# *exc-2,* an intermediate filament gene, maintains tubular excretory canals in *Caenorhabditis elegans* along with *ifa-4* and other novel genes.

**By: Hikmat Imad Al-Hashimi**

Submitted to the Department of Molecular Biosciences and the Faculty of the Graduate School of the University of Kansas in partial fulfillment of the requirements for the degree of Doctor of Philosophy

_____
Chairperson Dr. Matthew Buechner

_____
Dr. Erik Lundquist

_____
Dr. Brian Ackley

_____
Dr. Liang Xu

_____
Dr. Deborah Smith

Date Defended: May 3rd, 2018

The Dissertation Committee for Hikmat Imad Al-Hashimi certifies that this is the approved version of the following dissertation:

# ***exc-2,*** **an intermediate filament gene, maintains tubular excretory canals in *Caenorhabditis elegans* along with *ifa-4* and other novel genes.**

_____

Chairperson: Dr. Matthew Buechner

Date Approved: May 8th, 2018

## Abstract

The excretory canals of *Caenorhabditis elegans* are a model for understanding the maintenance of apical morphology in narrow single-celled tubes. Light and electron microscopy shows that mutants in *exc-2* start to form canals normally, but these swell to develop large fluid-filled cysts that lack a complete terminal web at the apical surface, and accumulate filamentous material in the canal lumen. Here, whole-genome sequencing and gene rescue show that *exc-2* encodes intermediate filament protein IFC-2. EXC-2/IFC-2 protein, fluorescently tagged via CRISPR/Cas9, is located at the apical surface of the canals independently of other intermediate filament proteins. EXC-2 is also located in several other tissues, though the tagged isoforms are not seen in the larger intestinal tube. Tagged EXC-2 binds via pulldown to intermediate filament protein IFA-4, which is also shown to line the canal apical surface. Overexpression of either protein results in narrow but shortened canals. These results are consistent with a model whereby three intermediate filaments in the canals, EXC-2, IFA-4, and IFB-1, restrain swelling of narrow tubules in concert with actin filaments that guide the extension and direction of tubule outgrowth, while allowing the tube to bend as the animal moves. Additionally, a focused reverse genomic screen of genes highly expressed in the canals found 21 new genes that significantly affect outgrowth or diameter of the canals. These genes nearly double the number of candidates that regulate canal size. Two genes act as suppressors on a pathway of conserved genes whose products mediate vesicle movement from early to recycling endosomes. The encoded proteins provide new tools for understanding the process of cellular recycling and its role in maintaining the narrow diameter of single-cell tubulogenesis.

## Dedication

To my Father … The greatest man I have ever known.

To Gada and Meral …  I love you so much and I am so lucky to have you.

Without you I wouldn't have gone this far …

## Acknowledgment

I am grateful to all who supported me through the years of my study. I am grateful to my mentor Dr. Matthew Buechner for his scientific guidance including all meetings that discussed my results and troubleshooted my experiments. I am thankful for encouraging me to attend, and financially supporting me, many local and international meetings. I am greatly appreciative to his time and efforts he invested in helping me write my manuscripts. His kindness and humbleness is a model to follow.

I owe a big thank you to my committee members who always have been a source of support and help to me. Dr. Lundquist for his contributions and support in genome sequencing and analysis of *exc-2* alleles. Additionally, for the helpful feedback during my committee meetings. Dr. Ackley for sharing his confocal microscopy and for all the advice he provided. Dr. Xu for sharing his western-blot imager and Dr. Smith for the support that she has showed over the course of my graduate studies. I would like also to thank my previous committee members Dr. Robert Cohen and Dr. Kathy Suprenant for all the feedback and recommendations they provided and their contribution in establishing my main project.

Finally, I am thankful for all the sources of funds that supported me. Specially, the GRF support which helped me into focusing on my research during summers and the K-INBRE which generously provided a grant to sequence three alleles of *exc-2*.

# Table of contents

# Chapter 1: Introduction

## 1.1 Focus of Research

Biological tubes are found ubiquitously in living organisms; they are connected to form networks in order to exchange gases and fluids. These tubes develop through different mechanisms and can be found in various lengths, widths, and functions [2]. While narrow tubes are usually made from a single cell, wider tubes are built up from multiple cells that are connected to each other through cell-cell junctions to form an interior lumen [12]. Developing biological tubes with the optimal diameter is vital for proper function to transport the required amount of substance. An alteration in nephron diameter in the kidney, for example, leads to Polycystic Kidney Disease (PKD). In PKD, clusters of cysts are formed in the nephrons within the kidneys which leads to their enlargement in size and loss of function over time. Hence, understanding the mechanism by which a biological tube maintains its diameter is vital in order to avoid diseases such as PKD.

The goal of my research is to gain further insight into the mechanism of maintaining diameter of narrow tubes. I utilized the excretory canal of the nematode *Caenorhabditis elegans* to address my questions and to test my hypothesis. The single-celled and seamless excretory canal is made of two very narrow tubes that extend over the full length of the worm. The relatively long tubes with narrow diameter facilitate the detection of any alterations in the canal diameter or length. Hence, the excretory canal provided a simple yet effective model for our research goals. I cloned and characterized *exc-2* and found that it encodes a cytosolic intermediate filament, IFC-2, and characterized its interaction with IFA-4. In addition, through a dsRNA screen, I identified novel genes that maintain the tubular structure of the excretory canal, including two suppressors for a previously cloned gene; *exc-5*.

## 1.2 Epithelia form biological tubes

Epithelial cells represent one of the four cell types in animal tissues. The epithelial cells are polarized cells where the apical surface often is oriented towards the inner side of the organ while the basal side secretes the basement membrane as a scaffold towards the outer surface. A simple epithelium is made from a layer of cells aligned next to each other and attached to each other by cell-cell junctions to form a sheet-like structure. Polarization of epithelial cells is fundamental for tissue function. Separation of cell surfaces is a key step toward polarization to form apical and basolateral sides for the cell. The phospholipid compositions on cell surfaces are altered and rearranged during polarization. $PIP_2$ is enriched on the apical membrane while $PIP_3$ is enriched at the basal and lateral membrane of the cell. This enrichment/rearrangement is facilitated through different sets of proteins such as the PAR-proteins, PTEN, and aPKC [6-8]. Epithelial cells are anchored to each other through different sets of junctions; the tight junction, for example, is made from a network of transmembrane proteins that bind two cells together (figure 1.1b) [6, 9]. Beside their function in holding two cells together, these junctions act as a barrier for materials by preventing passive movement of material among the cells throughout the tissue. Tight junctions also facilitate polarization by serving as a scaffolding structure and recruiter for proteins that initiate polarization, such as those mentioned above. In addition, these junctions maintain the polarity of the cell by preventing diffusion of the lateral proteins into the apical membrane surface

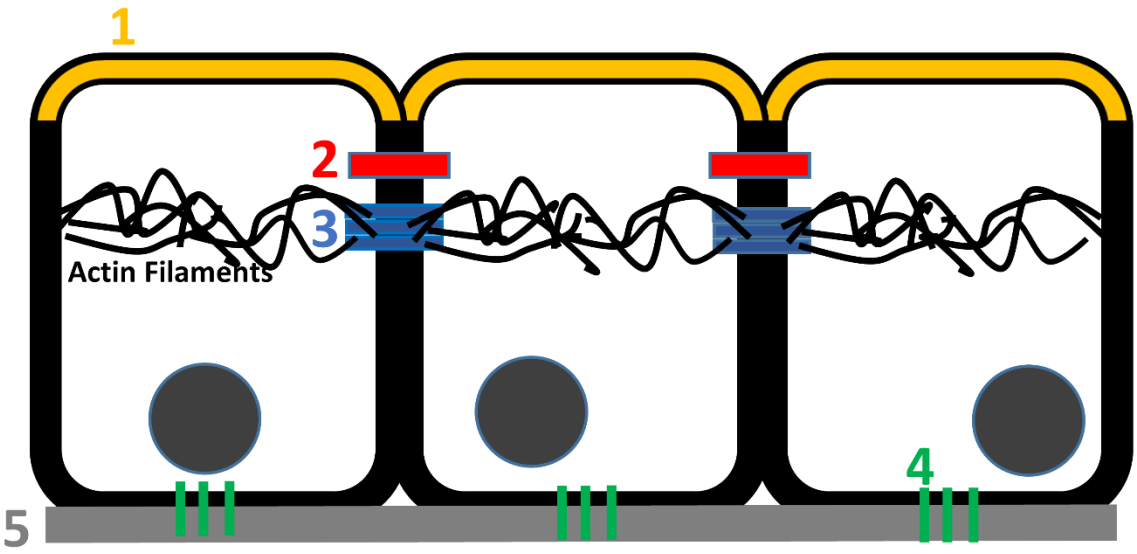


**Figure 1.1 Simplistic diagram of a monolayer of epithelial cells.**

- The apical membrane of cells (yellow) is oriented toward the inner side of an organ or the lumen of a tube and is enriched with $PIP_2$ phospholipids.
- Tight junctions (red) hold cells together and seal the tissue from passive movement between the apical and basolateral sides. Tight junctions also play a role in enriching the apical membrane with $PIP_2$ through interactions with polarizing protein such as PAR-proteins, PTEN, and aPKC.
- Adherens Junctions (blue) hold cells together, bind to actin filaments to give further support to the tissue, and also play roles in intracellular signaling and transcriptional regulation.
- Integrins (green) facilitate adhesion of the basal side of the cells to basement membrane.
- The basement membrane (grey) is a layer of proteins that helps to anchor epithelial basal side of the cell to the extracellular matrix.

[6, 9]. In addition to tight junctions, epithelial cells contain adherens junctions, which in invertebrates is more basal than tight junctions. The adherens junctions are composed of cadherin proteins, and play a role in regulating actin cytoskeleton and link the cell to bundles of actin filaments to give further support to the tissue. Finally, adherens junctions contribute to intracellular signaling and transcriptional regulation. On the basal surface, the transmembrane receptors, including integrin, facilitate adhesion of cells to the basement membrane. Once these receptors are activated, a cascade of cellular events take place, such as cytoskeleton organization [10, 11].

Given their wide distribution in the body, epithelial cells play a variety of important functions such as excretion (kidney), gas exchange (lung sacs and blood vessels), protection (skin), secretion (glands), and absorption (intestine). While epithelia can take the shape of a sheet in the skin to function in protecting and insulating the body, they can also take a tubule shape and function in excretion such as the nephrons in the kidney or as carries and transporters such as in blood vessels. Hence, a growing body of work focuses on tubulogenesis in order to gain further understanding of formation and maintenance of epithelial tubes.

Biological tubes vary in length and diameter; while the diameter of the trachea in *Drosophila* is 0.1 micron (one cell) the gut of an adult elephant is about 20 cm (multicellular tube). Regardless of tube complexity, diameter size, and length, all need the polarization and the support for the apical membrane in order to maintain normal diameter [12].

There are six major mechanisms to form biological tubes [2, 4, 12, 13]:

1- Wrapping: The epithelial sheet curls until one end is attached to the other forming a tube. This step is followed by separation from the rest of the sheet. The neural tubes of vertebrates

form using the wrapping method.

2- Budding: When cells start to extend from epithelial plane of a previously formed tube and start to form a tube in an orthogonal direction from the epithelial cells. This process takes place in many tracheal branches in *Drosophila.*

3- Cavitation: In this method, the cells form a mass in the shape of a cylinder and then start to eliminate the cells in the middle of that cylinder to form a central cavity that later forms the lumen of the tube. This method take place during *Drosophila* salivary gland morphogenesis.

4- Cord hollowing: In this method, the cells arrange in the shape of cylinder and form a lumen in between the cells, without cell elimination as described in 'Cavitation'. The intestine of *C. elegans* forms using this method.

Unicellular tubes can be formed in the following methods:

5- Cell wrapping and autofusion: A single cell forms a tube by use of the wrapping method, and the two sides use forming an adherence junction from one side of the cell to the opposite side of the same cell (autofusion). In some cells, such as the excretory duct cell of C. elegans, the adherens junction as the membrane between the two sides is removes, to form a seamless tube.

6- Cell hollowing: The lumen forms from vacuoles within the cytoplasm of the cell and eventually become the lumen in a tubular cell. The excretory canals of *C. elegans* form using this method, which will be the focus of this dissertation [2, 4, 12].

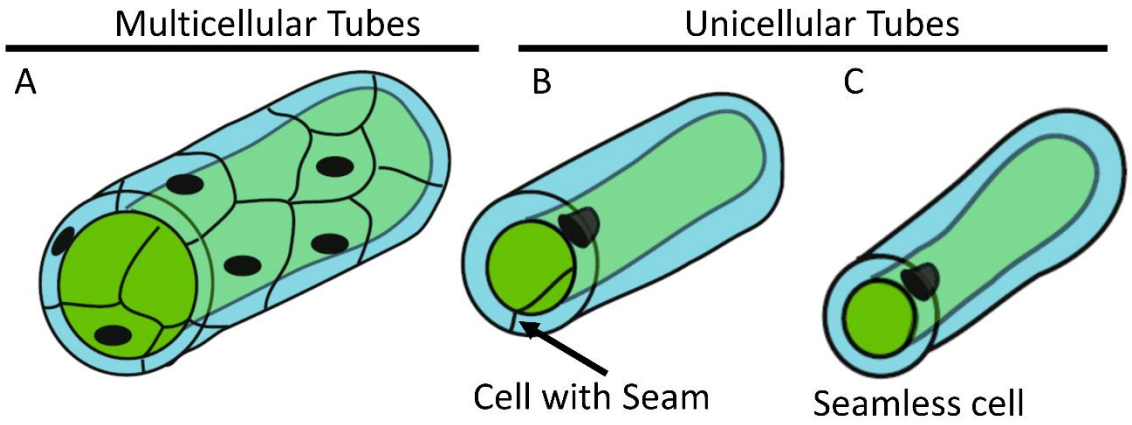


**Figure 1.2. Multicellular Vs. Unicellular Tubes.**

A- Multicellular tube, cell-cell junctions hold cells together in a tube shape.
B- Unicellular tube, a single cell for a tube with a seam sealing the tube.
C- Unicellular tube, a single cell without a seam in the wall of the tube.
Adapted with permission from [2]. (Receipt number 2342110067840)

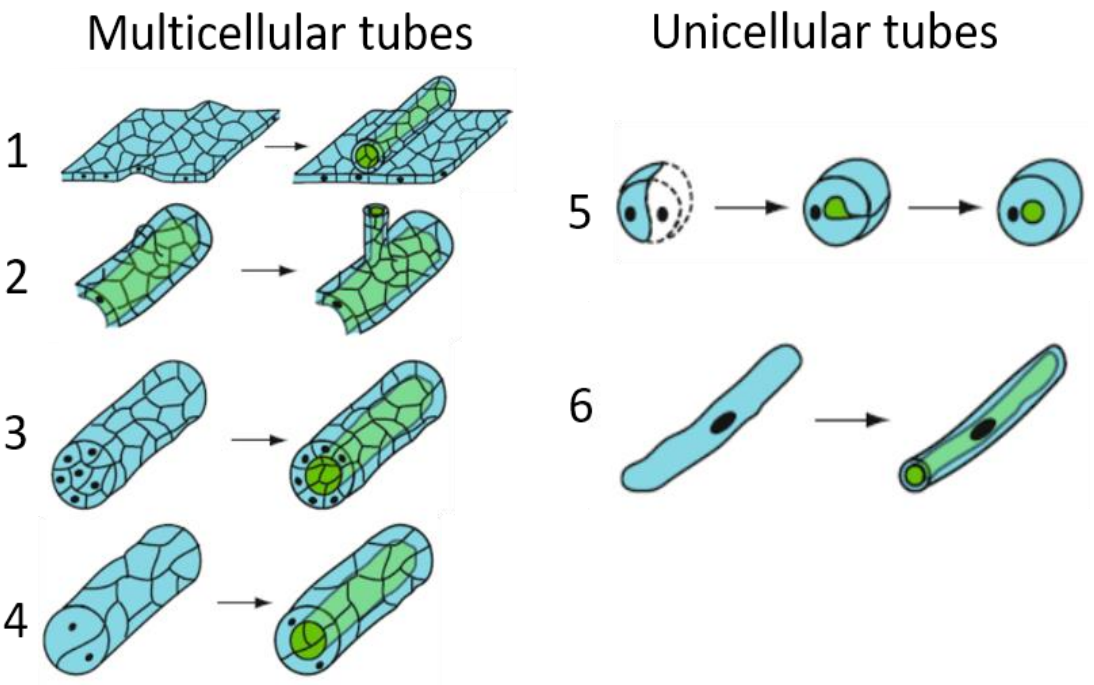


**Figure 1.3 Methods of biological tube formation.**

1- Wrapping (neural tubes) 2- Budding (tracheal branches in *Drososphila*)
3- Cavitation (salivary gland) 4- Cord hollowing (intestine of *C. elegans*)

5- Cell wrapping and autofusion (excretory duct of *C. elegans*) 6- Cell hollowing the excretory canals of *C. elegans*)

Adapted with permission from [2]. (Receipt number 2342110067840)

### 1.3 *Caenorhabditis elegans*:

#### 1.3.1 Living conditions and life-cycles:

*C. elegans* is a non-parasitic nematode species that inhabits the soil in a range of temperatures between 15 and 25ºC. Adults of *C. elegans* can grow to reach the length of 1 mm, and have two reproductive systems, nonsexual (hermaphroditic) and sexual (through rare males, 0.5%). The life cycle of *C. elegans* in preferable conditions includes: embryonic stage (~9 hours long); followed by 4-larval stages L1-L4 (total time ~46 hours); and finally adulthood where the worm is capable of laying its own eggs (can last up to three weeks). At the end of each larval stage, the worm undergoes a process of molting in order to prepare the body for further growth. Alternatively, the *C. elegans* life cycle can undergo a different path in the case of food depletion. By the end of L1 stage, the worm has a checkpoint where a decision is made whether to continue growing normally or to enter the dauer stage if nutrients are scarce. A worm in dauer stage closes its mouth and anus and stops acquiring food, the fat is lost from the body, and the worm become much skinner. In this stage, worms can survive for several months until the nutrients are available again, at which point the worm will exit this stage and molt into L4-stage larvae [2, 14-16].

#### 1.3.2 A great biological model to maintain in a laboratory:

Many characteristics of *C. elegans* attracted Sydney Brenner in 1966 to study the nervous system. The transparency of the skin facilitates the study of cells and tissues in a living organism, while the small size of the worm and its ability to grow in a small Petri dish while feeding on *E. coli* made its maintenance relatively easy and inexpensive. In addition, the worms can be frozen and be kept in liquid nitrogen for an undefined time, which enables easy maintenance of genetic strains [14, 16].

### 1.3.3 A great biological model to study genetics and cell biology:

*C. elegans* reproduces relatively fast, where the whole life cycle from an egg to a egg-laying adults takes only three days. In addition, *C. elegans* has a large progeny size where a healthy worm can lay between 200-250 eggs during its life span. All of these factors make *C. elegans* a great model for genetic studies, especially that it has a hermaphrodite system of self-fertilization which makes the maintenance of a genotype easy, yet males can still be used to exchange genes [14].

On the top of all the previous points, *C. elegans* is a truly amazing model and powerful for its ability to express genes ectopically by injecting the gene into the gonad of the worms to detect the any phenotypic alterations among its progeny. Furthermore, gene knockdown can be achieved relatively easy compared with other model organisms. Gene knockdown can be achieved by injecting the gonad with dsRNA complementary to the gene of interest, or by feeding the worms bacteria that synthesize/contain the dsRNA, or even by soaking the worms in a solution containing the dsRNA. Recently, multiple methods were published describing CRISR/Cas9 genome editing in worms, making *C. elegans* an inexpensive, easy to maintain, and powerful model in genetics and cell biology [14, 17, 18].

### 1.3.4 Scientific achievements from study of *C. elegans*:

Many important scientific findings have been achieved through studies of *C. elegans*. The complete pattern of cell fate for the somatic cells was described during the late 1970s. The steps during embryogenesis are therefore perhaps best characterized and studied in *C. elegans.* The transparency of the skin facilitated monitoring and tracking each cell in the body of *C. elegans*, which made this organism an excellent system to study apoptosis. Indeed, in 2002 Sydney

Brenner, Horvitz, and John E. Sulston were awarded the Nobel Prize in Medicine for their earlier work in identifying genes regulating apoptosis. Another big milestone achievement is the discovery of RNA interference (RNAi), which was first described in *C. elegans* by Andrew Fire and Craig C. Mello, who shared a Nobel Prize in Physiology or Medicine in 1998. A small, transparent, and simple system is a very powerful system for a scientist to address a basic question in biology.

Green Fluorescent protein (GFP) was first discovered in the jellyfish *Aequorea victoria* by Osamu Shimomura, who split the 2018 Nobel prize with Martin Chalfie and Roger Y. Tsien. Chalfie demonstrated the value of using GFP as a biological tag to detect and track proteins in living organisms. He utilized the transparent *C. elegans* for his research and labeled six different neurons in the worm and tracked their development [19]. Since then, GFP protein-tagging has become one of the most powerful techniques in developmental and cellular biology.

In my study, I used the excretory canal cell of *C. elegans* to study the mechanisms by which a biological tube maintains its diameter during the lifespan of a living organism. All the advantages mentioned above made my work possible and provide further insights into this process.


**Fig. 1.4 *C. elegans* worm.**

A DIC image of an adult hermaphrodite of *C. elegans* worm, showing the pharynx where food is ground up, the vulva around the middle of worm's body, and the anus at the end of the worm. Scale bar = 0.1mm

(Adapted from http://www.wormatlas.org.)

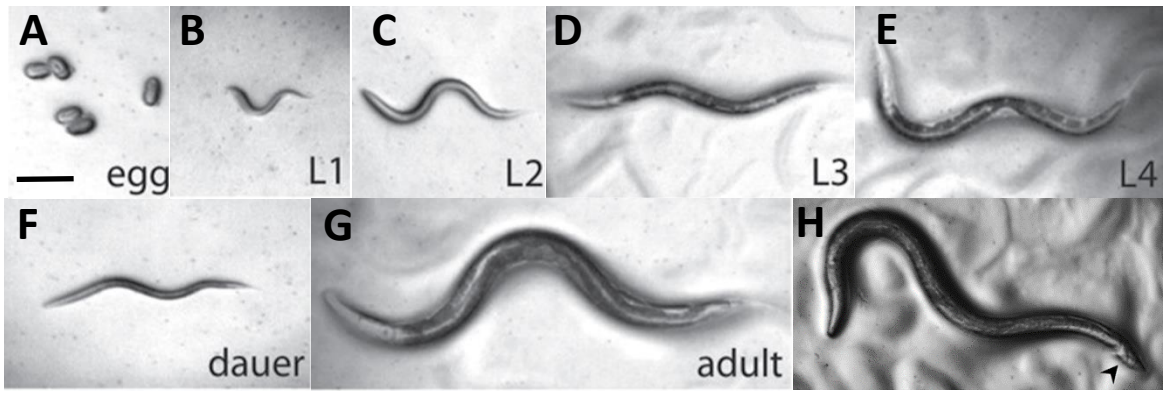


**Fig. 1.5 *C. elegans* life cycle.**

A- Eggs (9 hours) Bar = 0.1 mm
B- L1 (9-12 hours)
C- L2 (8 hours)
D- L3 (5.5 hours)
E- L4 (16 hours)
F- Dauer stage (in food-depletion condition- can survive up to 4 months)
G- Adult hermaphrodite (up to 3 weeks)
H- Adult male worm – black arrow head points to male gubernaculum and tip of the tail.

(A-G adapter from [3]) "This image is in the public domain in the origin country of the publication"

(H adapted from [5]) "Copyright © 2015 Corsi, Wightman, and Chalfie.Creative Commons Attribution Unported Licens"(http://creativecommons.org/licenses/by/3.0/), which permits unrestricted use, distribution, and reproduction in any medium, provided the original work is properly cited."

### 1.4 Excretory canals of *C. elegans*:

The excretory canals of *C. elegans* represent a great model to study tubulogenesis and tube maintenance. The canal cell is a part of the excretory system which also includes the excretory duct and excretory pore cells, and two excretory gland cells. All of these cells are connected to each other and share a common continuous lumen. The excretory canal represents the largest epithelial cell in the worm. The worm cannot survive in the absence of the canals, as ablation of the canal cell body by use of a laser beam showed that water accumulates inside the worm body cavity and soon kills the worm [4, 15, 20].

The canal cell body is located directly beneath the terminal pharyngeal-bulb, in proximity to the other cells of the excretory system. Two hollow tubes extend laterally from the cell body to the lateral hypoderm, then branch anteriorward and posteriorward until the four tubes reach the distal ends of the worm, taking the shape of the letter 'H' [20-23]. The function of this simple network is to collect excess water from the worm to excretes through the duct and pore cells. This process regulates osmolarity inside the worm and hence the canal functions in part similarly to the vertebrate kidney [15].

Many studies provided insights into the mechanism of excretory-canal function and development. Perhaps one of the most important structures in the canal are the canaliculi at the apical membrane. These small hollow vesicular structures highly increase the luminal surface and contain vacuolar ATPase (proton pumps) and the water channel/pump protein Aquaporin AQP-8. Both the vacuolar ATPase and AQP-8 play essential roles in canal lumen elongation and regulation of osmolarity [24, 25]. The extension of the apical surface of the canal depends in part on the luminal fluid pressure toward the growing distal tip of the canal. AQP-8 is believed to pump water into the canal lumen in order to provide the needed pressure, although *aqp-8*-null

mutants form only slightly short canals, which suggests that additional player(s) participate in this process [25]. Vacuolar ATPase is important for alternating and balancing the ionic balance in the canal in response to changing osmotic conditions [26].

The canal cell is born toward the end of gastrulation, about four and half hours after the first cell cleavage. Thirty minutes to one hour after birth, vacuoles start to appear in the cell, which represent the kernel for what will later become the lumen of the canals. In the meantime, the cell starts to slightly change its shape and projects two arms dorsolaterally. After an hour of development, the vacuoles accumulate and start to merge to form the first defined lumen in the cell. At this time, the arms extend farther and reach the lateral hypoderms. At the 2-fold stage of embryogenesis, the canals reach the lateral hypodermis and bifurcate to extend both in the anterior direction (anterior canals short and thinner) and in the posterior direction (posterior canals long and wider). At hatching, the posterior canal length reaches about half the length of the worm, and continues to extend anteriorly and posteriorly until reaching their full length just posterior to the anus by late first larval stage. After the canal tubes reach the distal tips of the worm, they elongate at the same rate as the worm grows and elongates [21-23].

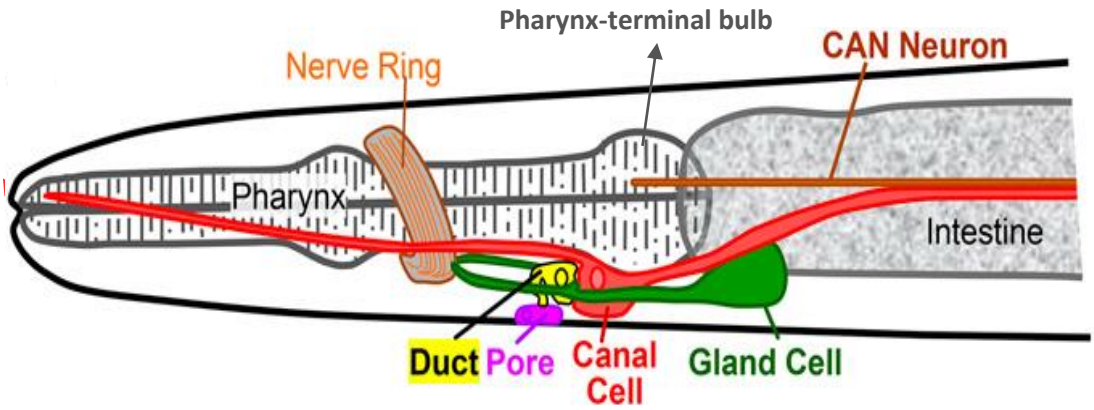


**Figure 1.6 The anatomy of the excretory system in *C. elegans*.**

Excretory-canal (in red) cell body beneath the terminal bulb of the terminal pharyngeal bulb. The canal cell forms a continuous lumen with the excretory pore and duct cells.

(Adopted from [4]) (Permission order detail ID: 71158594  Order License Id: 4342131335545)

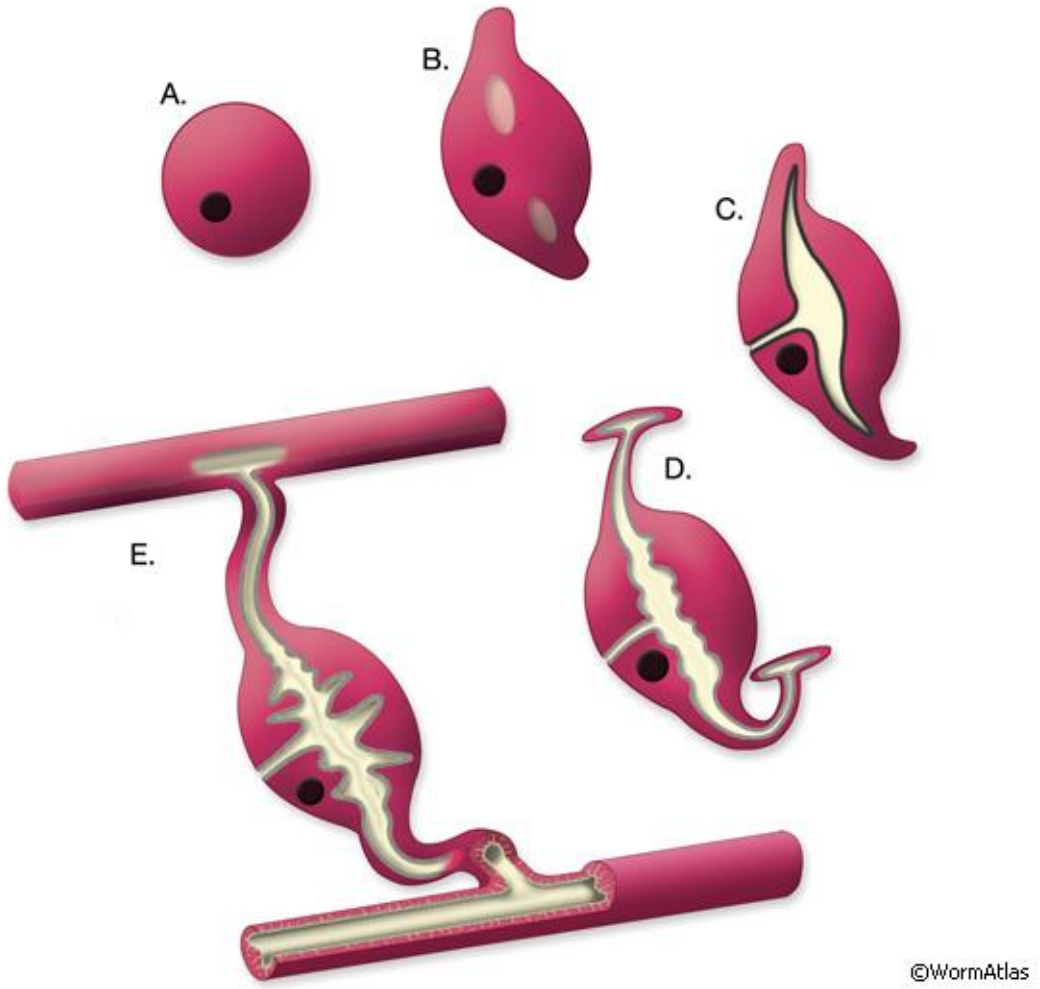


**Figure 1.7 Excretory canal development.**

A- Excretory canal cell born ~270 minutes after fertilization occurred.
B- Vacuoles start to appear and develop starting from 300 to 330 minutes after fertilization.
C- The vacuoles start to merge and form one continuous lumen, and the cell starts to change its shape and send two extensions dorsolaterally at 400 to 430 minutes after fertilization.
D- The arms reach the hypodermis and starts to bifurcate and form the posterior and anterior canal tubes, at about the two-fold stage.
E- At hatching the canal is almost fully developed, with canaliculi all around the apical surface of the canal. The canal keeps growing until it has fully developed and reaches the full length of the worm.
(From http://www.wormatlas.org.)

### 1.5 Unicellular tubes:

#### 1.5.1 Unicellular tubes in our bodies:

Until recently, unicellular seamless tubes were poorly understood. The small size of the structures and the difficulty of imaging and studying them were major factors that hindered study of these structures. As technology advanced and new techniques were acquired, more evidence emerged that seamless tubes play important functions in our bodies. Capillaries in our cardiovascular system are perhaps the best example, as multiple diseases and have been shown to be related to defects in capillaries; such as hypertension (higher blood pressure), coronary microvascular disease (a major cause of heart attacks), and cerebral small vessel disease (a major contributor for age-related strokes and dementia).

Defects and poor maintenance of single-celled tubes can also be detected in genetic diseases such as Cerebral Cavernous Malformation (CCM), in which enlarged blood vessels form irregular shapes. These vessels lack elasticity, which leads to blood leakage, most noticeably in the brain. The list of inheritable diseases affecting unicellular tubes is extensive, which emphasizes the importance of studying these structures in more depth [27].

#### 1.5.2 Unicellular studies in biological models:

Unicellular tubes are studied in many biological models besides *C. elegans*. The tracheal system in *Drosophila* is a great example. The trachea forms a small network in the animal; this network is made from different types of tubule-forming cells that are fused to each other. The biggest tracheal processes are multicellular tubes, and attached to these large multicellular tubes are multiple smaller unicellular tubes made from stalk cells. The stalk cells are seamed tubes that often connect at the stalk distal end to two seamless tube cells; a fusion cell and a terminal cell.

The function of the very short fusion cell is to interconnect multiple branches in trachea. The terminal cell forms multiple narrow branches that extend throughout nearby tissues. The function of the terminal cells is to exchange gases between trachea and other organs. This model is suitable to study tubulogenesis, since the *Drosophila* larva is almost transparent and the tracheal tubes can be easily visualized. Indeed, many phenotypes were observed and studied among these cells. Mutants in the tracheal gene *uninflatable,* for example, fail to inflate the tracheal tube, which results in crushed or twisted tubes. The mutant flies fail to complete embryogenesis and often dies as a larva [28-31].

The Palatocerebral Artery (PLA) in zebrafish represents another interesting example of tube formation and morphogenesis. The lumen in the cell forms via invagination as a normal unicellular tube. Interestingly, this unicellular tube is a transient step in formation of a mature multicellular tube. Antibody staining of apical membrane and cell-cell junctions showed obvious characteristics of a multicellular tube, with the presence of cell-cell junctions within the tube. The cell undergoes a series of dynamic cell rearrangements to become a multicellular tube from a unicellular one [32-34].

### 1.6 The *exc* family genes.

A genetic screen was conducted to identify genes that are important for excretory canal formation and maintenance in *C. elegans*. This screen identified nine novel genes, *exc-1* through *exc-9*. In *exc*-gene mutants, the canal is born and appears to develop normally initially, until tube diameter maintenance is compromised and the canal starts to accumulate fluid-filled cysts [22]. Many of the *exc*-genes have been cloned, and some functions of the encoded proteins identified, while others are yet to be cloned and studied. Three of the cloned *exc*-genes work in a common genetic pathway: *exc-9, exc-5,* and *exc-1*. The encoded proteins work in vesicle transportation between the early endosomes and the apical recycling endosomes. It is believed that blocking this pathway leads to accumulation of some substance in early endosomes, followed by weakening of the apical surface, and subsequent formation of fluid-filled cysts. In epistatic studies, it was shown that *exc-9* acts upstream of the other two *exc* genes, *exc-1* and *exc-5*, while *exc-1* acts upstream of *exc-5*. The EXC-1 and EXC-9 proteins bind each other directly [1, 35, 36].

EXC-4, on the other hand, was found to be a chloride (CLIC) channel at the apical membrane, the phenotype of *exc-4* mutants shows the most severe and obvious cysts in the canal among the *exc* genes [21]. EXC-7 is an RNA-binding protein; one of its targets is *sma-1* mRNA [37]. SMA-1 ($\beta_H$spectrin) docks the actin-filaments to the apical membrane in order to provide the needed support for the apical surface [38, 39]. *exc-6* encodes for formin INF2, which regulates F-actin and microtubule formation in the canal [40]. As noted in table 1.6.1, two genes are still to be identified among the *exc* gene family: *exc-3* and *exc-8*.

Beside the *exc*-genes, other genes were also identified as players in canal diameter maintenance

(Table 1.6.2). *ifb-1* and *erm-1* will be discussed later in this work in reference to the interacting functions that they have with the cloned *exc-2* gene.

### 1.6.2 Gene of interest: *exc-2*.

The *exc-2* mutants show one of most pronounced phenotypes among the *exc* mutants. The canal partially extends to only 30-40% of the normal length, with multiple fluid-filled cysts all along the canal. Previously, via three-point mapping, *exc-2* was roughly mapped on the X-chromosome in the locus between *mec-2* and *dpy-8* (~415 kb with 170 genes). The *exc-2* mutants show slightly smaller brood size and their bodies look somewhat pale as compared to those of wild-type worms. It is also worth mentioning that *exc-2* mutants share a similar phenotype with other *exc*-gene mutants in having defects in structure of the tail tips. The tail tips of *exc-2* worms form a distinctive onion-dome shape instead of a smooth tail tip like those found in wild-type animals. This phenotype is not 100% penetrant among *exc-2* mutants and hence will not be discussed in detail in this study.

The genetic screen generated four different alleles of *exc-2*: *rh90*, *rh105*, *rh209*, and *rh247*. Phenotype severity of the 4 alleles is approximately equivalent with regards to cyst size and canal length. The fact that random mutagenesis generated four alleles of the same gene (most other exc genes were represented by only one or two alleles) suggests that the gene is relatively large in size. The multiple cysts along the canal suggest a uniform weakening throughout the apical surface of the entire canal tube. In contrast, a specific regional weakening, as observed in *exc-5* for example, where cysts appear primarily or solely at the distal tips of the canals, indicates that most of the canal tube is structurally. Additionally, the very short length of *exc-2* mutant canals suggests a fundamental function for the EXC-2 protein; since the canal length is shorter

than half the length of the worm, luminal failure and cyst formation likely begins early in canal cell formation in late embryogenesis.

**Table 1.1 A list of the *exc* genes along with known functions.**

| ***exc*-gene** | **Function** |
|---|---|
| *exc-1** | GTPase (human IRGC homologue) |
| ***exc-2*** | **The gene of interest in this dissertation** |
| *exc-3* | Unknown-not cloned |
| *exc-4* | Chloride-channel (human CLIC) |
| *exc-5** | Guanine Nucleotide Exchange Factor, (human FGD4) |
| *exc-6* | Formin (human INF2) |
| *exc-7* | mRNA binding protein, (*Dros.* ELAV, human HuR) |
| *exc-8* | Unknown-not cloned |
| *exc-9** | LIM domain protein, (human CRIP) |

*Work in a common pathway.

**Table 1.2 A partial list of genes, beside *exc*-genes, known to play a role in canal tube maintenance, along with their functions.**

| **Gene name** | **Function** |
|---|---|
| ***ifb-1*** | Intermediate filament protein B |
| ***erm-1*** | Cytoskeleton linkers |
| ***sma-1*** | $\beta_H$-Spectrin |
| ***let-4*** | an extracellular leucine-rich repeat |

# Chapter 2: Cloning and characterization of *exc-2*

## 2.1 ABSTRACT

The excretory canals of *Caenorhabditis elegans* are a model for understanding the maintenance of apical morphology in narrow single-celled tubes. Light and electron microscopy shows that mutants in *exc-2* start to form canals normally, but these swell to develop large fluid-filled cysts that lack a complete terminal web at the apical surface, and accumulate filamentous material in the canal lumen. Here, whole-genome sequencing and gene rescue show that *exc-2* encodes intermediate filament protein IFC-2. EXC-2/IFC-2 protein, fluorescently tagged via CRISPR/Cas9, is located at the apical surface of the canals independently of other intermediate filament proteins. EXC-2 is also located in several other tissues, though the tagged isoforms are not seen in the larger intestinal tube. Tagged EXC-2 binds via pulldown to intermediate filament protein IFA-4, which is also shown to line the canal apical surface. Overexpression of either protein results in narrow but shortened canals. These results are consistent with a model whereby three intermediate filaments in the canals, EXC-2, IFA-4, and IFB-1, restrain swelling of narrow tubules in concert with actin filaments that guide the extension and direction of tubule outgrowth, while allowing the tube to bend as the animal moves.

## 2.2 INTRODUCTION

Polarized cells form tubular structures ubiquitously in living organisms [12, 41, 42]. Tubes vary in width, length, and in mechanism of formation [12, 43]. The mechanism by which a narrow biological tube grows and maintains a uniform diameter throughout the lifespan of an organism is poorly understood, however. The excretory system of the nematode *Caenorhabditis elegans* provides a useful model of "seamless" (no intracellular adherence junctions) single-celled tubular structures [4] such as vertebrate capillaries or the tip cells of the *Drosophila* trachea [12]. The core excretory system consists of a large excretory cell plus a duct and pore cell [44]. The excretory cell, located beneath the pharynx, extends four hollow canals throughout the length of the worm roughly in the shape of the letter "H" (Fig. 1A, B). The canals collect and excrete excess water from the body through the duct and pore to regulate organismal osmolarity [15]. Worms with defects in excretory canal function exhibit pale bloated canals and bodies, and have less tolerance to high-salt environments [22, 45, 46].

In genetic screens, mutations in nine "*exc*" genes were discovered to affect canal structure to allow fluid-filled cysts to accumulate during canal extension during late embryogenesis and early first larval stage [22]. Other studies found similar mutations that affect additional tubular structures in the nematode, including the seamed single-cell excretory duct cell [47-50]and the multicellular intestine [25, 51-55]. In the canal cell, proteins implementing tubule structure comprise apical cytoskeletal elements [24, 25, 38-40], vesicular trafficking and exocyst proteins [1, 35, 36, 56, 57], and ion and lipid transporters [21, 25], among others.

Cytoskeletal components play an essential role in maintaining canal structure [13]. Actin filaments are aligned over the apical surface of the canal lumen and docked to apical membrane via the ezrin/radixin/moesin homologue ERM-1 [58] and the apical $\beta_H$spectrin [38], while

mutations in the formin gene *exc-6* compromise nucleation of microtubules along the length of the canal [40]. *C. elegans* contains eleven cytosolic intermediate filament (IF) proteins, plus one nuclear lamin protein [59, 60]. Three intermediate filaments proteins are highly expressed in the canal cell: IFC-2, IFA-4, and IFB-1 [61]. Knockdown of the *ifb-1* gene causes cystic defects in both the canal and the multicellular intestine [24, 62].

While most of the original *exc* genes have been cloned [1, 4], mutations in the *exc-2* gene cause particularly severe canal defects. In these mutants, the canal length is shortened by over half, the animals accumulate multiple cysts in the canals, and are sensitive to growth at low osmolarity [22]. Four alleles of this gene were discovered in the original screen, which suggested that it encodes a large protein. Here we report that *exc-2* encodes the intermediate filament IFC-2, and additionally found that mutations in the *ifa-4* intermediate filament gene also cause cystic canal defects similar to those of *exc-2* mutants. Overexpression of either *exc-2* or *ifa-4* results in shortened canals with small or no cysts. EXC-2 and IFA-4 proteins bind to each other and are located at the apical membrane of the canals. The position of EXC-2 at the apical membrane occurs independently of IFB-1 and IFA-4 function in the canals. These results indicate the importance of these three intermediate filaments in forming and maintaining the uniform diameter of the canals in this single-celled model of long, narrow tubular structure.

## 2.3 MATERIALS AND METHODS

### 2.3.1 DNA constructs and dsRNA synthesis

This study utilized two canal markers: pCV01 (used at 15ng/µl) contains the *gfp* gene driven by the canal-specific *vha-1* promoter; and pBK162 (used at 25ng/µl) contains the *mCherry* gene driven by the *exc-9* promoter. Fosmid WRM0630A_E08 was provided by the Max Planck Institute, Dresden, Germany. Genomic DNA was used for *exc-2* rescue and was prepared via PCR with LongRange enzyme (Qiagen, Venlo, NL) to amplify the full-length *ifc-2* gene, including 2kb upstream and 500bp downstream. The translational construct of *ifa-4* was made by ligating *ifa-4* cDNA in-frame with the *gfp* gene in plasmid pCV01.

Double-stranded RNA (dsRNA) constructs were synthesized via PCR-amplification of 250-350bp regions of selected exons in genes of interest (Supp. Table 2.1). A MEGAscript T7 kit (ThermoFisher, Waltham, MA) was used for transcription. For *ifb-1*, RNAi constructs were created by placing two constructs, each containing a complementary sequence corresponding to exon 4, under control of the canal-specific *vha-1* promoter.

Constructs for CRISPR/Cas9-mediated mutation were created according to the method of the Goldstein laboratory [17]. The sgRNA constructs were made by amplifying plasmid pDD162 using primers containing a 20-base sequence specific for the gene of interest. The PCR product was self-ligated after treatment with T4 kinase. Goldstein group construct pDD282 was used for tagging *exc-2*, and pDD287 to tag *ifa-4*. Repair constructs were prepared through Gibson assembly of constructs containing the gene-specific tags in four overlapping amplified fragments, and ligated via NEBuilder® HiFi DNA Assembly Cloning Kit (NewEngland Biolabs, Ipswich, MA).

### 2.3.2 Nematode genetics and genetic mapping

Strains of *C. elegans* are shown in Table 1. They were maintained on lawns of bacterial strain BK16 (a streptomycin-resistant OP50 strain) on NGM agar plates as described [63].

By means of complementation tests and deficiency mapping, *exc-2* was previously mapped to the left end of the X chromosome [22]. Strains of *exc-2* to be sequenced were each outcrossed to a wild-type Hawaiian isolate (CB4856) as described [64]. For each of four mutant allele strains, twelve F2 progeny homozygous for the *exc-2* mutation were selected, and grown to populations that were combined for whole-genome sequencing. Sequencing was completed at the Genome Sequencing Core at the University of Kansas. Genome data analysis was carried out to identify mutations in the expected genetic area by use of the Galaxy cloud-map website (https://usegalaxy.org).

Genetic rescue assays of *exc-2*(*rh247*) mutants were performed through co-injection into the gonad of carrier DNA pCV01, plus either Fosmid WRM0630A_E08, or PCR-amplified genomic *exc-2* DNA. Injected animals were allowed to lay eggs, which were screened for expression of the GFP-expressing carrier DNA. F1 progeny expressing GFP were examined for canal morphology.

Rescue of the *ifa-4* deletion mutant strain RB1483 was performed through gonad co-injection of an *ifa-4* cDNA construct at 40ng/µl together with marker plasmid pBK162. Injection of these *exc-2* and *ifa-4* constructs was also used to cause overexpression of the genes in wild-type worms. RNAi-knockdown of specific *exc-2* isoforms was accomplished through co-injection of forward and reverse RNA together with carrier pCV01 into gonads of young adult wild-type worms.

Complementation tests were carried out by mating male *exc-2*(*rh247*) to hermaphrodites of the BK530 (CRISPR'd *ifc-2* deletion) strain. Fluorescent hermaphrodite cross-progeny all showed the strong cystic canal phenotype of *exc-2* (n=30).

CRISPR/Cas9-mediated knock-in strains were created through injection of repair constructs from modifications to pDD282 and pDD287 CRISPR reagents (AddGene.org, Cambridge, MA) to make plasmids pBK301 and pBK302 in order to insert a fluorescent marker and epitope tag between the 5'UTR and coding region of *exc-2* and *ifa-4*, respectively. Selection of strains containing the constructs was performed on NGM plates containing 250 μg/ml hygromycin (Sigma-Aldrich, St. Louis). Heat-shock at 35C for 4-5 hours was used to activate removal of the selection cassette via self-excision. As the *exc-2* and *ifa-4* genes are located close together on the X chromosome, the doubly-tagged *exc-2*; *ifa-4* strain BK533 was created via CRISPR/Cas9-mediated tagging of BK531 (tagged *exc-2*) with pBK302.

### 2.3.3 Microscopy and Canal Measurement

Worms were examined through a Zeiss Axioskop microscope with Nomarski (DIC) optics and epifluorescence. Animals were placed on 3% agarose pads in water and immobilized either through addition of Polybeads® polystyrene beads (Polysciences, Warrington, PA) or of sodium azide (35 mM). Non-confocal images were taken using an Optronics MagnaFire Camera. Some images of larger worms required 2 or 3 photographs that were "stitched" together to provide picture of the entire animal. Contrast on DIC images was uniformly enhanced over the entire image to increase clarity. For protein subcellular location, worms were examined using an Olympus Fluoview FV1000 laser-scanning confocal microscope. Lasers were set to 488nm excitation and 520nm emission (GFP), or 543nm excitation and 572nm emission (mKate2). All

images were captured via FluoView optics (Olympus, Tokyo, JP) and collocation was analyzed using ImageJ software by drawing a straight line perpendicular to the length of the canal. Fluorescence plot profiles were then recorded and analyzed as shown in each image.

Electron microscopy was performed as described [22]. Young adult worms were cut and fixed in buffered glutaraldehyde and $OsO_4$, encased in agar, dehydrated, and embedded in resin. Serial sections are ~70 nm thick, and stained in uranyl acetate and lead citrate.

Canals were measured for length and cysts size as described [36]. The length of each canal was scored between 0 and 4, where 4 indicates a full-length canal; 3 for canals that extended between the vulva and full-length; 2 for canals extending to the vulva; 1 for short canals that extended between the cell body and the vulva; 0 for canals that did not extend past the cell body. Cyst size was scored by measuring cyst diameter relative to worm body width. Large cysts have a diameter similar to that of the worm body width, medium cysts have a diameter of approximately half-worm width, and small cysts are smaller than half the worm body width. A 3x2 Fisher's Exact Test was used to compare number of animals with short, medium-length, and full-length canals; and separately to compare number of animals with cysts, no cysts but canals with enlarged diameter, and normal-diameter canals.

### 2.3.4 Biochemistry and Binding Assays

Worms were collected after growth on strain BK16 cultured on twelve 100mm plates of NGM medium until the bacterial lawn was consumed, then washed in M9 solution and frozen in liquid nitrogen until needed. Worm lysates were prepared through vortexing 500µl thawed worms in a mixture of 300µl dry 425-600 µm-diameter glass beads (Sigma-Aldrich, St. Louis, MO) and 700µl lysis buffer (0.5% NP40, 150mM NaCl, 50mM Tris pH 8.0, 0.5mM EDTA, 5% glycerol, 1mM DTT, and Protease-inhibitor tablet (Thermo Fisher Scientific, Waltham, MA)). The

mixture was vortexed for 15min at maximum speed at 4°C, followed by 15 minutes on ice to cool down the samples, and again for another 15 minutes at 4°C. The lysate was then centrifuged in an Eppendorf centrifuge at maximum speed for 5 minutes at 4°C, and protein concentration of the supernatant was measured.

Protein samples for co-immunoprecipitation were incubated with pre-blocked (using 5% BSA) anti-FLAG® M2 magnetic beads (Sigma-Aldrich) at 4°C for 30 minutes. Samples were then washed thoroughly with PBS-T and eluted using 3X FLAG peptides (Sigma-Aldrich).

Samples for western blots were loaded onto Mini-PROTEAN® TGX™ gels with a 4-20% gradient of bis-acrylamide (Bio-Rad, Hercules, CA). For immunoprecipitation samples, an equal volume was loaded in each well, while for lysate samples an equal amount of protein was loaded each well. Nitrocellulose membranes were blocked in 5% instant milk in TBS-T.
Tagged EXC-2 protein was detected via monoclonal anti-FLAG® M2 antibody (Sigma-Aldrich) at a final concentration of 1µg/ml in blocking buffer, and tagged IFA-4 protein was detected via HRP-bound anti-c-Myc antibody (Sigma-Aldrich) at a final concentration of 0.5µg/ml in blocking buffer.

## 2.4 RESULTS

Mutants in all alleles of *exc-2* show severely cystic canal phenotypes, with multiple fluid-filled cysts evident along the entire length of the greatly shortened canals (Fig. 2.1C and C', Supp. Fig. 2.1). Canal length is only 30-40% of that of wild-type canals, and cysts have an average diameter 4 times as wide as that of a wild-type canal lumen. Electron microscopy images of *exc-2* canals show areas where the electron-dense actin-rich terminal web of the apical membrane has been thinned or lost (Fig. 2.2B and B') in comparison with that of wild-type canal (Fig. 2.2A and A'), consistent with a loss in apical membrane support. The thinned areas lack canalicular vesicles relative to other areas where the terminal web is still intact. These vesicles connect transiently to the canals and are believed to regulate acidification and osmotic regulation of the animal (Kolotuev, Hyenne et al. 2013). The lumen of the cystic canals contains visible long filaments (Fig 2B') that have not been detected in wild-type canals or in most other *exc* mutant canals, save for mutants in the *sma-1* $\beta_H$spectrin gene. These defects are specific to the excretory canals; electron microscopy of the intestine shows an apparently normal terminal web surrounding well-formed and normally arranged microvilli, with no cystic effects (Fig. 2.2C and C').

Whole-genome sequencing of four *exc-2* alleles revealed that the intermediate filament gene *ifc-2* is mutated in all four strains (Fig. 2.3A, Supp. Fig. 2.2). Two of these alleles, *rh209* and *rh247*, encode nonsense mutations in exon ten and twelve, respectively. Alleles *rh90* and *rh105* include deletions of multiple coding regions that cause frameshift mutations that lead to early stop codons (Fig. 2.3A). In order to confirm the identity of the *exc-2* gene, a null-allele (*qp110*) in *ifc-2* was generated via

**Table 2.1. List of strains used in this study, with genotype descriptions.**

| STRAIN | GENOTYPE | DESCRIPTION | REFERENCE |
|---|---|---|---|
| N2 | Wild-type | Bristol isolate | [16] |
| CB4856 | Wild-type | Hawaiian isolate | [65, 66] |
| RB1483 | *ifa-4*(*ok1734*) | *ifa-4* deletion mutation | [67] |
| BK36 | *unc-119*(ed3); *qpIs11*[*unc-119*; $P_{vha-1}$::*gfp*] I | Wild type with integrated GFP marker expressed in excretory canal cytoplasm | [36] |
| NJ242 | *exc-2*(*rh90*) | *exc-2* deletion mutation | [68] |
| NJ340 | *exc-2*(*rh105*) | *exc-2* deletion mutation | [68] |
| NJ602 | *exc-2*(*rh209*) | *exc-2* nonsense mutation | [68] |
| NJ678 | *exc-2*(*rh247*) | *exc-2* nonsense mutation | [68] |
| BK530 | *exc-2*(*qp110*) | CRISPR-induced deletion of part of 5'UTR and part of first coding exon of *exc-2*. | This study |
| BK531 | *exc-2*(*qp111* [$P_{exc-2}$::*gfp*::3X*flag*::*exc-2*]) X | CRISPR-induced insertion into N2 of *gfp*::3x*flag* between promoter and starting codon of *exc-2*.<br>= tagged *exc-2* | This study |
| BK532 | *ifa-4*(*qp112* [$P_{ifa-4}$::*mKate2*::3X*Myc*::*ifa-4*])X | CRISPR-induced insertion into N2 of *mKate2*::3x*Myc* between promoter and starting codon of *ifa-4*.<br>= tagged *ifa-4* | This study |
| BK533 | *exc-2*(*qpIs111* [$P_{exc-2}$::*gfp*::3X*flag*::*exc-2*]) *ifa-4*(*qpIs113* [$P_{ifa-4}$::*mKate2*::3X*myc*::*ifa-4*])X | CRISPR-induced insertion into BK531 of *mKate2*::3x*Myc* between promoter and starting codon of *ifa-4*<br>= tagged *exc-2* & *ifa-4* | This study |
| BK534 | *ifa-4*(*ok1734*); *exc-2*(*qpIs111* [$P_{exc-2}$::*gfp*::3X*flag*::*exc-2*]) X | *ifa-4* deletion mutant crossed to BK531 line expressing labeled EXC-2::GFP<br>= *ifa-4* ko; tagged *exc-2* | This study |
| BK535 | *ifa-4*(*ok1734*) X; *qpIs11*[*unc-119*; $P_{vha-1}$::*gfp*] I | *ifa-4* deletion mutant crossed to BK36 line expressing strong cytoplasmic canal fluorescence<br>= *ifa-4* ko; canal marker | This study |
| BK536 | *exc-2*(*rh247*) X; *qpIs11*[*unc-119*; $P_{vha-1}$::*gfp*] I | *exc-2* null mutant crossed to BK36 line expressing strong cytoplasmic canal fluorescence<br>= *exc-2* ko; canal marker | This study |

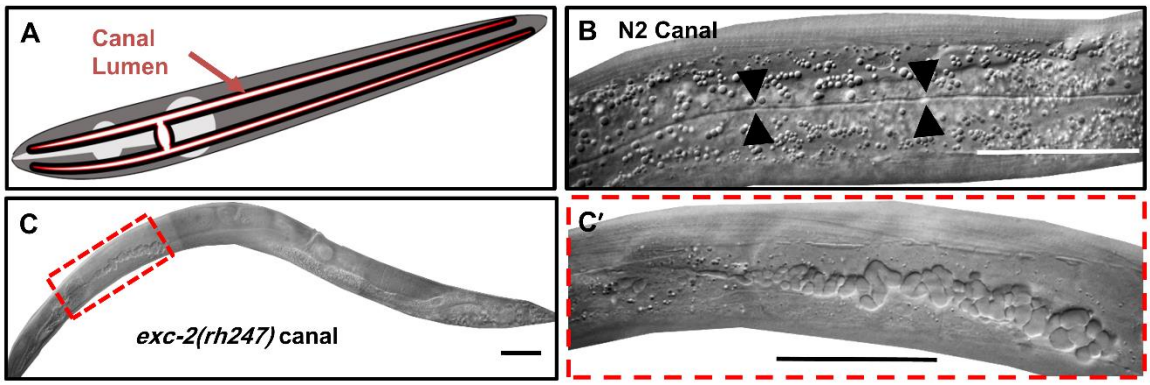


**Figure 2.1. *exc-2* mutant shows short and cystic canals.**

(A) Diagram showing the excretory canals in wild-type *C. elegans* with two tubes (red apical surface, black basolateral surface, lumen in white) extended over the entire length of the worm and connected at the canal cell body. Canals extend from cell body in both directions anteriorward and posteriorward. (B) DIC image of excretory canal of wild-type worm (N2); arrows indicate narrow canal lumen with uniform diameter. (C) DIC image of *exc-2*(*rh247*) mutant shows canal extending to only ~30% of the wild-type length. Area outlined in red is magnified in C' to show the fluid-filled cysts accumulated throughout entire canal. Scale bars, 50µm.

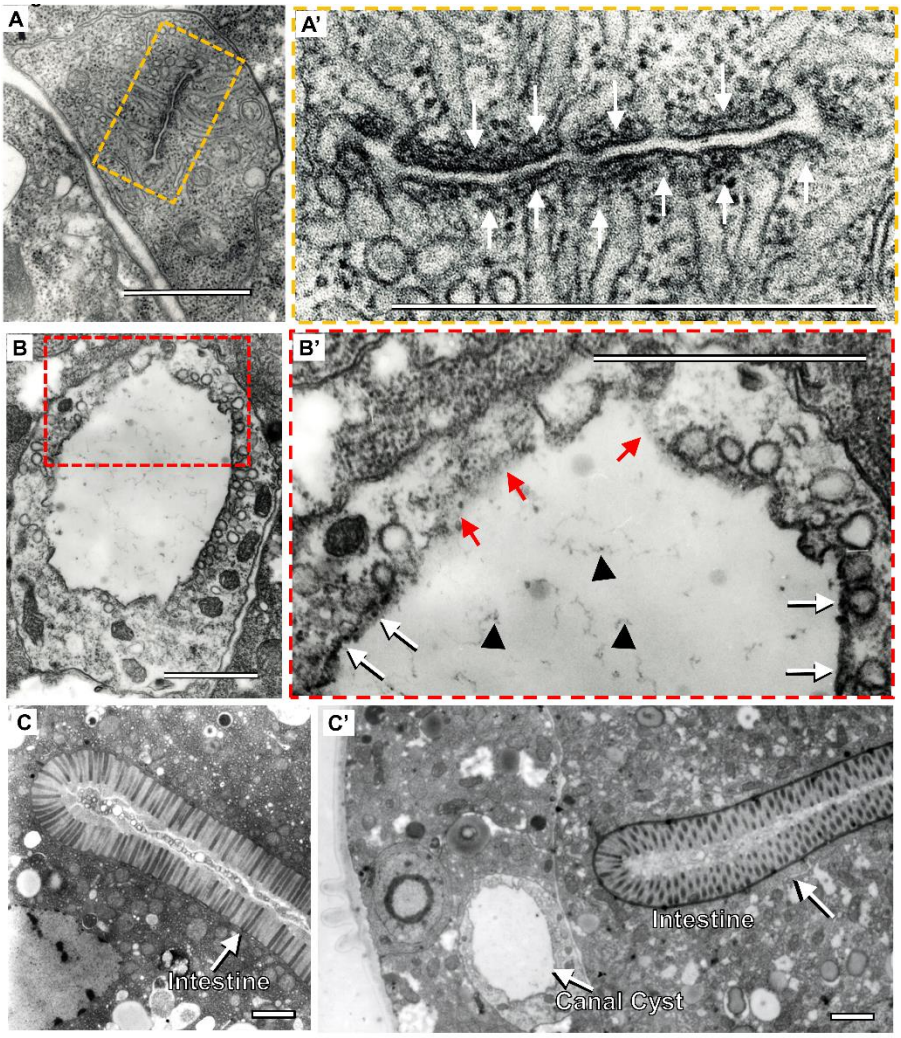


**Figure 2.2. Electron microscopy of *exc-2*(*rh209*) excretory canal and intestine.**

Cross-sectional electron-microscopic images of wild-type (N2) and mutant (*exc-2*(*rh209*)) tissues. (A) Wild-type canal; area outlined in yellow contains lumen (connected to myriad small canaliculi) and is magnified in A'. White arrows point to the dark actin-rich terminal web surrounding the lumen on all sides. (B) *exc-2* (*rh209*) canal; area outlined in red is magnified in B'. White arrows point to thick terminal web where present; red arrows point to regions of apical membrane lacking visible terminal web. Black arrowheads indicate presumed luminal scaffold material accumulating abnormally in the lumen of multiple *exc-2* mutant alleles, but not visible in lumen of wild-type canals or other *exc* mutants. (C) Lower-magnification image of intestine in (C) wild-type and (C') *exc-2* (*rh209*) shows intact intestine with normal arrangement of microvilli and normal basal membrane surrounded by intact terminal web surrounding entire apical surface. Mutant also shows cystic canal. Scale bars, 1µm.

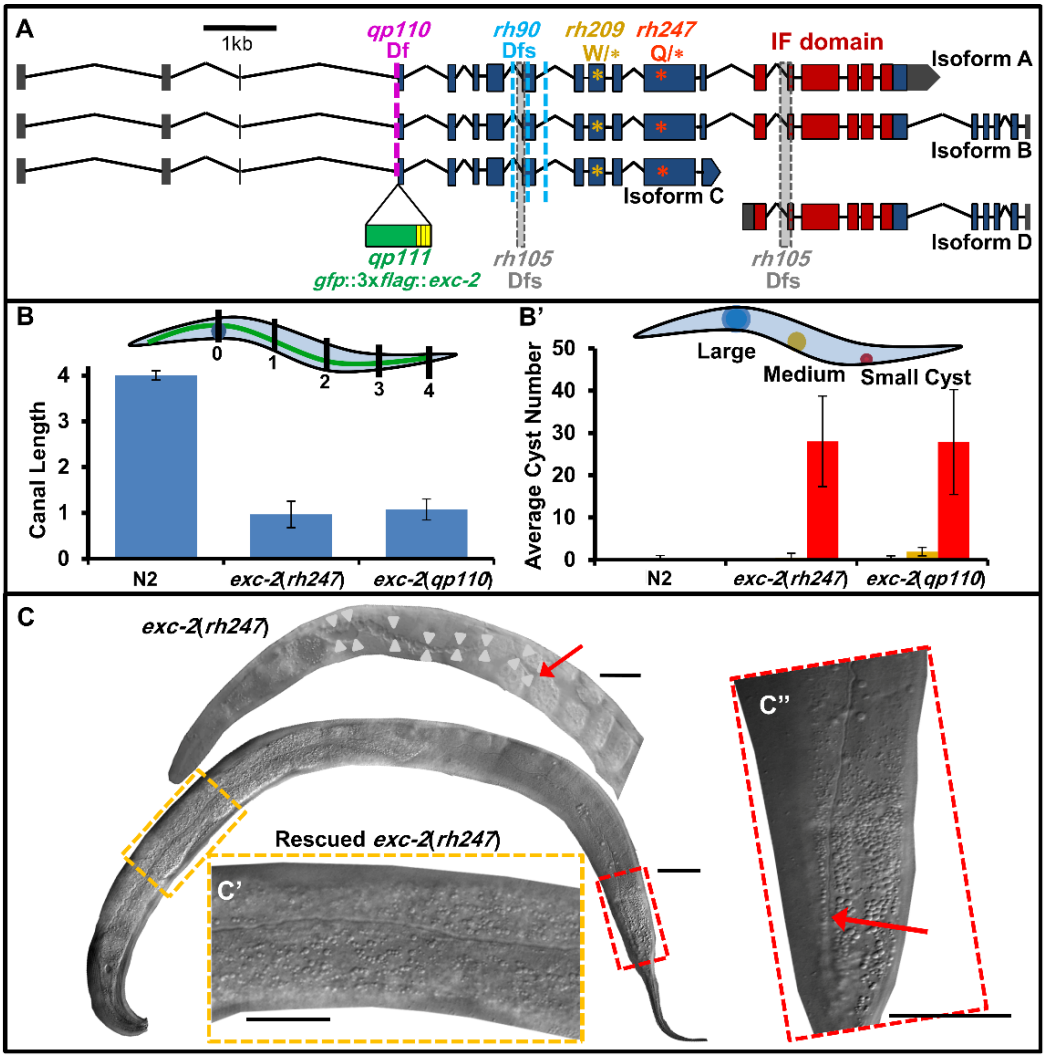


**Figure 2.3. *exc-2* encodes the intermediate filament protein IFC-2.**

(A) Structure of *exc-2* gene (from Wormbase, release WS262). Conserved region homologous to Intermediate Filament Domain is shown in dark red. Alleles *rh209* and *rh247* contain nonsense mutations in exon ten and twelve, respectively. Alleles *rh90* and *rh105* include deletions in multiple coding regions that cause frameshift mutations, while CRISPR/Cas9-generated allele *qp110* deletes part of the promoter and 2 bases of the start codon of Isoforms A, B, and C. CRISPR/Cas9-generated allele *qp111* inserts *gfp* linked to 3 copies of FLAG-tag sequence at the start codon of isoforms A, B, and C. Bar, 1kb. (B) *exc-2*(*qp110*) mutants (CRISPR/Cas9-generated deletion at the start codon) exhibit similar canal defects to those of other *exc-2* mutants, as measured by canal length (B) and cyst size (B'); n=50. (C) Phenotypic rescue of progeny animal of *exc-2*(*rh247*) animal injected with PCR-amplified *ifc-2* gene, including 2kb upstream and 500bp downstream at 15 ng/ml. 19% of animals were completely rescued, 15% were partially rescued by this concentration of injected gene (Table 2). C' and C'' show magnification of boxed areas. Red arrows indicate terminus of canal. Bars, 50 µm.

CRISPR/Cas9-induced deletion; this allele harbors a deletion in the 5' region of the gene, including the third exon of the 5'UTR along with part of first exon of the coding sequence of the gene (Fig. 2.3A). The *qp110* strain showed similar canal length and cyst number and size as for *exc-2*(*rh247*) (Fig. 2.3B and B'), and these two alleles failed to complement each other. To further confirm the identity of the *exc-2* gene, dsRNA targeting the twelfth exon of the *ifc-2* coding region was injected into wild-type worms. These worms exhibited canal defects equivalent to those in *exc-2* mutant animals (Fig. 2.4B and B'). As a control, injection of this dsRNA into *exc-2* animals did not noticeably exacerbate canal defects. Finally, a rescue assay was conducted via injection, either of the ~51kb fosmid WRM0630A_E08 containing the *ifc-2* gene (as well as *lpr-7*, *m6.11*, *pha-2*, *m6.4*, and a part of *rund-1*), or of the *ifc-2* gene and regulatory element (2kb upstream and 500bp downstream, total length 15.3kb) PCR-amplified from the WRM0630A_E08 fosmid, together with a GFP marker construct, into the gonad of *exc-2*(*rh247*) worms. Multiple concentrations were tested for injection (Table 2.2). Of the surviving progeny labeled in the canals, up to 16% showed complete rescue via fosmid injection at 12.5 ng/µl, with a full-length canal and complete absence of cysts (Fig. 2.3C). An additional 9% were partially rescued by fosmid, exhibiting canals shorter than wild-type, but much longer than those of *exc-2*(*rh247*) animals, with no cysts visible along the canal length. For the amplified gene at a concentration of 15 ng/µl, 19% were fully rescued plus 15% partially rescued. The relatively low rate of rescue was significantly higher than occurred through control injection of a different intermediate filament gene, *ifa-4*, 0% (Table 2.2). The *exc-2*(*qp110*) strain showed a similar low but significant rate of recovery (9%) when injected with the rescuing amplified *ifc-2* gene product

**Table 2.2. Rescue of Exc-2 phenotype by injection of *ifc-2* DNA.**

Phenotypes of progeny animals expressing GFP after injection into *exc-2*(*rh247*) or *exc-2*(*rh90*) hermaphrodites of the indicated constructs, as shown in Fig. 2.3A. Combined results for injection of Fosmid DNA at all concentrations attempted, and of PCR-amplified *ifc-2* DNA at all concentrations attempted, are also included. A Fisher's 3x2 test compared both lumen length and cyst size to canals of mutants of the appropriate genotype. Significant differences are underlined.

| | | | **CANAL LUMEN LENGTH** | | | **LUMEN WIDTH** | | ***p*-VALUE COMPARED TO *exc-2*** | |
|---|---|---|---|---|---|---|---|---|---|
| **GENOTYPE** | **INJECTED WITH** | **CONC. (ng/µl)** | **SHORT** | **MIDWAY** | **FULL-LENGTH** | **CYSTIC** | **NORMAL WIDTH** | **LUMEN LENGTH** | **LUMEN WIDTH** |
| *exc-2*(*rh247*) | - | - | 60 | 0 | 0 | 60 | 0 | - | - |
| Wild-type | - | - | 0 | 0 | 60 | 0 | 60 | $1.0x10^{-35}$ | $2.2x10^{-59}$ |
| *exc-2*(*rh247*) | Fosmid DNA | 10 | 49 | 16 | 6 | 49 | 22 | **$\underline{7.5x10^{-7}}$** | **$\underline{3.5x10^{-7}}$** |
| *exc-2*(*rh247*) | Fosmid | 12.5 | 33 | 4 | 7 | 33 | 11 | **$\underline{3.4x10^{-5}}$** | **$\underline{3.4x10^{-5}}$** |
| *exc-2*(*rh247*) | Fosmid | 25 | 25 | 0 | 1 | 25 | 1 | 0.30 | 0.30 |
| *exc-2*(*rh247*) | **Total Fosmid injections** | | **107** | **20** | **14** | **107** | **34** | **$\underline{1.8x10^{-5}}$** | **$\underline{2.0x10^{-6}}$** |
| *exc-2*(*rh247*) | PCR-amplified *ifc-2* | 5 | 9 | 1 | 0 | 9 | 1 | 0.14 | 0.14 |
| *exc-2*(*rh247*) | PCR'd *ifc-2* | 7.5 | 10 | 0 | 1 | 10 | 1 | 0.15 | 0.15 |
| *exc-2*(*rh247*) | PCR'd *ifc-2* | 10 | 7 | 0 | 2 | 7 | 2 | 0.015 | 0.015 |
| *exc-2*(*rh247*) | PCR'd *ifc-2* | 15 | 17 | 4 | 5 | 17 | 9 | **$\underline{6.8x10^{-6}}$** | **$\underline{6.8x10^{-6}}$** |
| *exc-2*(*rh247*) | PCR'd *ifc-2* | 25 | 51 | 3 | 1 | 51 | 4 | 0.049 | 0.049 |
| *exc-2*(*rh247*) | PCR'd *ifc-2* | 35 | 29 | 2 | 0 | 29 | 2 | 0.11 | 0.11 |
| *exc-2*(*rh247*) | **Total PCR'd *ifc-2*** | | **123** | **10** | **9** | **123** | **19** | **$\underline{7.5x10^{-3}}$** | **$\underline{1.1x10^{-3}}$** |
| *exc-2(qp110)* | | | 100 | 0 | 0 | 100 | 0 | | |
| *exc-2(qp110)* | PCR'd *ifc-2* | 15 | 91 | 6 | 3 | 91 | 9 | **$\underline{3.2x10^{-3}}$** | **$\underline{3.2x10^{-3}}$** |
| *exc-2(rh90)* | | | 60 | 0 | 0 | 60 | 0 | - | - |
| *exc-2(rh90)* | P*vha-1* ::*ifa-4* cDNA | 15 | 60 | 0 | 0 | 60 | 0 | 1.0 | 1.0 |
| *exc-2(rh90)* | *ifa-4* genomic (+ 5', 3' UTRs) | 40 | 60 | 0 | 0 | 60 | 0 | 1.0 | 1.0 |

(Table 2.2). The low but overall significant rescue rate for these injections is consistent with a dosage-dependent level of *exc-2* expression being necessary for wild-type canal formation. We conclude that the intermediate filament protein IFC-2 is encoded by the *exc-2* gene, and will refer here to the gene and protein by the prior name, EXC-2.

In order to identify the isoforms of EXC-2 that are responsible for the excretory canal phenotype, we directly injected dsRNA into wild-type worms (synthesized and transcribed *in vitro*) targeted to specific *exc-2* isoforms (Fig. 2.4A). The canals in progeny animals were then evaluated with regard to canal length, and cyst number and size (Fig. 2.4C and C'', Table 2.3). The first dsRNA (#1 in Fig. 2.4A) targeted the twelfth exon, which knocks down isoforms A, B, and C. These worms showed a canal phenotype similar to that of *exc-2*-null strains in both length and cyst size (Fig. 2.4B). dsRNA #2 targets the sixteenth exon to knock down isoforms A, B, and D, and this knockdown also resulted in a phenotype similar to that of *exc-2* mutants. As antibodies to Isoform D bind to the intestine [59], and long-term knockdown of Isoform D has been reported to affect intestinal structure [69], we also examined this organ in progeny animals, but saw no intestinal effects in progeny, even in animals exhibiting strongly cystic canals (Supp. Fig. 2.3). dsRNA #3 targeted the 3'UTR solely in isoform A, in exon nineteen. These worms showed a milder phenotype in which the canal length reached the vulva midway along the length of the animal, and displayed cysts, but smaller than those of *exc-2* knockout animals. dsRNA #4 targeted the coding sequence that is uniquely transcribed at the end of isoform C. This knockdown had no effect on canal length, and no cysts were formed. Finally, dsRNA #5 targeted the 5'UTR of isoform D. Canal length was as long as in wild-type animals, and no cysts were observed, and again, no intestinal effects were observed. To confirm the lack of effects of knockdown of isoforms C and D, we injected a mixture of dsRNA(s) targeting both isoforms.

These worms showed no deleterious effects on the canals. These results indicate that both isoforms A and B are needed for EXC-2 function in canal formation.

**Table 2.3. Effects of isoform-specific RNAi-knockdown of *exc-2*.**

Phenotypes of progeny animals expressing GFP after injection into hermaphrodites of the indicated dsRNAs, as shown in Fig. 4A. A Fisher's 3x2 test compared both lumen length and cyst size to canals of wild-type animals. Significant differences are underlined.

| | | CANAL LUMEN LENGTH | | | LUMEN CYST SIZE | | | *p*-VALUE COMPARED TO WILD-TYPE | |
|---|---|---|---|---|---|---|---|---|---|
| WILD TYPE INJECTED WITH RNAi# | ISOFORMS TARGETED | SHORT | MIDWAY | FULL-LENGTH | LARGE+ MEDIUM CYSTS | SMALL CYSTS | NO CYSTS | LUMEN LENGTH | CYST SIZE |
| **None (wild type)** | | 0 | 0 | 60 | 0 | 0 | 60 | - | - |
| **1** | A, B, D | 42 | 16 | 0 | 9 | 48 | 0 | **$4.2\times10^{-35}$** | **$8.5\times10^{-35}$** |
| **2** | A, B, C | 49 | 2 | 0 | 7 | 44 | 0 | **$7.3\times10^{-33}$** | **$7.3\times10^{-33}$** |
| **3** | A | 9 | 42 | 1 | 0 | 49 | 0 | **$2.07\times10^{-31}$** | **$3.5\times10^{-32}$** |
| 4 | C | 0 | 1 | 28 | 0 | 0 | 25 | 0.326 | 1.0 |
| 5 | D | 0 | 1 | 61 | 0 | 0 | 62 | 0.999 | 1.0 |
| 4 + 5 | C, D | 0 | 0 | 50 | 0 | 0 | 50 | 1.0 | 1.0 |
| **3 + 4 + 5** | A, C, D | 0 | 26 | 7 | 0 | 33 | 0 | **$5.4\times10^{-17}$** | **$6.2\times10^{-26}$** |

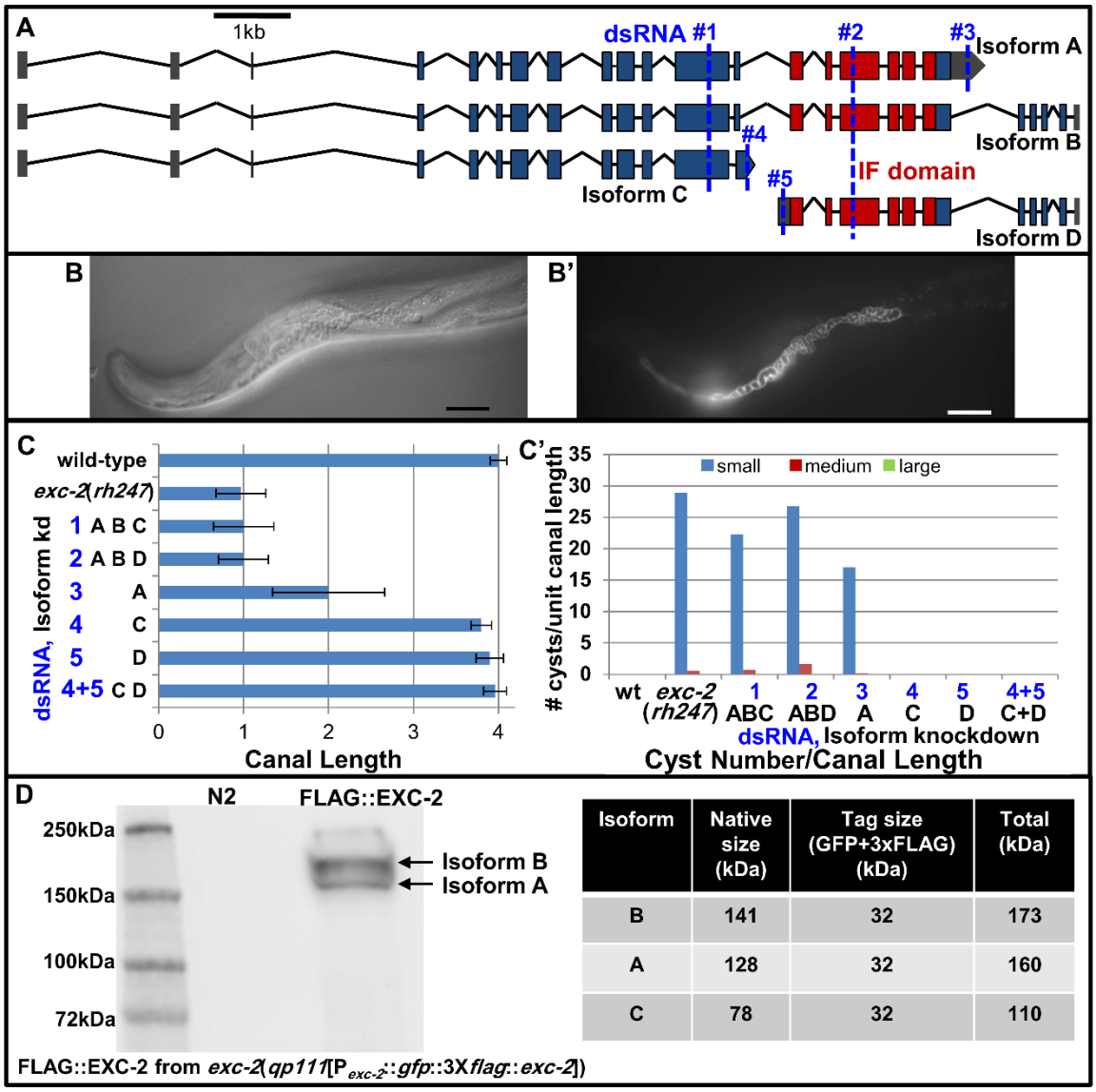


| Isoform | Native size (kDa) | Tag size (GFP+3xFLAG) (kDa) | Total (kDa) |
|---|---|---|---|
| B | 141 | 32 | 173 |
| A | 128 | 32 | 160 |
| C | 78 | 32 | 110 |

**Figure 2.4. EXC-2 Isoforms A and B maintain canal structure.**

(A) Schematic diagram of isoforms of *exc-2* (from Wormbase release 262) showing positions of RNAi-targeted regions (blue dashed lines). Bar, 1 kb. (B) DIC and (B') fluorescence images for progeny of injected worms with dsRNA #1 targeting the twelfth exon of *ifc-2*. Animals presented canals as short and cystic as those of *exc-2*(*rh247*) animals. (C) Measurements of canal length (C) and cyst number (C') in different isoform-specific RNAi knockdown animals. (n>50 each). (D) Protein expression of N-terminal FLAG-tagged EXC-2. Western blot shows two predominant bands corresponding to predicted sizes of isoforms A and B.

In order to validate the dsRNA data, we looked at total protein levels of isoforms A, B, and C in strain BK531 ("tagged *exc-2* strain") in which *exc-2* was modified via CRISPR/Cas9 to place *gfp* and three copies of a *flag* tag just upstream of the starting AUG codon of these three isoforms. The western blot (Fig. 2.4D) showed only two large isoforms in the worm lysate sample, corresponding to the size of isoforms A and B. It should be noted that the anti-FLAG antibody cannot detect isoform D; the result is still in agreement with the knockdown results, however. We conclude that both isoforms A and B are needed for EXC-2 function in the excretory canals.

Examination of strain BK531 (tagged *exc-2*) showed the expression pattern of the *exc-2* gene (Fig. 2.5). Labeled EXC-2 is located at the lumen of the excretory canal, in the corpus, posterior bulb, and pharyngeal-intestinal valve (PIV) of the pharynx, as well as in the uterine seam (UTSE) and intestinal-rectal valve (VIR). The subcellular location of EXC-2 in these tubes was compared to that of exogenously expressed cytosolic mCherry (Fig. 2.6). Labeled EXC-2 is located apical to canal cytoplasm (Fig. 2.6A-A''), as determined via cross-sectional fluorescence intensity measurements (Fig. 2.6A'''). This result was confirmed by evaluating the subcellular location of EXC-2 relative to a known apical membrane protein, ERM-1 [58]. The results demonstrate that EXC-2 and ERM-1 show overlapping expression at the canal apical (luminal) membrane (Fig. 2.6B-B''').

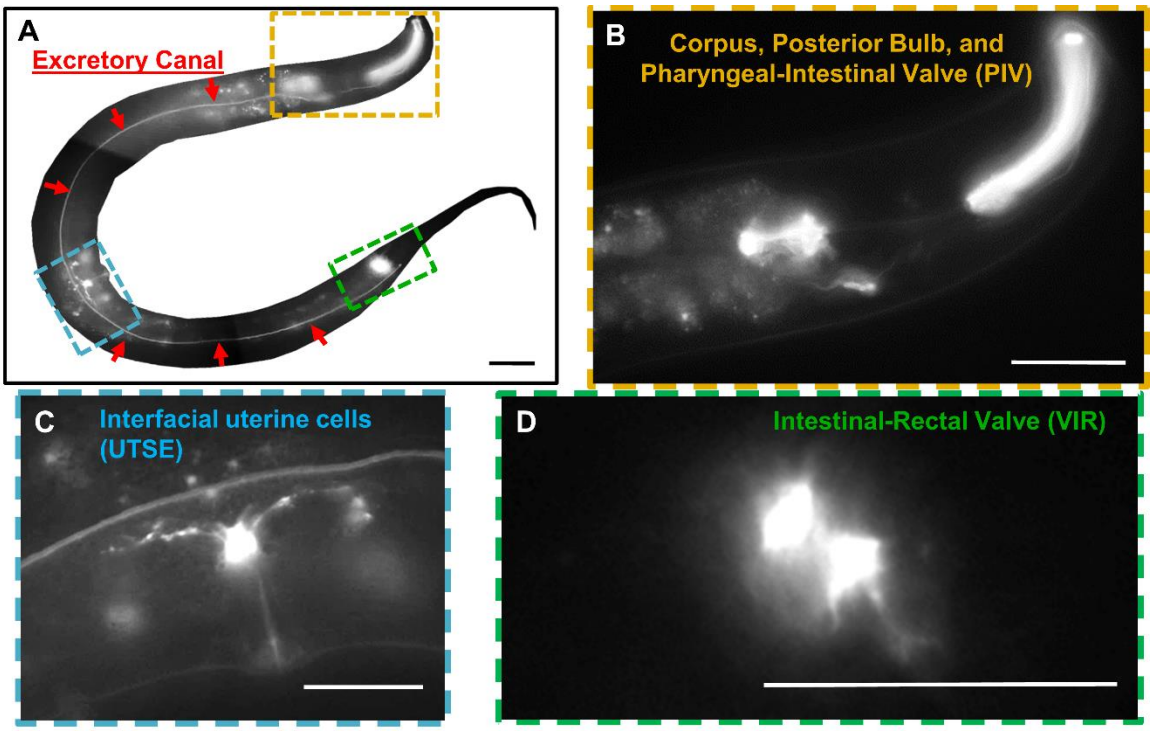


**Figure 2.5. EXC-2 is expressed in multiple epithelial cells.**

A) A CRISPR/Cas9 knock-in of *gfp* at the N-terminus of *exc-2* is expressed in four tissues: 1) The excretory canals (A,C); 2) The pharyngeal corpus, posterior bulb, and pharyngeal-intestinal valve (PIV) (B); 3) The interfacial uterine cell (UTSE) (C), and; 4) The intestinal-rectal valve (VIR) (D) Bar, 50µm.

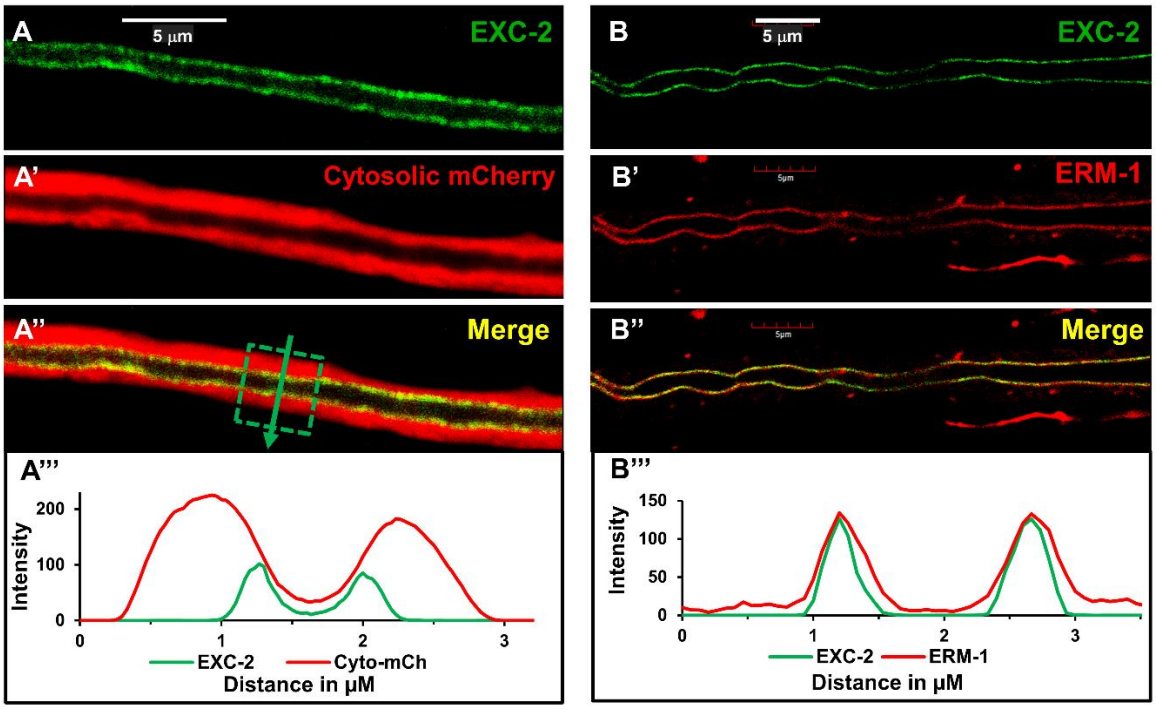


**Figure 2.6. EXC-2 is expressed at the apical membrane of the excretory canals.**

(A) Apical position of EXC-2 (GFP) relative to (A') canal cytosol labelled with mCherry; (A'') merged panel. (A''') Graph of fluorophore intensity for each color within canal section (box in A'') along length of arrow. (B) Coincident position of EXC-2 (GFP); with (B') apical epithelial marker ERM-1 labeled with mCherry; (B'') merged panel. (B'''') Graph of fluorophore intensity measurement within canal section boxed in B''. Bars, 5μm.

IFA-4 is the third intermediate filament gene that is highly enriched in the canal [61]. We investigated whether IFA-4 plays a role in canal maintenance similar to that of EXC-2 and IFB-1 [62]. The *ifa-4*(*ok1734*) strain from the CGC carries a deletion of the *ifa-4* coding sequence, and exhibits a canal phenotype similar to that of *exc-2* mutants (Fig. 2.7A-A''). Injection of dsRNA specific to *ifa-4* phenocopies the short cystic canals of the *ifa-4* deletion strain (Fig. 2.7B-B''). Strain BK532 ("tagged *ifa-4* strain") was created via CRISPR/Cas9 to tag *ifa-4* with *mKate2* and three *myc*-tags at the 5' end of the coding region (Fig. 2.7C). 40% of these animals exhibited wild-type morphology, while in 60% of these animals (which tended to have brighter expression) the canals were slightly shortened (to length ~3.5), but did not exhibit any cysts. IFA-4::mKate2 showed expression in several of the same locations as *exc-2*: the excretory canals, the pharyngeal-intestinal valve, and the intestinal-rectal valve. IFA-4 is additionally located in the spermathecal-uterine valve and cells in the vulva, including the uterine muscles and two neurons in the tail (Fig. 2.7C). The IFA-4 protein was also found in the gut of dauer-stage but not well-fed worms, and appeared as well in the tips of the rays and neurons of the male tail (Supp. Fig. 2.4). An overexpressing translational construct ($P_{vha\text{-}1}$*::ifa-4::gfp*) rescued the mutant canal phenotype of the *ifa-4*(*ok1734*) deletion mutant strain, and showed subcellular expression of this protein at the apical membrane of the canal, though with large inclusions protruding deeper into the cytosol (Fig. 2.8A-A'''). The 60% of BK532 (tagged *ifa-4*) animals that exhibited shortened canals also contained these subcellular inclusions. Finally, subcellular collocation of IFA-4 and EXC-2 at the canal apical membrane was confirmed in strain BK533 carrying CRISPR/Cas9-tagged insertions both of *gfp* into the 5' end of *exc-2* and of *mKate2* into the 5' end of *ifa-4* (Fig. 2.8B-B''').

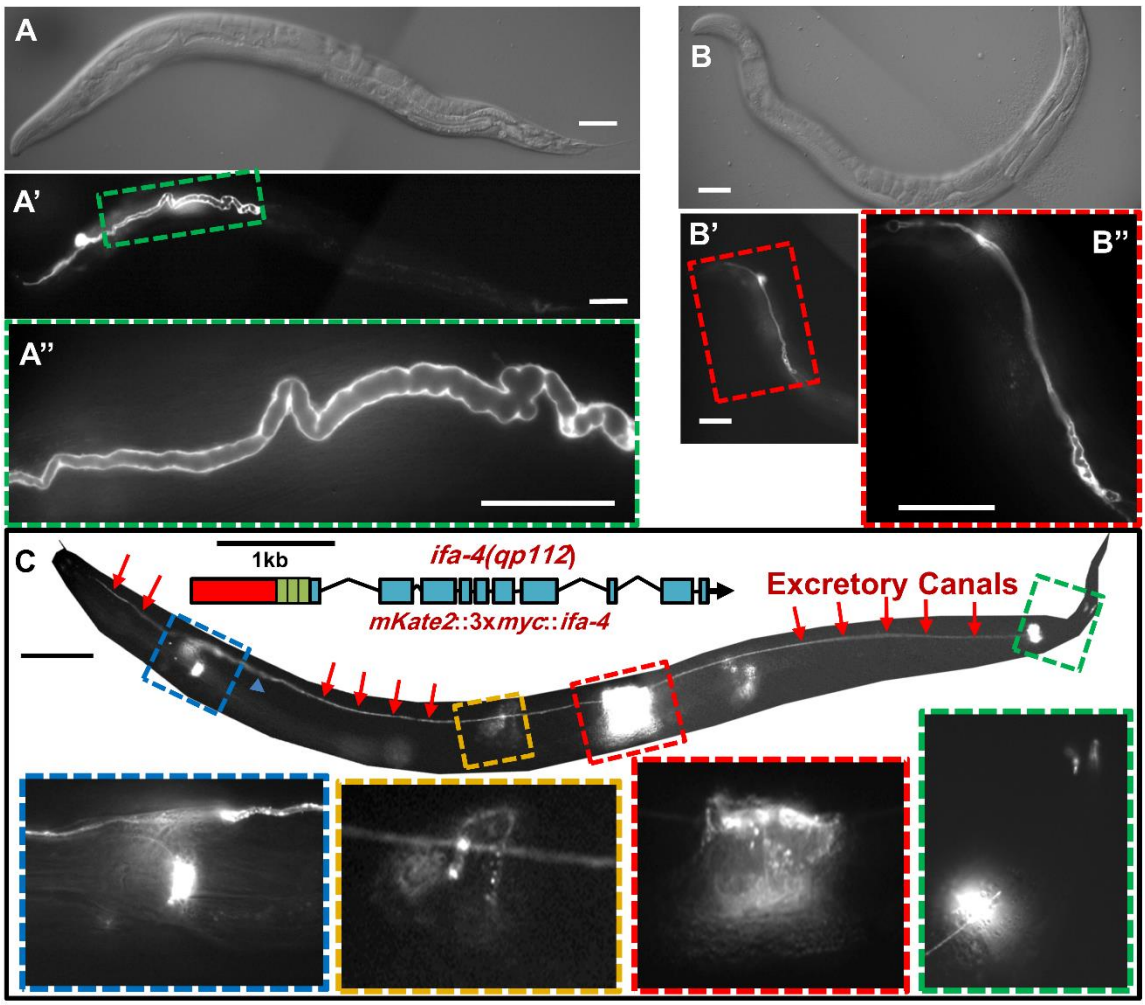


**Figure 2.7. IFA-4 effects canal maintenance.**

(A) DIC and (A', A'') fluorescence micrographs of excretory canal of strain BK535 (*ifa-4* ko; canal marker). Boxed area of (A') magnified in (A''). (B) DIC and (B') fluorescence micrographs for progeny of animal injected with dsRNA targeting the seventh exon of *ifa-4*. Animals exhibited short, cystic canals. Boxed area of (B') magnified in (B''). (C) Diagram of CRISPR/Cas9 knock-in of *mKate2* at the N-terminus of *ifa-4*. *ifa-4* is expressed in five tissues: 1) The excretory canals (red arrows); 2) Pharyngeal-intestinal valve (PIV) (blue box); 3) The spermathecal-uterine valve (yellow box); 4) Uterine muscles (red box), and; 4) The intestinal-rectal valve and neurons at the tip of the tail (green box). Boxed areas are below main image, outlined in boxes of the corresponding color. All bars, 50µm.

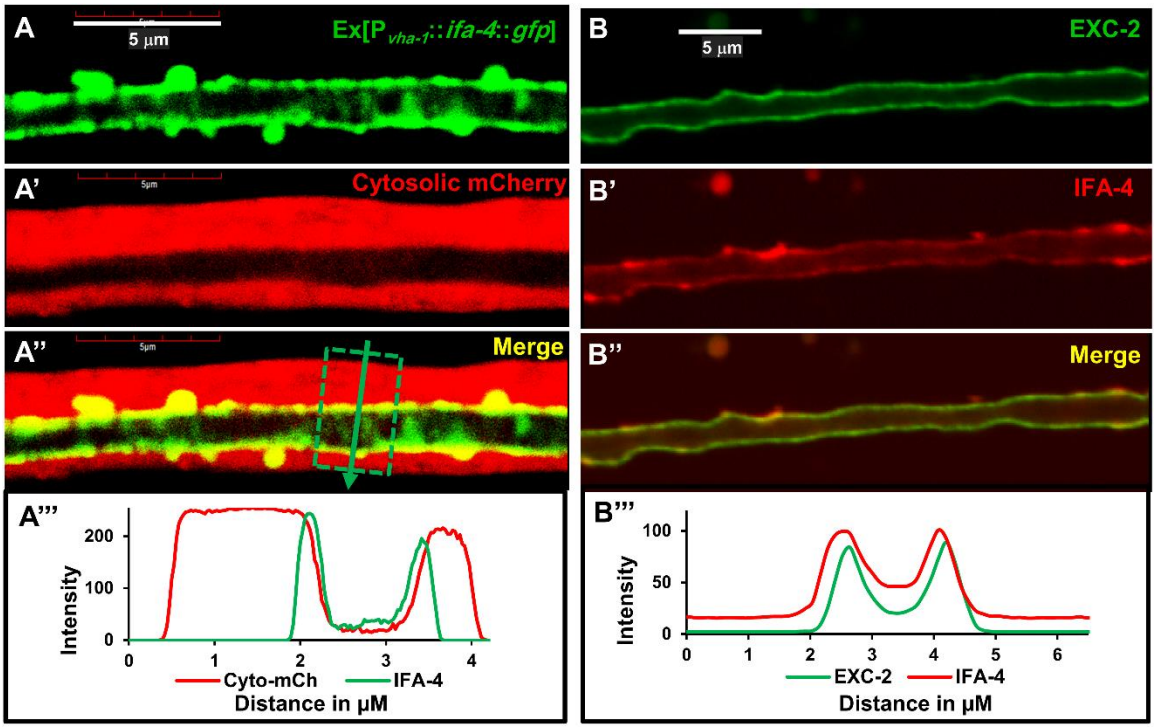


**Figure 2.8. IFA-4 is co-localized with EXC-2 to the apical membrane.**

(A). Fluorescence micrographs of injected (40ng/µl) translational construct ($P_{vha\text{-}1}$::*ifa-4*::*gfp*) ectopically expressed in *ifa-4*(*ok1734*) deletion mutant, which fully rescued canal morphology. (A') Cytosolic mCherry marker co-expressed in the canal; (A'') Merged image. (A''') Graph of fluorophore intensity for each color within canal section (box in A'') along length of arrow. (B) Fluorescence micrographs of CRISPR/Cas9-modified strains labelling *exc-2* and *ifa-4*. (B) shows GFP::EXC-2 expression, (B') mKate2::IFA-4 expression, (B'') merged image. (B''') Graph of fluorophore intensity for each color within canal section. Bars, 5µm.

Several *exc* genes (*exc-1*, *exc-5*, *exc-9*) with knockout canal phenotypes of large cysts also exhibit characteristic overexpression phenotypes that rescue the canal lumen diameter, while shortening canal length, and show epistatic genetic interactions [1, 35, 36]. We therefore looked at overexpression phenotypes of *exc-2* and *ifa-4*. PCR-amplified *exc-2* that rescued *exc-2* mutants (Fig. 2.3C) was injected (together with a fluorescent canal marker) into N2 wild-type worms (Fig. 2.9A). All progeny showing the injection marker also exhibited substantially shortened canals extending only to the vulva (average canal length of 2.1 (n=14)), but with small or no cysts. We created a similar construct of PCR-amplified *ifa-4* cDNA, linked to *gfp*, under the control of a strong canal-specific promoter. After injection into wild-type worms, progeny expressing GFP (Fig. 2.9A'). showed shortened canals, extending just beyond the vulva (length 2.5, n=30). The similarity of overexpression phenotype between the two intermediate filament genes is consistent with these proteins performing similar functions.

A co-immunoprecipitation assay was conducted to test whether EXC-2 and IFA-4 bind each other directly (Fig. 2.9B and B'). Protein lysates were prepared from three worm strains: Wild-type (N2); BK532 (tagged *ifa-4*), and BK533 (tagged *exc-2* & *ifa-4*). Tagged IFA-4 could be detected in blots of whole-worm lysates (Fig. 2.9B), but was only detectable in αFLAG pulldowns when tagged EXC-2 was present (Fig. 2.9B'), which indicates that the two proteins bind to each other.

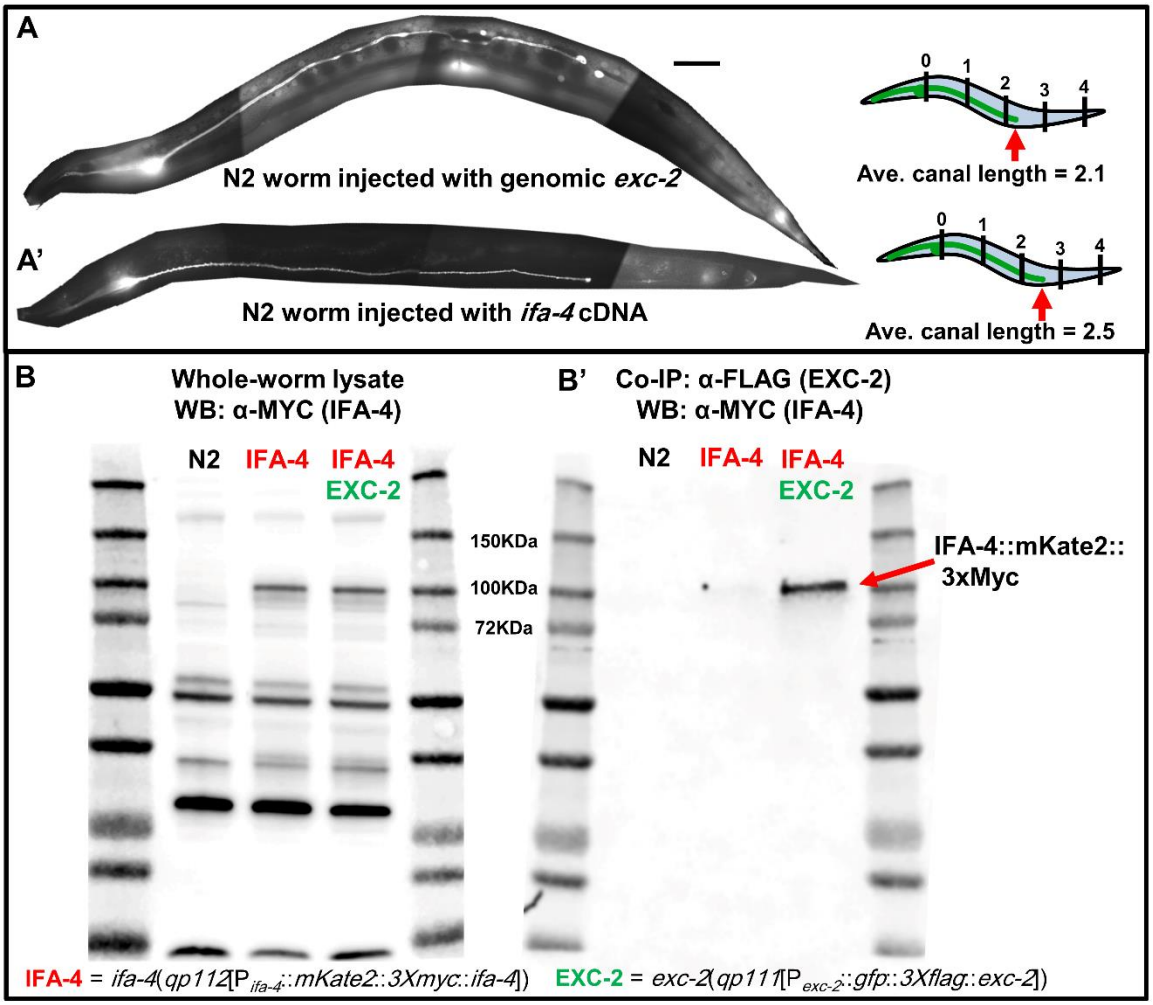


**Figure 2.9. EXC-2 and IFA-4 interact directly.**

A) Representative N2 worms injected with (A) *exc-2* genomic construct (including 2kb upstream and 500bp downstream of coding region) or (B) *ifa-4* cDNA construct under control of strong canal promoter *vha-1* to overexpress these proteins. Both lines exhibited shortened canal lumen of wild-type diameter with no cysts. For *exc-2* overexpression, length=2.1 (n=14); for *ifa-4* overexpression, length=2.5 (n=30). Bars, 50µm. B) Western blot of whole-worm lysates probed with antibody to MYC. (B') Western blot of lysates purified via anti-FLAG magnetic beads, which bind to FLAG-tagged EXC-2. Lysates are from wild-type animals (N2, left), animals expressing Myc-tagged IFA-4 (middle), and animals expressing both Myc-tagged IFA-4 and FLAG-tagged EXC-2 (right); lanes on blots are flanked by size marker lanes. Red arrow in blot on right indicates size of IFA-4 band at ~100kDa.

The interaction of EXC-2 with IFA-4 led us to investigate whether the apical localization of EXC-2 in the canals depends on the function of the other two intermediate filaments. Strain RB1483, carrying the *ifa-4*(*ok1734*) deletion, was crossed to strain BK531 (tagged *exc-2*) (Fig. 2.10A-A’’’’), then injected with a cytosolic mCherry marker construct. The subcellular location of EXC-2 at the apical membrane of the canal was unchanged in these *ifa-4* knockout mutants.

The apical location of EXC-2 was similarly tested in the absence of IFB-1. Due to embryonic lethality of *ifb-1* null mutants (due to hypodermal defects [62]), a construct expressing dsRNA to *ifb-1* under a canal-specific promoter was injected together with cytosolic mCherry marker construct into strain BK531 (tagged *exc-2*) (Fig. 2.10B-B’’’’). These animals exhibited cystic canals consistent with knockout of IFB-1, and EXC-2 retained its apical location in the presence of this *ifb-1* knockdown. Finally, we investigated whether the apical location of EXC-2 depends on the presence of either one of the other intermediate filaments, IFA-4 or IFB-1 (Fig. 2.10C-C’’’’). Injection of the same canal-specific dsRNA construct against *ifb-1* along with cytosolic mCherry marker construct into the *ifa-4*(*ok1734*) mutant strain and crossed to BK531 (tagged *exc-2*) resulted in the same location for EXC-2. The double knockout was sickly, with lethality higher than for either *ifb-1* knockdown or *ifa-4* mutation alone (n=97, Supp. Fig. 2.5), consistent with an additive function of IFA-4 and IFB-1. Death in these animals occurred throughout mid-larval stages, much later than the two-fold embryonic muscle failure and death of *ifb-1* null mutants [62], which suggests a general inability of canals to function effectively in the combined abseence of these two intermediate filament proteins. [22, 45].

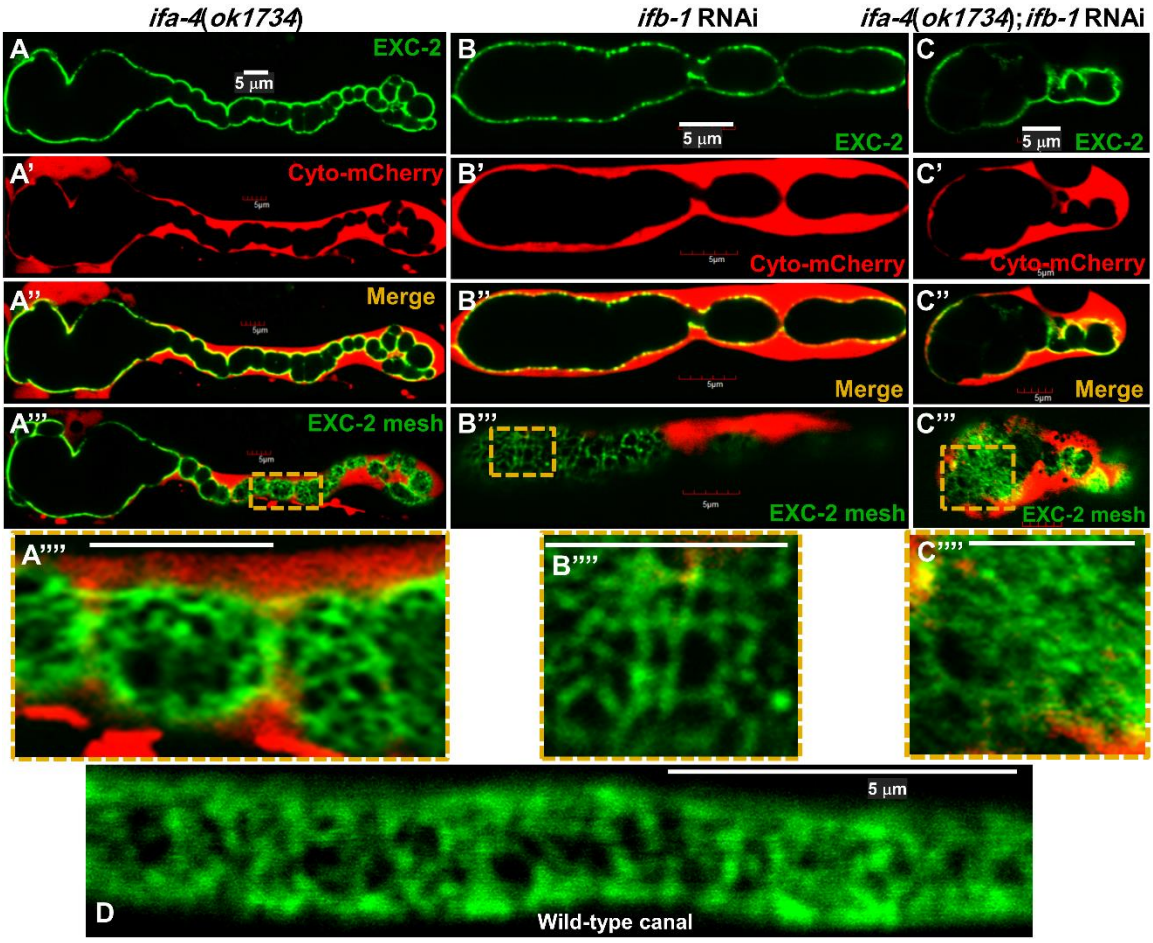


**Figure 2.10. EXC-2 apical location is independent of IFB-1 and IFA-4 function.**

Fluorescence micrographs of GFP-tagged EXC-2 in: (A) *ifa-4* knockout strain (*ok1734*); (B) animal exhibiting canal-specific RNAi-knockdown of *ifb-1*; (C) RNAi-knockdown of *ifb-1* in *ifa-4* knockdown strain. All animals express cytosolic mCherry marker. (A,B,C) GFP::EXC-2 fluorescence; (A',B',C') Cytosolic mCherry fluorescence; (A'',B'',C'') Merged images. (A''', B''', C''') Plane of focus higher in Z-plane, to observe merged fluorescence of GFP::EXC-2at apical surface of swollen cystic areas of canals flattened against hypoderm.. Boxed areas are magnified in panels A'''', B'''', and C''''. (D) Fluorescence of GFP::EXC-2 at the narrower surface next to hypoderm in wild-type canals. All bars, 5µm.

Finally, the subcellular expression pattern of EXC-2 formed a mesh-like network on the apical surface of the canals, both in wild-type canals (Fig. 2.10D) and in animals lacking IFA-4, IFB-1, or both (Figs. 2.10A’’’’, B’’’’, and C’’’’). This meshwork is more easily observed on cysts, where a larger surface area is in the focal plane, than in the narrow canals of wild-type animals, but the size and general arrangement of filaments appears similar in all cases, which indicates that EXC-2 filaments can be localized to the apical membrane even without the function of the other two canal intermediate filament proteins.

## 2.5 DISCUSSION

### 2.5.1 *exc-2* encodes for the intermediate filament IFC-2

This study has used multiple methods to confirm the identity of the *exc-2* gene: 1) Whole-genome sequencing of four alleles; 2) Injection of dsRNA to knock down multiple isoforms of the gene; 3) Rescue of a null allele by both fosmid and PCR-amplified DNA; 4) CRISPR/Cas9-mediated tagging of the *exc-2* gene showing the tissue and subcellular location of the encoded protein at the apical surface of the tissue affected by mutation; 5) Generating a new allele of the gene, via CRISPR/Cas9-induced deletion, which caused the same phenotype; 6) Noncomplementation between the CRISPR-induced deletion allele and a previous allele, and; 7) Pulldown of the expressed tagged EXC-2 protein to another intermediate filament that is expressed at the same location in the excretory canals, and has the same genetic effects on the excretory canals.

This cloning result is surprising, since it contradicts multiple previous studies that found IFC-2 not in the excretory canals, but primarily in desmosomes of the *C. elegans* intestine [51, 53, 69-72], though expression of one fluorescent construct showed expression at the intestinal apical surface [70]. These previous studies assumed Isoform D to be the full-length IFC-2, since this isoform is about the same size as other *C. elegans* intermediate filament proteins, and some confusion of RNA-sequencing results presented on earlier versions of Wormbase (e.g. Wormbase.org, release WS180) listed up to eight splice forms and suggested the possibility that the first 13 exons (i.e. Isoform C) comprised a separate gene. More extensive RNA sequencing since that time (summarized on current Wormbase release WS262) shows that although Isoform C and Isoform D do not overlap, both are transcripts from different parts of the same gene, and

that the large Isoform A in fact comprises the entire 24 exons of the gene. Western blot of FLAG-labelled EXC-2 protein in the present study (Fig. 2.4D) matches the current predicted protein sizes on Wormbase. We also note that the pioneering comprehensive study of *C. elegans* intermediate filament genes [60] reported eight intermediate filament genes, including *ifc-2*, and presents a Northern blot ([60], Fig. 2.4) showing two much larger transcripts that correspond in size to the Isoform A and B mRNAs. Subsequent work on IFC-2 from the Weber, Leube, and Karabinos labs [59, 69, 72, 73] created and used a polyclonal antibody to a fragment of the conserved intermediate filament domain of IFC-2; this antibody bound a single ~55kDa protein on blots [73], and further studies showed this antibody binding specifically to proteins in the intestine [71], as long-term treatment with RNAi to *ifc-2* removed intestinal staining but not staining of other tissues. Our CRISPR-tagged GFP was inserted at the first codon of Isoforms A, B, and C, and so cannot show expression of isoform D. It is therefore possible that Isoform D is expressed in the intestine, while the other isoforms are expressed in the excretory canals and other tissues shown here. Since Isoforms A, B, and D all include the conserved intermediate filament domain, however, we cannot explain why previous studies did not find expression within the excretory canals.

Previous studies ([69, 73] found that in worms fed RNAi specific to the intermediate filament domain over the course of three generations, the animal intestines slowly acquired gross morphological effects, although they saw that at the ultrastructural level, the microvilli and terminal web appeared intact. We directly microinjected dsRNAs specific to multiple isoforms into the gonad, and found that in all cases, progeny intestines were unaffected, while the excretory canals uniformly were strongly cystic, matching the phenotype of all five of our *exc-2* mutant alleles. In particular, this result obtained for dsRNA #2 (Fig. 2.4A), a knockdown of the

conserved intermediate filament domain of Isoforms A, B, and D. Finally, the *rh105* allele has deletions in the conserved domain of these three isoforms (Fig. 2.3A), and exhibits large canal cysts with no intestinal defects (Supp. Fig. 2.1). In summary, our results strongly suggest that, while Isoform D may be expressed in the intestine, the major locus of function of the EXC-2/IFC-2 intermediate filament isoforms is in the excretory canals.

### 2.5.2 EXC-2, IFB-1, and IFA-4 maintain tubular morphology at the apical membrane

At 12.7kb, the *exc-2* gene is easily the largest IF gene in *C. elegans*, which helps explain the relatively high frequency of alleles of this gene identified in genetic screens for cystic canal mutants [22]. The two large Isoforms A and B of this protein had clear effects within the canals as seen by mutations at multiple sites and effects of dsRNA to all areas of the gene. No effects were noticed from knockdown solely of Isoform C or Isoform D.

A map of gene expression for specific tissues of *C. elegans* [61] examined expression in the excretory canal cell, and in addition to *exc-2*, found two other highly expressed intermediate filament genes, *ifb-1* and *ifa-4*, confirming earlier studies of intermediate filament expression [73]. Knockdown of *ifb-1* has previously been found to cause formation of cysts in the canal, as well as surprising breaks in canal cytoplasm during cell outgrowth [24, 62, 73]. The present study shows that IFA-4 also is necessary to maintain canal morphology. Intermediate filaments form homo- and hetero-polymers to carry out their functions [74]. While IFA-4, IFB-1, and EXC-2 are all expressed at the apical (luminal) surface of the excretory canals, they each have varied expression (and presumably function) in other tissues, both overlapping and non-overlapping. IFB-1, in particular, has an essential role in embryonic muscle attachment and hypodermal cell elongation [62], tissues where IFA-4 and EXC-2 are not expressed. Future

studies of these tissues may find other functions for these intermediate filament proteins. For example, as stretching of dissected intestines can be measured [75], it may be possible to determine the role of IFA-4 in intestinal integrity during dauer formation, as compared to intestines in other stages where IFA-4 is not expressed.

Ultrastructural analysis of *exc-2* mutants found visible fibrous material in the lumen (Fig. 2.2B'), which has also been seen only in other excretory system mutants affecting apical cytoskeleton proteins: *sma-1* (encoding $\beta_H$spectrin), *erm-1* (ezrin-moesin-radixin homologue), and the excretory duct cell gene *let-653* (mucin) [22, 25, 39, 48]. Future studies may show whether the fibrous material represents proteins or other material normally anchored to the membrane directly or indirectly by these cytoskeletal proteins.

### 2.5.3 Three intermediate filament proteins support the canal apical membrane.

The three intermediate-filament proteins EXC-2, IFA-4, and IFB-1 are collocated at the apical membrane of the canal, have similar knockdown effects, and bind to each other in pulldown assays (Fig. 2.9B) and [73]). The ratio between these proteins affects their function, as overexpression of either IFC-2 or IFA-4 allows formation of small cysts in short canals (Fig. 2.9A and A').

EXC-2 forms homo- and heterodimers in *in vitro* studies [76], which may be necessary in order to form a strong meshwork at the canal apical surface, as seen for lamins and other intermediate filament proteins at cell membranes. Lamin, for example, is bound directly to the membrane to form such structures at the inner nuclear membrane [77-79], through farnesylation of the CAAX domain at the lamin C-terminus [78, 80]. EXC-2, IFA-4, and IFB-1 do not have a

CAAX domain, so do not appear to be bound to the apical canal membrane through the same mechanism as lamin. Other intermediate filament proteins such as keratin and vimentin form such meshworks linked to mammalian cell cytoplasm through a scaffolding protein, Plastin1 [81, 82] Though *C. elegans* does not have an obvious plastin homologue, it will be interesting to see if a protein yet to be identified serves a similar purpose to link EXC-2 to the canal apical surface. Since EXC-2 retains its location in the canal and meshwork appearance when *ifa-4* and *ifb-1* are mutated and knocked down, respectively (Fig. 2.10), EXC-2 appears to be located to the apical membrane independently of these other two IF proteins. All three proteins are necessary to prevent cyst formation, and overexpression of *ifa-4* does not rescue *exc-2* mutation; these results suggest that the three filament proteins provide complementary functions to regulate tubule diameter and length.

We present a working model of these three proteins at the surface of the excretory canal in Fig. 2.11. The three intermediate-filament proteins EXC-2, IFA-4, and IFB-1 are collocated at the apical surface of the canal. We do not know if they are linked as obligate heterodimers; as EXC-2 binds to IFA-4 in our pulldown assay, this heterodimer presumably makes up some of the filaments. But EXC-2 is properly placed even without IFA-4 function, so EXC-2 dimers, either homodimers of one isoform or heterodimers of two isoforms, are likely part of the makeup of the filaments in wild-type animals.

The actin cytoskeleton forms a thick terminal web around the canal lumen visible in electron micrographs, and much thicker than the narrow band of intermediate filaments visible in the fluorescently tagged confocal micrographs here. The terminal web is tethered to the luminal membrane through the action of the SMA-1 $\beta_H$spectrin [22, 37, 38] and the ezrin-radixin-moesin homologue ERM-1 [25]; we do not know if actin is closer to the membrane than are the

intermediate filament proteins, but actin certainly lies outside of the layer intermediate filaments. Future studies on the *in vivo* interactions between these intermediate filament isoforms and proteins, and between these intermediate filaments and the actin cytoskeleton, should provide further insights into the ability of this network of proteins to provide the rigidity to maintain a firm luminal diameter while maintaining the flexibility to allow these narrow tubes to lengthen and bend during growth and movement.

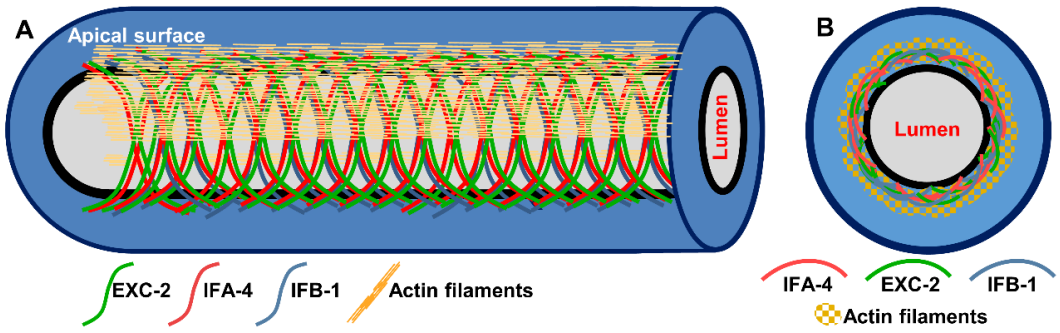


**Figure 2.11. Proposed model of EXC-2, IFA-4, and IFB-1 in excretory canals.**

(A) Lateral section of the excretory canal, where intermediate filaments (green, red, blue) surround the apical membrane (black). Actin filaments make up the thick terminal web extending from the apical membrane and extending into the cytoplasm of the canals. Actin filaments are cut away in bottom half of drawing to show intermediate filaments more clearly. (B) Cross-section of the canal shows intermediate filaments forming a meshwork that surrounds the lumen surrounded by actin filaments.

## 2.6 Supporting Data

### Supplemental Table 2.1.

Primers sequences used to synthesize dsRNA specific for *exc-2* isoforms. T7 promoters are underlined.

| Primer | Sequence ( 5'-to-3') |
|---|---|
| *exc-2* isoforms A, B, C (Fwd) | **TAATACGACTCACTATAGGG**accacatcgagttgagcctacaag |
| *exc-2* isoforms A, B, C (Rev) | **TAATACGACTCACTATAGGG**ctctcaggcggttgtgatctgtc |
| *exc-2* isoforms A, B, D (Fwd) | **TAATACGACTCACTATAGGG**tcaacgccgtcaaagctcatc |
| *exc-2* isoforms A, B, D (Rev) | **TAATACGACTCACTATAGGG**cataatcggcacggatgtcacg |
| *exc-2* isoform A (Fwd) | **TAATACGACTCACTATAGGG**cttcacaacttgttgccgttcc |
| *exc-2* isoform A (Rev) | **TAATACGACTCACTATAGGG**catgcgcagcatcttgattagc |
| *exc-2* isoform C (Fwd) | **TAATACGACTCACTATAGGG**acctgaactttgcgggac |
| *exc-2* isoform C (Rev) | **TAATACGACTCACTATAGGG**ctaagtacaaagaaagtagtgtataaaatgaactg |
| *exc-2* isoform D (Fwd) | **TAATACGACTCACTATAGGG**agaagtagtataggccgcgtaag |
| *exc-2* isoform D (Rev) | **TAATACGACTCACTATAGGG**cataggtggagtcgcaagg |

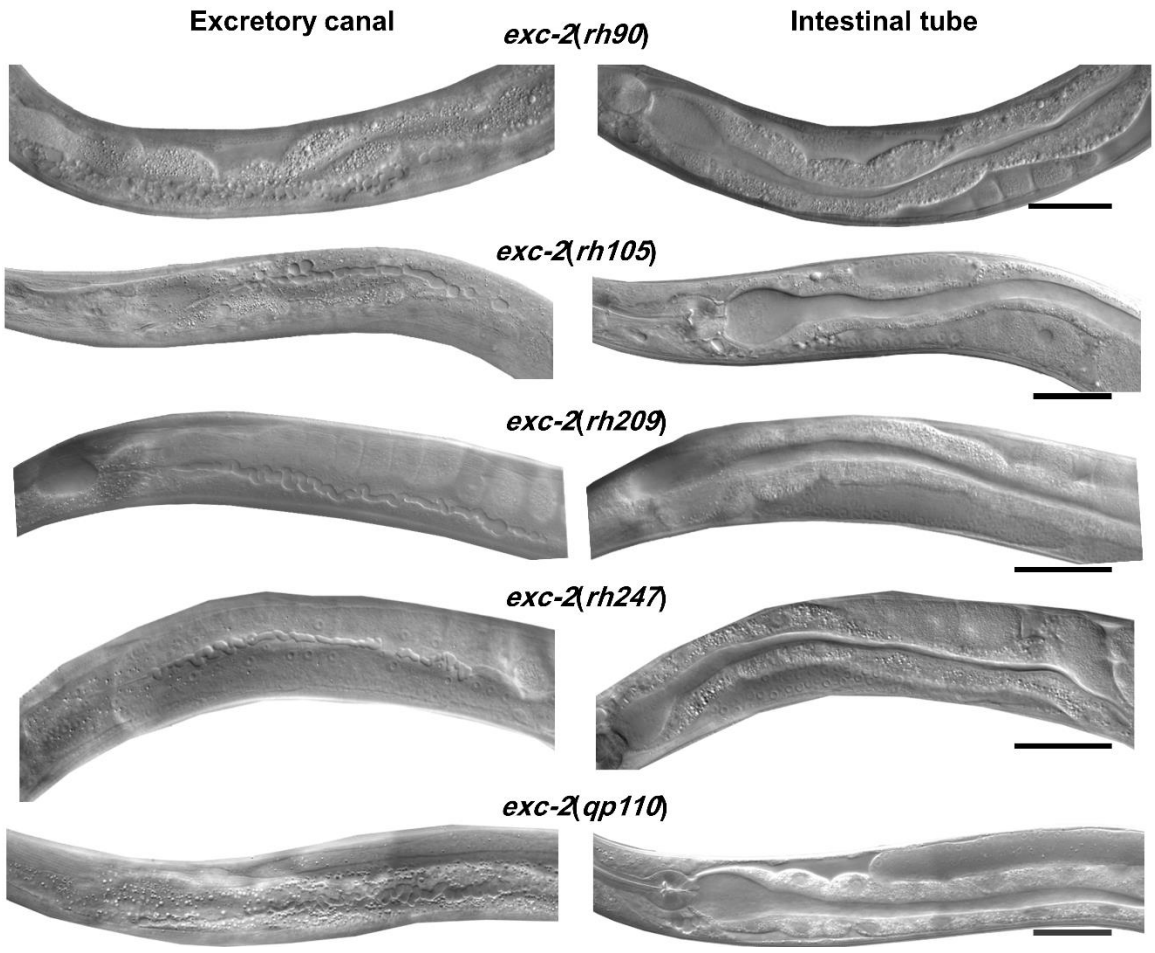


**Supplemental Figure 2.1. Phenotype of all *exc-2* alleles.**

DIC images of excretory canals (left) and intestine (right) in all four EMS-derived mutant strains, and in strain BK530 [CRISPR/Cas9-induced *exc-2* deletion]. All animals showed characteristically strong cystic defects comparable to those in other *exc-2* alleles in 100% of canals examined. No defects were seen in intestinal diameter. Top to bottom: *exc-2*(*rh90*), *exc-2*(*rh105*), *exc-2*(*rh209*), *exc-2*(*rh247*), and *exc-2*(*qp110*) CRISPR/Cas9-induced deletion strain.

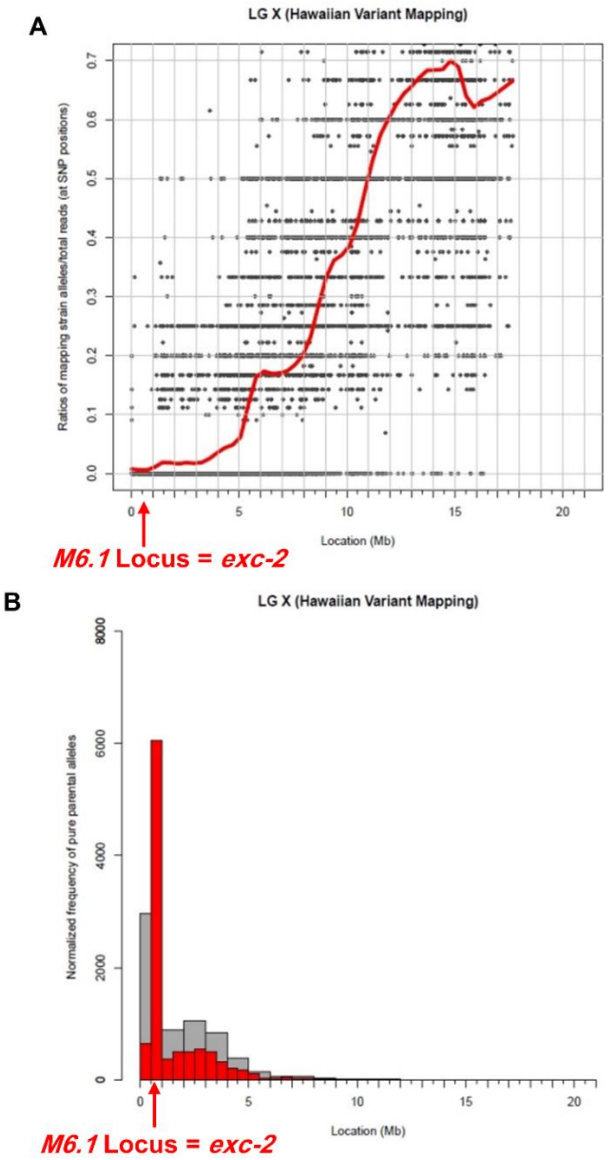


**Supplemental Figure 2.2.** Cloudmapping data output of *exc-2* whole-genome sequencing.

(A) Ratio of mapping-strain reads of CB4856 (Hawaiian wild-type) SNPs to total SNPs in populations of F2 progeny selected for homozygous Exc phenotype. CB4856 was crossed to *exc-2* mutant animals (in Bristol background) and F1 progeny allowed to self-cross. Upon selection for Exc animals, the locus of the *exc-2* mutation is located where the ratio of CB4856 to N2 reads equals zero (i.e. 100% SNP composition of the Bristol background of *exc-2*).

(B) Data from panel A normalized via LOESS regression. The highest peak shows where pure parental (*exc-2*) SNP is located along the X-chromosome.

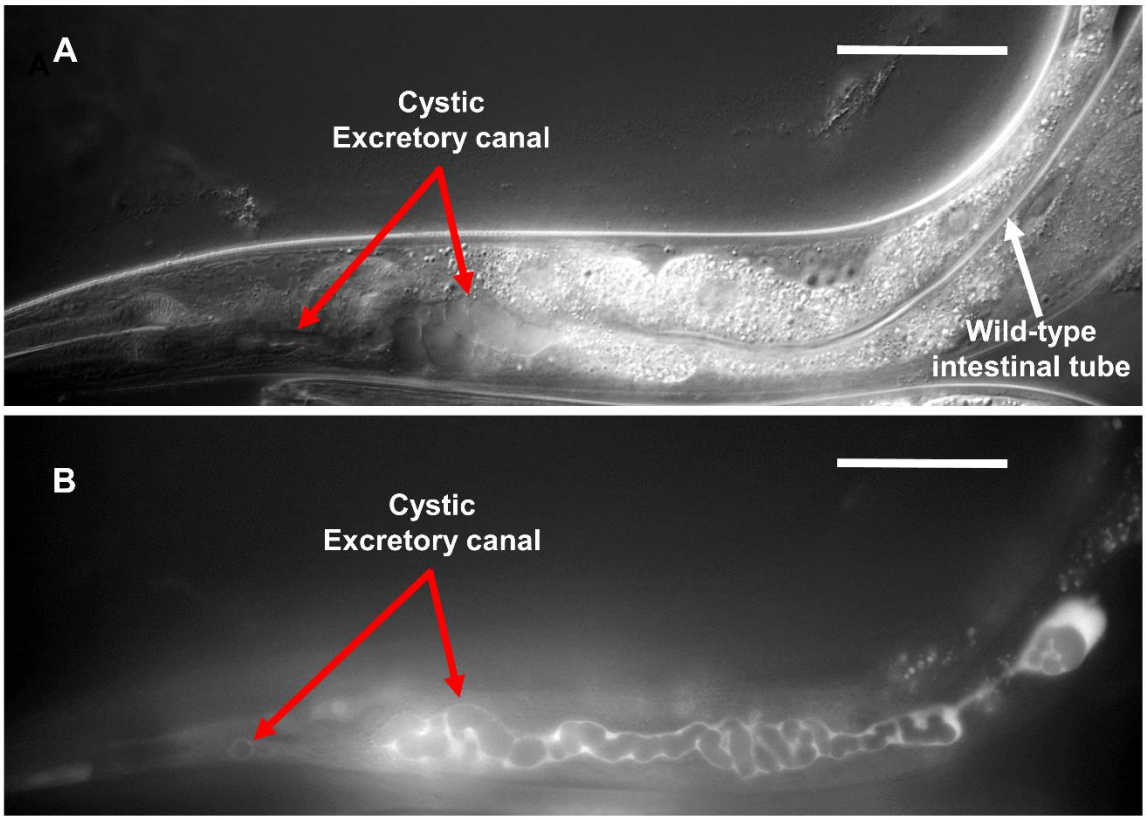


**Supplemental Figure 2.3.** Typical animal treated with injected dsRNA #2 specific for knockdown of *exc-2* isoforms A, B, and D. Top, DIC image shows cystic anterior and posterior canals, and intestine with wild-type lumen. Bottom, Fluorescent image shows cystic short canals. Bars, 50µm**.**

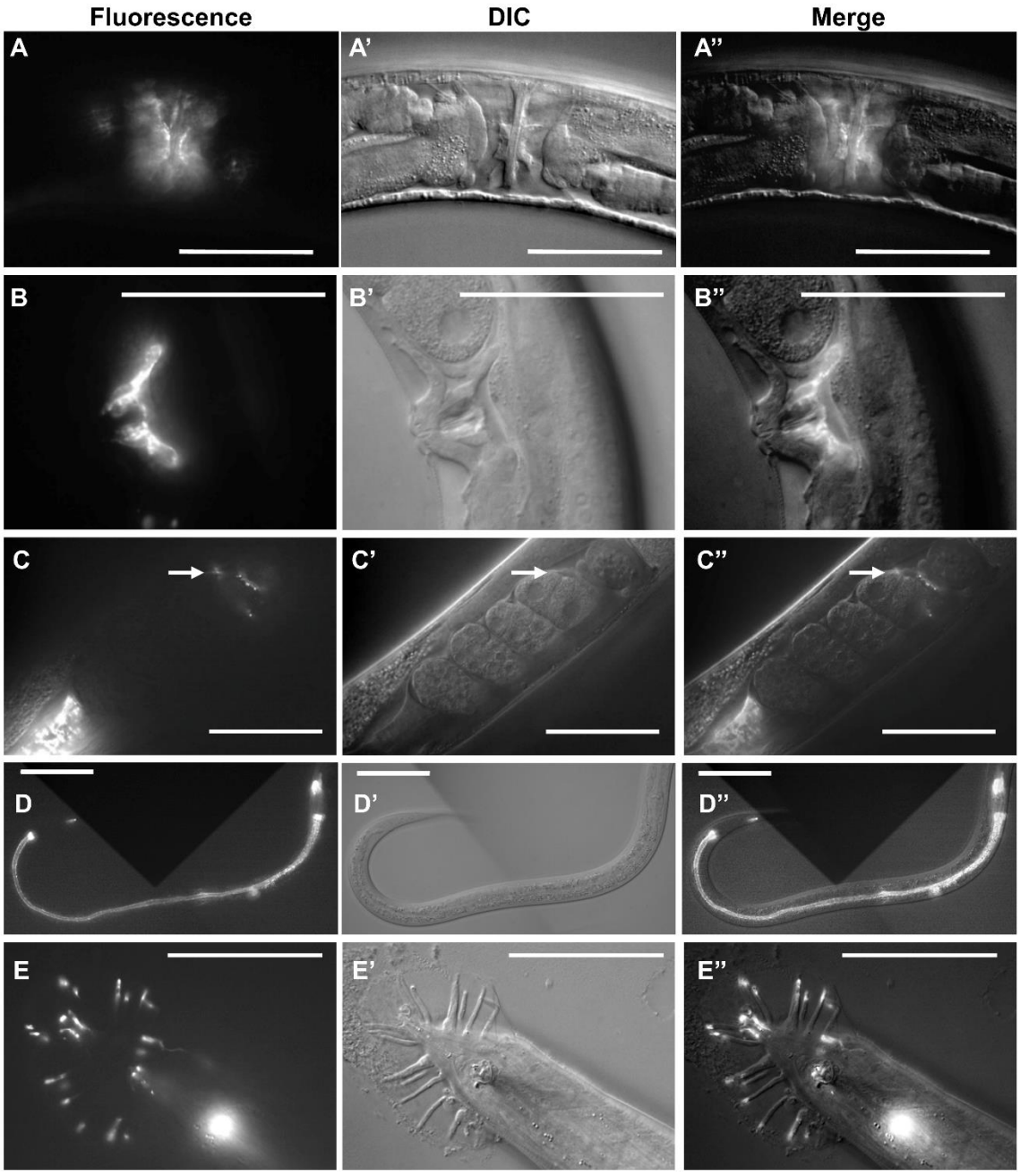


**Supplemental Figure 2.4. Locations of *ifa-4* expression.**

Images of mKate2-labeled IFA-4 expression outside of the excretory canals. Left, fluorescent image; center, DIC image of tissue; right, merged images. (A) Ventral view of IFA-4 in the uterine muscles; (B) Lateral view of uterine muscle; (C) Spermathecal-uterine valve (white arrow); (D) Intestine of long-lived dauer stage (starved) worm; (E) IFA-4 at tips of the 18 male-tail rays and hook sensillum.

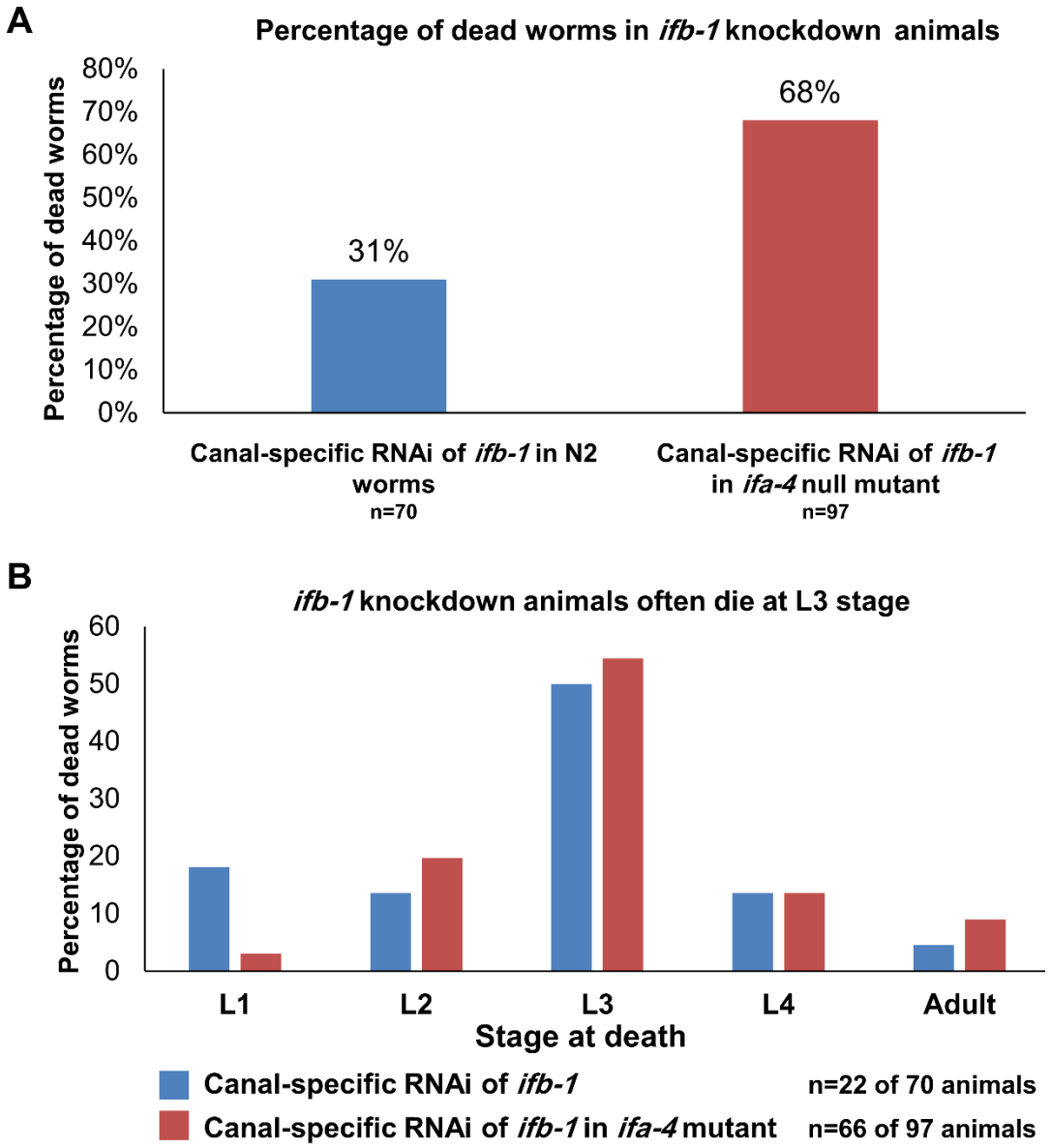


**Supplemental Figure 2.5.** Measurements of lethality of canal-specific knockdown of *ifb-1* in N2 (blue bars) and in the *ifa-4*(*ok1734*) deletion mutant (red bars). (A) Percentage of dead animals observed. (B) Stage of dead animals.

# Chapter 3: RNAi Screen for Novel EXC Tubulogenesis Genes

## 3.1. ABSTRACT

Regulation of luminal diameter is critical to the function of small single-celled tubes, of which the small tubular excretory canals of *C. elegans* provide a tractable genetic model. Several sets of genes regulate the diameter of the canals, including genes encoding intermediate filaments and other cytoskeletal proteins, genes affecting vesicular formation and movement, and genes encoding ion transport. Here, a focused reverse genomic screen of genes highly expressed in the canals found 21 new genes that significantly affect outgrowth or diameter of the canals. These genes nearly double the number of candidates that regulate canal size. Two genes act as suppressors on a pathway of conserved genes whose products mediate vesicle movement from early to recycling endosomes. The encoded proteins provide new tools for understanding the process of cellular recycling and its role in maintaining the narrow diameter of single-cell tubulogenesis.

## 3.2. INTRODUCTION

Tubule formation is an essential process during development of multicellular organisms, with the narrowest tubes occurring in structures as diverse as *Drosophila* trachea, floral pollen tubes, and mammalian capillaries [12, 43]. In *C. elegans*, the excretory system is comprised of cells that form single-celled tubules of three types: pore cells that wrap around a lumen to form a tube with an autocellular junction ("seamed tube"); a larger duct cell that forms a similar seamed tube followed by dissolution of the seam to form a "seamless" tube; and the large excretory canal cell that extends four long thing seamless tubules ("canals") throughout the length of the organism [4].

Many mutants have been discovered that affect the length, guidance of outgrowth, or lumen diameter of the excretory canals. An initial set of such identified "*exc*" mutants were mapped [22], and found to include multiple alleles of some *exc* genes, but only single alleles of others. The frequency of mutations suggested that additional genes should have excretory lumen defects. Studies by multiple laboratories indeed found alleles of other genes with Exc phenotypes [24, 25, 48, 56, 57, 83]. Almost all of the original *exc* genes have now been cloned {Grussendorf, 2016 #11;Al-Hashimi in press, Berry, 2003 #12;Mattingly, 2011 #13;Shaye, 2015 #14;Fujita, 2003 #15;Suzuki, 2001 #16;Tong, 2008 #17;Praitis, 2005 #18}, and found to affect multiple well-conserved cell processes, including cytoskeletal structures, ion channels, and vesicle recycling pathways. The initial screen sought primarily non-lethal genetic effects, but several of the subsequently identified genes were lethal when null.

Several screens have identified genes that affect excretory canal tubulogenesis [4]. RNAi studies were particularly useful in determining roles of excretory canal genes where the null allele is lethal, such as gene encoding the NHR-31 nuclear hormone receptor [45], the ABI-1

Abelson-Interactor [84], and PROS-1 transcription factor [24]. In addition, null mutations in genes that connect the excretory canal cell to the excretory duct (e.g. LET-4 [49] and LPR-1 [83]) are lethal, and have been studied

In order to identify other genes affecting the process of tubulegenesis and tubule maintenancein the excretory canals, we undertook a targeted genomic RNAi screen to identify excretory canal genes that exhibit lumen alterations ("Exc" phenotypes) when knocked down. This screen identified 23 specific canal-expressed genes that showed effects on lumen and/or outgrowth of the excretory canals, including eight genes with no prior known phenotypic effects. In addition, two knockdowns suppressed effects of mutation of the *exc-5* vesicle-recycling gene, and therefore represent potential regulators of vesicle transport needed for single-cell tubulogenesis.

## 3.3 MATERIALS AND METHODS

### 3.3.1. Nematode genetics:

*C. elegans* strains (Table 1) were grown by use of standard culture techniques on lawns of *Escherichia coli* strain BK16 (a streptomycin-resistant derivative of strain OP50) on nematode growth medium (NGM) plates [63]. All strains were grown and evaluated for canal phenotypes at 20$^{o}$C. Worms subjected in this study were young adults or adults.

Each nematode strain (wild-type N2, and *exc-1, exc-2, exc-3, exc-4, exc-5, exc-7, and exc-9*) harbored a chromosomal insertion of canal-specific marker driving cytoplasmic GFP expression ($P_{vha-1}$*::gfp*). All strains were sensitized for RNAi treatment by crossing them to mutant strain *rrf-3*(*pk1426*) and selecting in the F2 generation for homozygous *rrf-3* deletion allele, canal fluorescence, and appropriate *exc* mutation. The *rrf-3* deletion was confirmed via PCR using the following forward and reverse primers, respectively: $^{5'}$TGCTTTGGATATTGCCGAGCAC$^{3'}$ and $^{5'}$GGAGATCTCCGAGCCCTAGAC$^{3'}$, and a reverse nested primer: $^{5'}$CATCGCCAGGCCAACTCAATAC$^{3'}$.

### 3.3.2. RNAi Screen:

The Ahringer RNAi bacterial library [85] was utilized for this study. Overnight cultures were prepared by inoculating bacteria in 5 ml LB + ampicillin (100µg/ml) + tetracycline (12.5µg/ml), and cultured at 37$^{o}$C for 16 hours. In order to induce the bacteria with IPTG, overnight cultures were moved to fresh media, incubated at 37$^{o}$C with rotation until cultures reached an $O.D._{600}$ in a range from 0.5 to 0.8. IPTG was then added to the culture to a final concentration of 95 µg/ml along with ampicillin at 100µg/ml. The cultures were then incubated with rotation at 37$^{o}$C for ninety minutes followed by re-induction with IPTG and ampicillin, and another ninety minutes of incubation at 37$^{o}$C with rotation. Finally, IPTG and ampicillin were

added for the last time right before using these bacteria to seed NGM 12-well plates and Petri dishes. Plates were then incubated at room temperature for 24 hours in order to dry. L2 worms were added to the plates, and their F1 progeny were evaluated for phenotypes in the excretory canals. Each set of genes tested were induced together with induction of two control strains: a plate of bacteria induced to knock down *dpy-11* (which affects the hypoderm but not the canals) [16], and a plate of bacteria induced to knock down *erm-1* bacteria, which causes severe defects in excretory canal length and lumen diameter [25], respectively. Induction was considered successful and plates were screened only if worms grown on the control plates showed the appropriate phenotypes in at least 80% of the surviving progeny.

For each tested gene, the induced bacteria were seeded on one 12-well plate and one 10cm plate. Two or three L2 nematodes were placed on the bacterial lawn of each well, and screened for phenotypes in the $4^{th}$, $5^{th}$, and $6^{th}$ days of induction. Each gene was tested via RNAi treatment of twelve different strains of worms, shown in Table 1, while the one 10cm plate was used for further analysis of animals with wild-type canals grown on RNAi bacteria.

**3.3.3. Microscopy:**

Living worms were mounted on 3% agarose pads to which were added 0.1μm-diameter Polybead® polystyrene beads (Polysciences, Warrington, PA) to immobilize the animals [86]. Images were captured with a MagnaFire Camera (Optronics) on a Zeiss Axioskop microscope equipped with Nomarski optics and fluorescence set to 488 nm excitation and 520 nm emission. Adobe Photoshop software was used to combine images from multiple sections of individual worms and to crop them. Contrast on images was increased to show the excretory canal tissue more clearly.

### 3.3.4. Canal Measurements:

Measurements of excretory canal length and determination of cystic phenotype were carried out as described (Tong and Buechner 2008). Canal length was scored by eye on a scale from 0 – 4: A score of (4) was given if the canals had grown out to full length; canals that extended past the vulva but not full-length were scored as (3); at the vulva (2); canals that ended between the cell body and the vulva were scored as (1); and if the canal did not extend past the cell body, the canal was scored as (0). Cyst size was measured via assessment of size relative to normal canal width. Cysts wider than a normal canal up to ¼ the diameter of the worm were scored as small, cysts between ¼ diameter and ½ the diameter of the worm were scored as medium, and any cysts larger than ½ the diameter of the worm were scored as large. In cases where cyst diameter was ambiguous relative to worm size, photographs of the canal were analyzed via NIH software ImageJ (http://imagej.nih.gov/ij/) and Adobe Photoshop (https://www.adobe.com). Statistical analyses of canal length were conducted as previously (Tong and Buechner 2008): Canals were binned into 3 categories for length (scores 0-1, scores 2-3, and score 4), and again for cyst size (none, small, and binned medium and large). The results were then analyzed via a 3x2 Fisher's Exact Test. P-values of 0.000001 ($1x10^{-6}$) or lower were regarded as strong statistical significance of an effect on the canal; scores between 0.000001 and 0.0001 as a partial effect.

## 3.4 Results and discussion.

### 3.4.1. A focused RNAi screen for new *exc* mutations

A study of genomic expression in *C. elegans* was previously undertaken by the Miller lab [61]. In that study, lists of genes highly expressed in various tissues, including 250 genes preferentially expressed in the excretory canal cell, were made public on the website WormViz (http://www.vanderbilt.edu/wormdoc/wormmap/WormViz.html). Of the corresponding strains in the Ahringer library of bacteria expressing dsRNA to specific *C. elegans* genes [87], we found that 216 grew well, and were tested for effects on *C. elegans* strains.

The excretory canal cell has some characteristics similar to neurons (long processes guided by netrins and other neural guidance cues [88], as well as early expression of the gene EXC-7/HuR[89], the homologue of the *Drosophila* neural marker ELAV), and so was considered potentially refractory to feeding RNAi [90]. We crossed the strain BK36, containing a strong canal-specific fluorescent transgene, to a mutant in the *rrf-3* gene (*pk1426*) in order to increase sensitivity to RNAi [91]. In addition, we also crossed the resultant strain (*BK540*) to known excretory canal mutants *exc-1*, *exc-3*, *exc-5*, and *exc-9*, in order to determine if knockdown of the genes to be tested interacted with known *exc* genes affecting excretory canal tubulogenesis, as double mutants in some *exc* genes (e.g. *exc-3*; *exc-7* doubles [22]) exhibit more severe canal phenotypes than either mutant alone.

We demonstrated the effectiveness of the treatment by performing successful knockdowns of canal-specific and –non-specific genes in these strains. Control knockdowns of *dpy-11* resulted in short worms with normal canal phenotypes, while knockdown of *exc-1* caused

**Table 1. Strains and genotypes of worms.**

Each gene knockdown (dsRNA) was tested with the following strains.

| STRAIN | GENOTYPE | DESCRIPTION | Reference |
|---|---|---|---|
| BK36 | *unc-119(ed3)*; qpIs11[*unc-119; Pvha-1::gfp*] I | N2 harbor integrated GFP marker expressed in excretory canals | [35] |
| BK540 | *rrf-3*(*pk1426*); qpIs11[*unc-119; Pvha-1::gfp*] I | RNAi sensitized strain with integrated canal cytoplasmic GFP-marker | This study |
| BK541 | *sid-1(pk3321)*; qpIs11[*unc-119; Pvha-1::gfp*] I | Systemic RNAi impaired strain with integrated canal cytoplasmic GFP-marker | This study |
| BK542 | *exc-2*(*rh90*); qpIs11[*unc-119; Pvha-1::gfp*] I | *exc-2*(*rh90*) with integrated canal cytoplasmic GFP-marker | This study |
| BK543 | *exc-3*(*rh207*); qpIs11[*unc-119; Pvha-1::gfp*] I | *exc-3*(*rh207*) with integrated canal cytoplasmic GFP-marker | This study |
| BK544 | *exc-4*(*rh133*); qpIs11[*unc-119; Pvha-1::gfp*] I | *exc-4*(*rh133*) with integrated canal cytoplasmic GFP-marker | This study |
| BK545 | *exc-5*(*rh232*); qpIs11[*unc-119; Pvha-1::gfp*] I | *exc-5*(*rh232*) with integrated canal cytoplasmic GFP-marker | This study |
| BK546 | *exc-7*(*rh252*); qpIs11[*unc-119; Pvha-1::gfp*] I | *exc-7*(*rh252*) with integrated canal cytoplasmic GFP-marker | This study |
| BK547 | BK540; *exc-2*(*rh90*) | *exc-2*(*rh90*) with integrated canal cytoplasmic GFP-marker in RNAi sensitized background | This study |
| BK548 | BK540; *exc-3*(*rh207*) | *exc-3*(*rh207*) with integrated canal cytoplasmic GFP-marker in RNAi sensitized background | This study |
| BK549 | BK540; *exc-4*(*rh133*) | *exc-4*(*rh133*) with integrated canal cytoplasmic GFP-marker in RNAi sensitized background | This study |
| BK550 | BK540; *exc-5*(*rh232*) | *exc-5*(*rh232*) with integrated canal cytoplasmic GFP-marker in RNAi sensitized background | This study |

formation of variable-sized cysts in a shortened excretory canal, with no other obvious phenotypes (Fig. 1). Knockdown of the ezrin-moesin-radixin homologue gene *erm-1* caused severe malformation of the canals visible in 50% of surviving treated worms [25, 58]. A deletion mutant of this gene is often lethal due to cystic malformation of the intestine as well as the canals Gobel, 2004 #13, while our treatment allowed many animals to survive to adulthood and reproduce. This result is consistent with our RNAi treatment causing variable levels of gene knockdown in the excretory canals.

Of the 216 genes tested, 186 caused no obvious phenotypic changes to the canals (Supp. Table 1). Knockdown of 26 genes caused noticeable defects in the development of the excretory canals, 3 were induced as controls and we found one to be lethal. The length of the canals were rated according to a measure shown in Fig. 1A, in which no extension past the excretory cell body was rated 0, extension to the animal midbody marked by the position of the vulva was measured as 2, and full extension was rated as 4. The average canal length was characteristic for the gene knocked down, although RNAi knockdown via feeding is intrinsically variable in the strength of gene induction and amount of bacteria eaten, so in general the stated length reflects the average of the canals in more strongly affected animals. Diameter of the canals ALSO varied greatly, depending on the gene knocked down; in cases where fluid-filled cysts became evident (as in previously-described *exc* mutants), cyst size was rated as large (cyst diameter at least half the width of the animal), medium (one-quarter to one-half animal width), or small (up to one-quarter animal width).

### 3.4.2. Excretory Canal Phenotypes

The common feature of all of these knockdown animals is that the posterior canals did

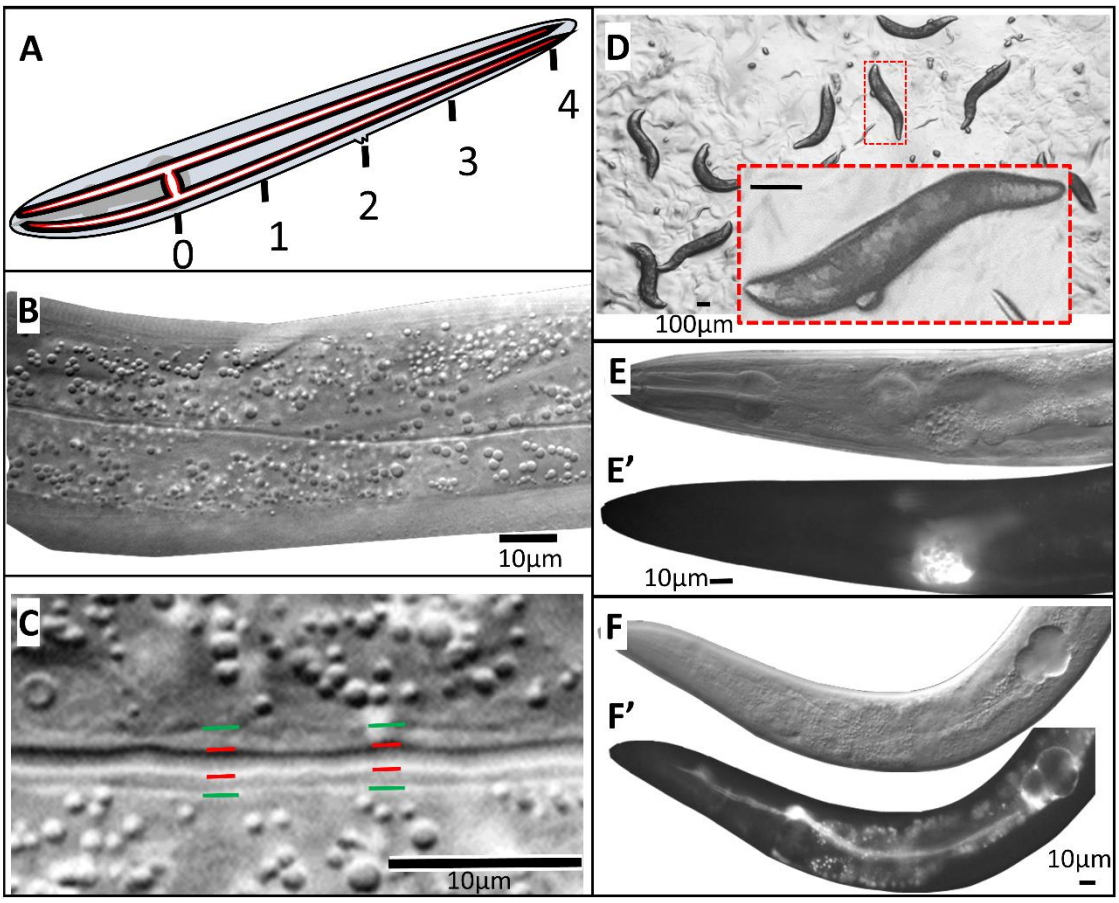


**Figure 1. The excretory canal and induction controls.**

(A) Schematic diagram of the excretory canals extending over the full length of the worm with basal membrane (black) and apical membrane (red) surrounding a narrow lumen (white). Numbers 0-4 represent numerical assignments used to assess canal length. (B) DIC image of section of posterior excretory canal of wild-type worm (N2); canal is narrow with uniform diameter. Bar, 10µm. (C) Magnified DIC image of excretory canal of wild-type worm (N2). Lines indicate boundaries of canal lumen/apical surface (red) and cytoplasmic/basal surface (green). (D-F) Controls to ensure strong induction of dsRNA synthesis for RNAi screen, in *rrf-3*(*pk1426*) animals expressing GFP in the canals: (D) Knockdown of cuticle collagen gene *dpy-11.* Boxed image: Magnification of single worm. Bar = 100µm. (E) DIC and (E') GFP image of *erm-1* knockdown in *rrf-3* worms. Bar, 10µm. (F) DIC and (F') GFP image of *exc-1* knockdown in *rrf-3* worms. Bar, 10µm.

not extend fully to the back of the animal (Table 1). The length of the canal lumen was often the same as the length of the canal cytoplasm, but in many cases the visible lumen (seen as a dark area in the center of the GFP-labelled cytoplasm) was substantially shorter than the length of the canal cytoplasm.

In addition to effects on canal length, the shape and width of the canal lumen and/or canal cytoplasm was affected by specific gene knockdown: A) Several knockdowns resulted in the formation of fluid-filled cysts reminiscent of those in known *exc* mutants; B) Canals appeared normal in diameter, but had frequent thickenings of cytoplasm around otherwise normal (but short) lumen similar to the 'beads" or "pearls" seen in growing first-larval-stage canals or in canals of animals undergoing osmotic stress [24]; C) Canal lumen ending in a large swelling of convoluted tubule or a multitude of small vesicles, and often with a "tail" of very thin canal cytoplasm without any lumen continuing distally; D) a series of vesicles filling much of the cytoplasm outside the normal-diameter lumen, and; E) an irregular shape of the basal surface of the cytoplasm, varying widely in diameter. Each of these phenotypes will be discussed below, together with the genes whose knockdown resulted in that phenotype. The complete list of genes tested is shown in Table S1, while photographs of gene knockdowns not discussed in detail are shown in Fig. S1.

CYSTIC CANALS: Two gene knockdowns, of *ceh-6* and of T25C8.1 (which will be referred to as *exc-10*) resulted in the formation of large fluid-filled cysts (Fig. 2), similar to those seen in *exc-2*, *exc-4*, and *exc-9* mutants (encoding an intermediate filament, a CLC chloride channel, and a CRIP vesicle-trafficking protein, respectively {Al-hashimi, 2018 in revision? Tong, 2008 #1;Berry, 2003 #3}). The homeobox gene *ceh-6* encodes a well-studied transcription factor that defines expression of many genes in the canal

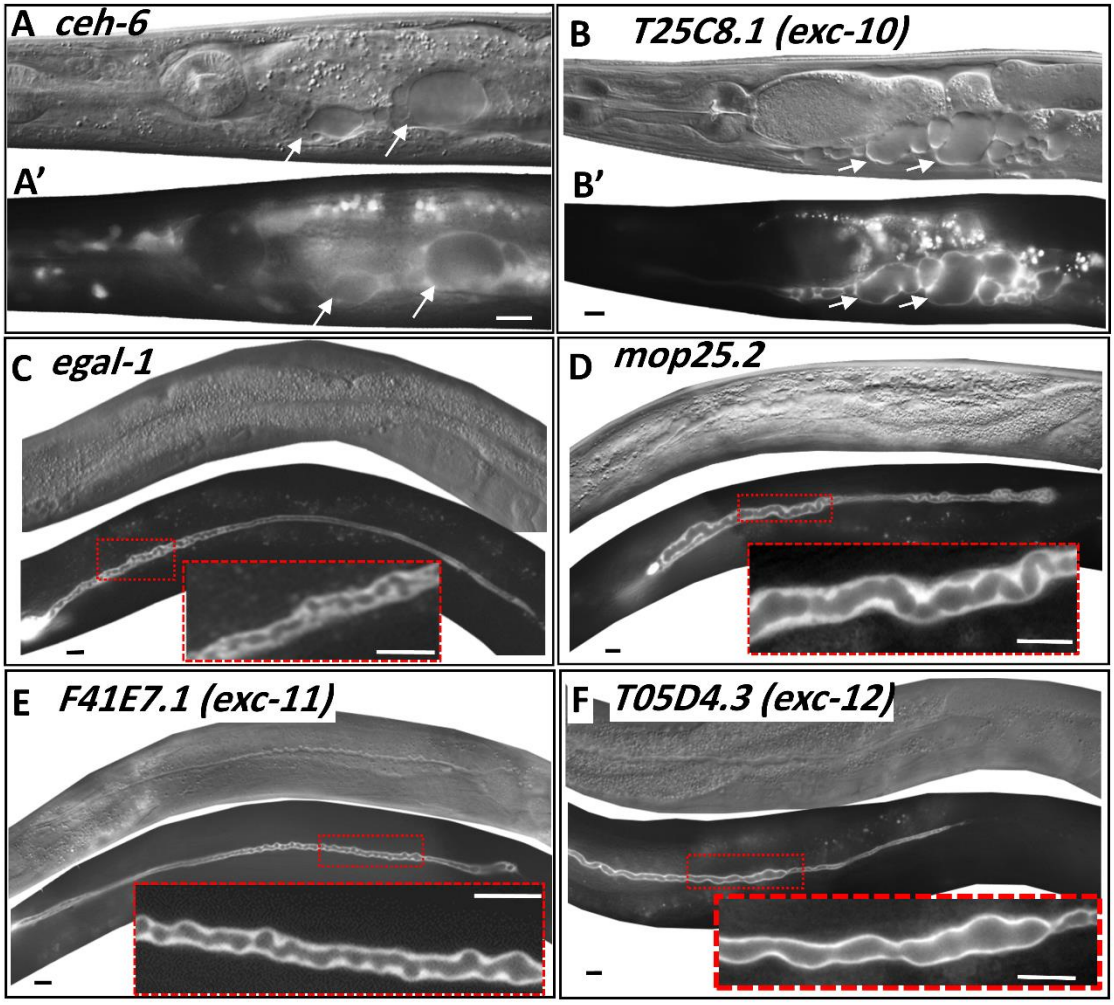


**Figure 2. RNAi knockdowns causing formation of fluid-filled cysts or swollen lumen.**
(A-F) DIC images and (A'-F') GFP fluorescence of representative animals exhibiting RNAi knockdown phenotypes: (A) *ceh-6*; (B) *T25C8.1* (*exc-10*); (C) *egal-1*; (D) *mop-25.2*; (E) *F41E7.1* (*exc-11*); (F) *T05D4.3* (*exc-12*). Arrows: Medium and large fluid-filled cysts. All bars, 10 µm.

[92, 93]. Null mutants of this gene are lethal. The knockdowns had very short canals with large fluid-filled cysts. The effect of *ceh-6* knockdown could reflect lower transcription of many of the known *exc* genes, the excretory aquaporin *aqp-8* {Mah, 2007 #26}, or of a novel gene.

The second gene, T25C8.1 (*exc-10*) encodes a carbohydrate kinase (homology to sedoheptulose kinase) of unknown function in nematodes, although the human homologue SHPK has been linked to a lysosomal storage disease {Wamelink, 2008 #27;Phornphutkul, 2001 #28}.

Knockdowns in *egal-1*, *mop-25.2*, F41E7.1 (*exc-11*), and T05D4.3 (*exc-12*) exhibited small-to-medium sized cysts (Fig. 2). In these animals, cystic regions of the lumen often appear to contain a series of hollow spheres, which may be connected or separate from each other along the lumen length (Fig. 2C-E). MOP-25.2 is a protein with close homology to yeast Mo25 and its homologues in all animals, and acts as a scaffolding protein for activating kinases including germinal center kinase in the STRIPAK complex, which also regulates endocytic recycling in the excretory canal morphology and gonadal lumen formation in *C. elegans* {Lant, 2015 #10;Pal, 2017 #31}. The *Drosophila* Mo25 also regulates transepithelial ion flux in the osmoregulatory Malpighian tubules {Sun, 2018 #29}.

The EGAL-1 protein is a homologue of the *Drosophila* Egalitarian exonuclease, involved in RNA degradation, and also interacts with dynein as part of a dynein-regulating complex at the face of the nucleus {Fridolfsson, 2010 #33}. The excretory canal cell is rich in microtubules along the length of the canals.

F41E7.1 (*exc-11*) encodes a solute carrier with high homology to the $Na^+/H^+$ exchanger. The excretory cell lumen is associated with canaliculi that have high levels of the vacuolar ATPase to pump protons into the lumen{Oka, 2001 #34}, so the presence and function of a

$Na^+/H^+$ exchanger is likely used for canal osmoregulatory function as well as luminal shape.

Finally, T05D4.3 (*exc-12*) is homologous only to genes in other nematodes, and has no obvious function, other than the presence of several putative transmembrane domains.

PERIODIC CYTOPLASMIC SWELLINGS: These "beads" or "pearls" are commonly seen in wild-type animals with growing canals at the L1 stage and in animals under osmotic stress {Kolotuev, 2013 #8}. These sites are hypothesized to be locations of addition of membrane to allow the canal to continue to grow together with the animal. The knockdown animals here were measured in young adulthood, and so should not exhibit such beads. Knockdown of the *inx-12* or *inx-13* genes (Fig. S1, Fig. 3), which encode innexins highly expressed in the canals, gave rise to these structures. Innexins form the gap junctions of invertebrates {Hall, 2017 #2202}, and the excretory canals are rich in these proteins along the basal surface, where they connect the canal cytoplasm to the overlaying hypodermis {Nelson, 1983 #37}. The mutant phenotype here suggests that these proteins regulate balancing of ionic content to allow normal canal growth.

A similar phenotype is seen in animals knocked down for *ceh-37*, which encodes an Otx Homeobox protein expressed solely in the excretory cell in adults, but additionally in a wide range of tissues in embryos{Hench, 2015 #38}. Expression of *ceh-37* is itself regulated by CEH-6 {Burglin, 2001 #25}, so the difference in phenotypes of knockdowns of these two genes suggests that CEH-6 regulates a wider range of genes than does CEH-37.

Knockdown of *dhhc-2* shows a similar phenotype, although bead size and placement appears more irregular than for the above mutants (Fig. 3). Close examination of the beads

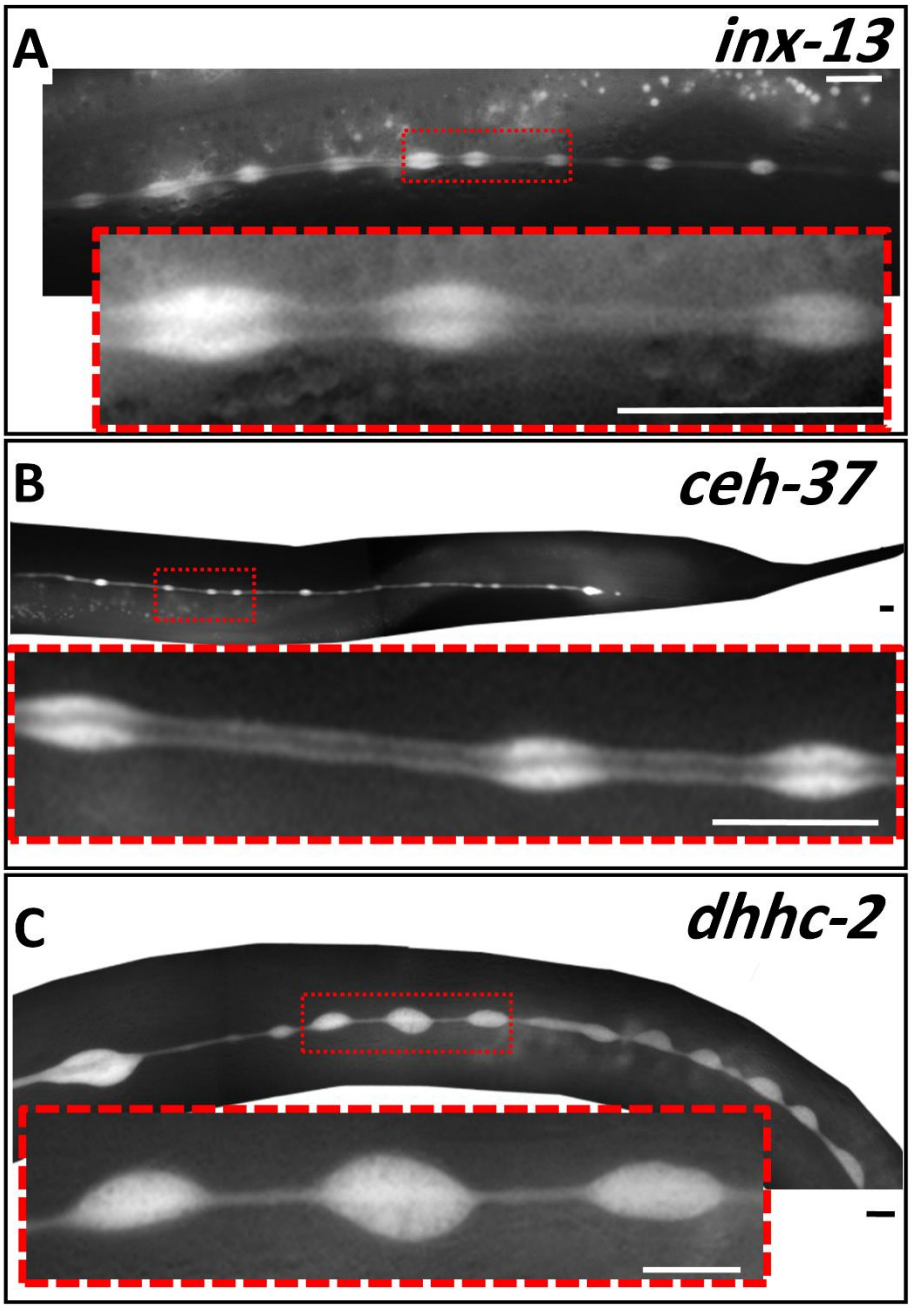


**Figure 3. RNAi knockdowns causing periodic cytoplasmic swellings.**

GFP fluorescence images of swellings ("beads") along length of canals. Boxed insets of marked areas are magnified to show width of lumen in regions within and between beads. (A) *inx-13*. (B) *ceh-37*. (C) *dhhc-2*. Inset in (C) is of region posterior to end of lumen, so lumen is not visible. Note visible vesicles in cytoplasmic beads in (C). All bars, 10 μm.

shows numerous small dark spots consistent with the presence of many vesicles of varying sizes within the beads (Fig. 3C) This gene encodes a zinc-finger protein homologous orthologous to , human ZDHHC18, which acts as a protein palmitoyltransferase {Ohno, 2012 #39}. This phenotype (BEADS) is also seen in knockdown of *mxt-1*, an RNA-binding protein that affects translation {Peter, 2015 #62} (Fig. S1A).]

SWELLING AT END OF LUMEN: The largest group of knockdown animals showed a substantial swelling at the distal tip of generally normal-diameter canals (Fig. 4). In some cases, the swelling appears to be caused by accumulation of a convoluted lumen folded back on itself, while in other knockdowns this swelling could reflect accumulation of a large number of vesicles at the end of the lumen. A combination of these structures also appears in many animals. Reflecting the variable effects of RNAi knockdown, some animals knocked down in genes discussed above, *ceh-37*, or *mop25.2*, showed effects primarily at the distal tip of the lumen (Fig. 4C, 4G), likely reflecting weaker knockdown than in other examples where the entire lumen was affected. These animals showed a highly convoluted lumen. Knockdown of another gene, *glt-5*, showed a similar effect. This gene encodes one of three glutamate transporters strongly expressed in the canals {Mano, 2007 #40}.

Knockdowns of *gst-28* and of *fbxa-183* (Fig. 4A, 4D) show clear and dramatic accumulation of vesicles at the swelling at the tip of the lumen. Vesicle transport defects are the cause of canal malformations in *exc-1*, *exc-5*, and *exc-9* mutants [1, 35, 36], so the knockdown effects shown in these and the following genes may reflect similar defects in vesicular transport.GST-28 is a glutathione-S-transferase orthologous to the human prostaglandin D synthase, which isomerases $PGH_2$ to form prostaglandin {Chang, 1987 #41}. FBXA-183 is one of the very large family of F-box proteins

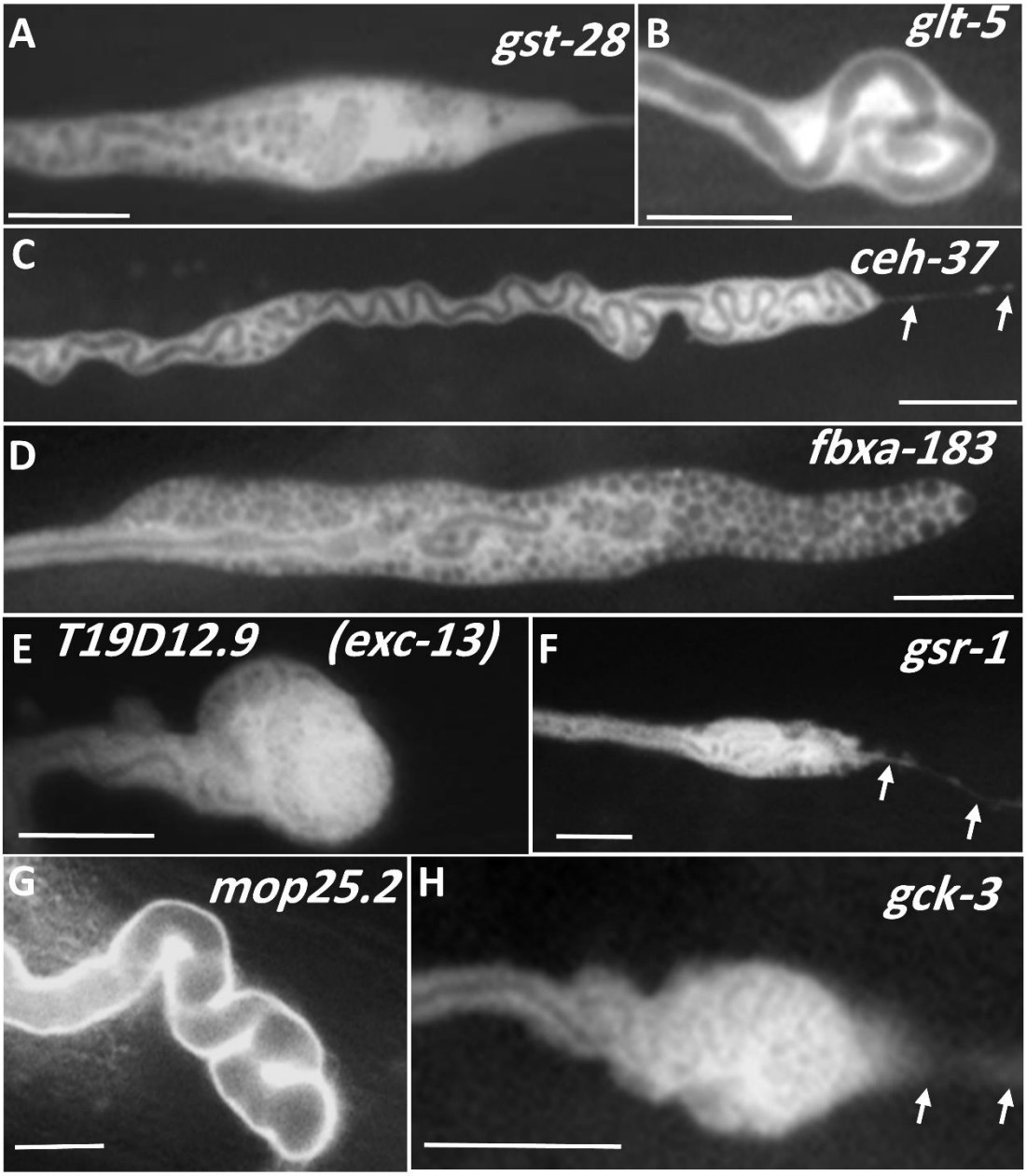


**Figure 4. RNAi knockdowns causing swelling at end of lumen.**

GFP fluorescence images of swollen canals at termination of lumen caused by RNAi knockdown of genes: (A) *gst-28*; (B) *glt-5*; (C) *ceh-37*; (D) *fbxa-183*; (E) *T19D12.9* (*exc-13*); (F) *gsr-1*; (G) *mop25.2*; (H) *gck-3*. All images show regions of convoluted canals. Some areas in panels A, D, E, and H show additional areas that are appear as individual separated small cysts or large vesicles. Arrows: Cytoplasmic tail continuing past termination of lumen (panels C, F, and H). All

in *C. elegans* that binds substrate for ubiquitin-mediated destruction. This protein also contains a FOG-2 Homology (FTH) domain, presumed to mediate protein-protein binding.

Knockdown of three genes produced animals with a swollen tail filled with a mixture of convoluted tubule and individual vesicles. T19D12.9 (to be referred to as *exc-13*) (Fig. 4E) encodes another homologue of the human SLC family of solute carriers, including the ubiquitous lysosomal membrane sialic acid transport protein sialin (SLC17A5), which transports sialic acid from the lysosome, and nitrate from the plasma membrane in humans {Qin, 2012 #43}. The *gsr-1* gene encodes the sole glutathione reductase in *C. elegans*, necessary for rapid growth and embryonic development as well as canal morphology {Mora-Lorca, 2016 #44}. Finally, knockdown of the germinal center kinase gene *gck-3* caused the same phenotype. As noted above, germinal center kinase is part of the STRIPAK complex that helps maintain canal morphology; malformations in STRIPAK are the cause of tubule defects such as cavernous cerebral malformations in humans {Lant, 2015 #10}.

A very narrow canal "tail" completely lacking a visible lumen often extends substantially past the end of the lumenated portion of the canal in these animals. This tail follows the path of wild-type canal growth, and in a few rare instances even reaches the normal endpoint of the canal. In wild-type animals, the lumen and tip of the canal grow together and reach the same endpoint {Buechner, 1999 #4}, with a widening suggestive of a growth cone at the tip of the growing canal in the embryo and L1 stage {Fujita, 2003 #15}. The tip of the canal is enriched in the formin EXC-6, which mediates interactions between microtubules and actin filaments and may mediate connections between the canal tip and end of the lumen {Shaye, 2015 #14}. The results here are consistent with the idea that canal lumens grow and extend separately from the growing basal surface that guides cytoplasmic outgrowth {Kolotuev, 2013 #8}.

VESICLES ALONG LENGTH OF CANAL: Two unexpected novel canal phenotypes were observed in which many vacuoles not associated with the central lumen accumulated along the length of the canals. Knockdown of the gene K11D12.9 (which will be referred to as *exc-14*) exhibited an extraordinary increase of vesicles in the cytoplasm of the canal, terminating in a large irregular swelling at the end of the canal (Fig. 5A). This swelling is unusual in that the lumen of the canal appears relatively normal in diameter (though short), but is surrounded by cytoplasm that puffs out at the basal side of the cell, which is surrounded by (and extensively connected via innexins to) the hypoderm and by basement membrane abutting the pseudocoelom {Nelson, 1983 #37}. GFP labelling of the cytoplasm showed the thick layer of canaliculi surrounding the lumen, which is surrounded by a cytoplasm packed with vesicles of variable size. K11D12.9 encodes a protein containing a RING finger domain at the C-terminus, with some BLASTP homology to potential ubiquitin E3-ligases found in plants and animals.

VESICLES AND IRREGULAR CYTOPLASM: Knockdown of several other genes gave rise to vesicles of varying size in the cytoplasm and irregular swellings to the side of the canal, some primarily at the terminus of the lumen, and in some cases along the length of the canals (Fig. 5B-5F). These included some animals knocked down in the F-Box gene *fbxa-183*, discussed above. Knockdowns of T08H10.1 (which will be referred to as *exc-15*) or of H09G03.1 (*exc-16*) showed increasing amounts of variable-sized vesicles in the canal cytoplasm towards the distal ends of the canals, together with increasing numbers of irregular cysts in the lumen (Fig. 5C, 5D). H09G03.1 has no conserved domains, and no clear homology to genes outside the *Caenorhabditis* genus. T08H10.1, however, encodes a well-conserved aldo-keto reductase, and in a previous RNAi screen was found to slow defecation rate by about 20% when knocked down possibly through effects on mitochondrial stress {Liu, 2012 #45}.

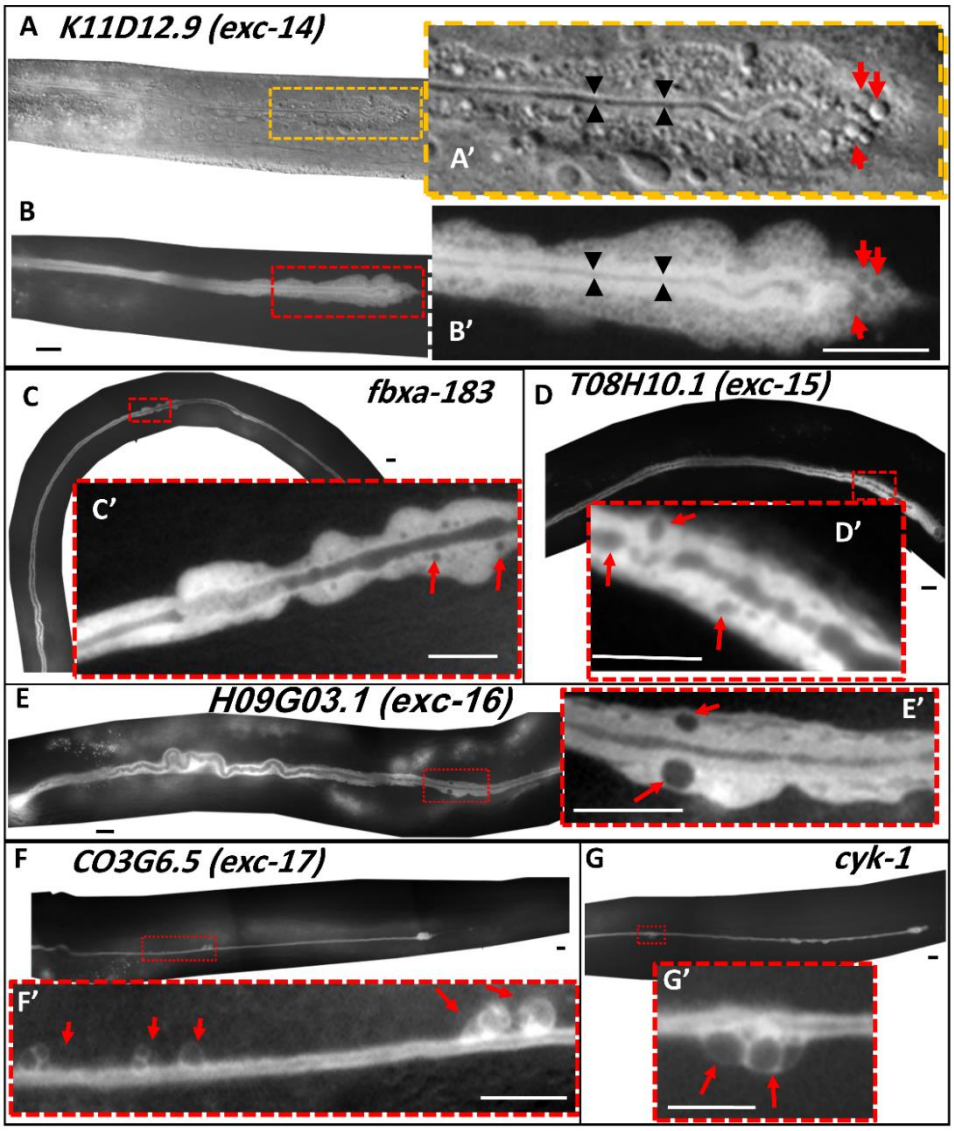


**Figure 5. RNAi knockdowns causing irregular basal membrane along canal length.**

(A) DIC and (B) GFP fluorescence images of distal tip of canal of representative animal knocked down for *K11D12.9* (*exc-14*). (A', B') Enlargement of boxed areas of panels A and B. Thin lumen indicated by arrowhead surrounded by area of bright GFP fluorescence. Distorted cytoplasmic shape is filled with large number of vesicles (red arrows). (C-G) GFP fluorescence of representative animals knocked down for genes: (C) *fbxa-183;* (D) *T08H10.1 (exc-15)*; (D) *H09G03.1(exc-16)*; (F) *C03G6.5 (exc-17)*; and (G) *cyk-1.* (C'-G') Enlargement of boxed areas of panels C-G, showing examples of areas along the canals where cytoplasm surface is swollen with vesicles, and basal surface is irregular and noticeably wider than in wild-type animals. Arrows show enlarged vesicles or cysts. Bars, 10 µm.

Knockdown of two other genes caused the appearance of large cysts or vesicles appearing on the basal surface of the canals in just a few seemingly random spots along the length of the canals (Fig. 5E, 5F). C03G6.5 (*exc-17*) is another protein found only in nematodes, with a Domain of Unknown Function (DUF19), possibly an extracellular domain, found only among several nematode and bacterial proteins. CYK-1, however, is a formin of the Diaphanous class, that has a well-investigated role in regulating microfilaments in cytokinesis {Severson, 2002 #46}, and in forming normal canal morphology through interactions with the EXC-6 formin, via regulation by EXC-5 (human FGD) guanine exchange factor and CDC-42{Shaye, 2016 #23}. Our RNAi knockdown of *cyk-1* produced a stronger phenotype (shorter canals with large cysts on the basal side) than seen in the temperature-sensitive mutant knockdown used by the Greenwald laboratory, but not as strong an effect as was seen in double mutants of *cyk-1*(*ts*) *exc-6*(*0*) {Shaye, 2016 #23}.

### 3.4.3. Variability and Range of Phenotypes:

Treatment of nematodes via feeding RNAi creates variable levels of knockdown between animals {Hull, 2004 #52}. This feature of the gene knockdowns has allowed observation of effects of genes that have a lethal null phenotype, and show a relationship between the phenotypes described above, as seen from RNAi-knockdown of the *vha-5* gene. This gene encodes a protein of the membrane-bound V0 subunit of the vacuolar ATPase, and is strongly expressed in the canalicular vesicles at the apical membrane of the canals {Kolotuev, 2013 #8}. Mutations of this gene are lethal, and a point mutation led to strong whorls of labelled VHA-5 at the apical surface {Liegeois, 2006 #47}. Our knockdown of this gene gave a wide range of phenotypes in different animals (Fig. 6). Some animals exhibited beads surrounding a normal-diameter lumen (Fig.6A), similar to animals under slow growth or osmotic stress, as in Fig. 3.

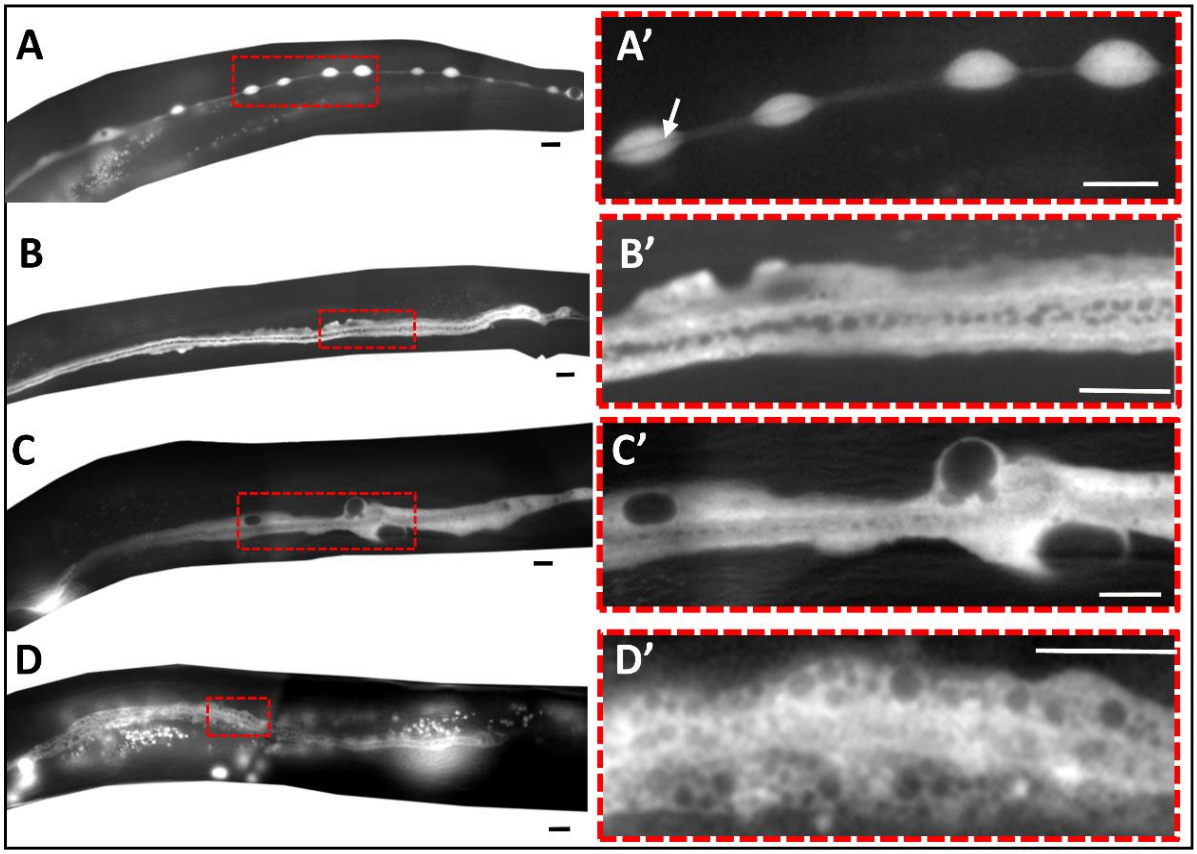


**Figure 6. knockdown of *vha-5* leads to a wide range of phenotypes.**

(A-D) GFP fluorescence of four different worms exhibiting a range of excretory canal phenotypic severity in response to *vha-5* knockdown. For each animal, the boxed area is enlarged on the right (A'-D'). (A, A') Periodic cytoplasmic swellings along lumen of canal. Arrows in A' show visible lumen of normal diameter. (B, B') Small septate cysts in the lumen of the canal, surrounded by area of bright GFP fluorescence, and somewhat irregular diameter cytoplasm. (C, C') Lumen with septate cysts similar to B, B', surrounded by cytoplasm of more irregular diameter containing large cysts/vesicles. (D, D') Wider-diameter lumen with larger cysts, surrounded by cytoplasm filled with vesicles in a wide range of sizes. Bar, 10µm.

Other animals showed small septate cysts in the canal lumen, but the canal lumen overall was generally of near-normal diameter, and the basal surface had mostly minor irregularities (Fig. 6B), similar to animals knocked down for *exc-15* (Fig. 5C). Other *vha-5* knockdown animals also exhibited a similar luminal phenotype, but also showed large vesicles within a highly irregularly shaped cytoplasm (Fig. 6C), similar to animals impaired in *exc-17* or *cyk-1* expression (Fig. 5E, 5F). Finally, the most extremely affected *vha-5* knockdown animals (Fig. 6D) showed cysts throughout the lumen, a swollen terminus to the lumen, and a range of variable-sized vesicles or cysts that pack the entire swollen cytoplasm of the canals. The wide range of defects seen in animals knocked down may reflect the very strong phenotype of the null mutant (embryonic lethal), and the wide range of expression of dsRNA that can occur through feeding RNAi. The variability of phenotype also indicates that the range of mutant phenotypes described above for various gene knockdowns may represent variable expression of dsRNAs that affect a common set of coordinated pathways that function to create and maintain the complicated shape of the excretory canals; these pathways include gene transcription, ion and small molecule transport, cell cytoskeleton, cell-cell communication, and movement and function of vesicles.

### 3.4.4. Suppressors of the Exc-5 Phenotype

In addition to carrying out the RNAi screen in labelled animals with wild-type canals, the RNAi screen was also carried out in animals carrying mutations in various *exc* genes, to try to find genes that interacted to form more severe phenotypes. Previous interactions have found, for example that *exc-3*; *exc-7* double mutants have much more severe canal phenotypes than either mutant alone {Buechner, 1999 #4}, and similar exacerbation of effects for *exc-5*; *exc-6* double mutants {Liegeois, 2006 #47}. It was surprising that no such effects were detected in this screen, but surprisingly, knockdown of two genes caused an unexpected phenotype: the

restoration of near-wild-type phenotype from strongly cystic homozygous *exc-5*(*rh232*) animals (Fig. 7), which carry a large deletion of almost all of the *exc-5* gene {Suzuki, 2001 #16}. The EXC-5 protein is a Guanine Exchange Factor (GEF) specific for CDC-42 and homologous to four human FGD proteins, including two that are implicated in Aarskog-Scott Syndrome and Charcot-Tooth-Marie Syndrome Type 4H, respectively. *exc-5* null mutants are characterized by large fluid-filled cysts at the terminus of both anterior and posterior canals (Fig. 7). Knockdown RNAi of these suppressor genes yielded a large number of progeny exhibiting near-normal canal phenotypes, with canal length extending near-full-length (Fig. 7D). We will refer to this phenotype as Suex, for SUppressor of EXcretory defects. In SUEX canals, no obvious septate cysts are evident, although parts of the canal lumen were slightly widened (Fig. 7B, 7C).

F12A10.7 (*suex-1*) encodes a small protein (113 aa) unique to *C. elegans*, expressed in the excretory canal cell and in some neural subtypes, with homology to genes in only a few other *Caenorhabditis* species. The C-terminal half of the protein contains a number of repeats of tri- and tetra-peptides GGY and GGGY. C53B4.1 (*suex-2*), however, encodes a protein with homologues in a wide range of animals, including humans. This gene encodes a cation transporter that has been implicated in distal tip cell migration through a previous RNAi screen {Cram, 2006 #48}. Multiple strong homologues in humans fall in the SLC (SoLute Carrier) family 22 class of proteins, with the closest homologue SLC22A1 (OCT1) encoding a 12-tm-domain integral membrane protein transporting organic cations {Nigam, 2018 #49} and expressed in the human liver and small intestine. The effect of knocking down this transporter implies that ionic milieu or lipid composition affects transport of vesicles mediated by EXC-5 signaling, but future work will be needed to determine the role that this transporter exerts on early and recycling endosomes.

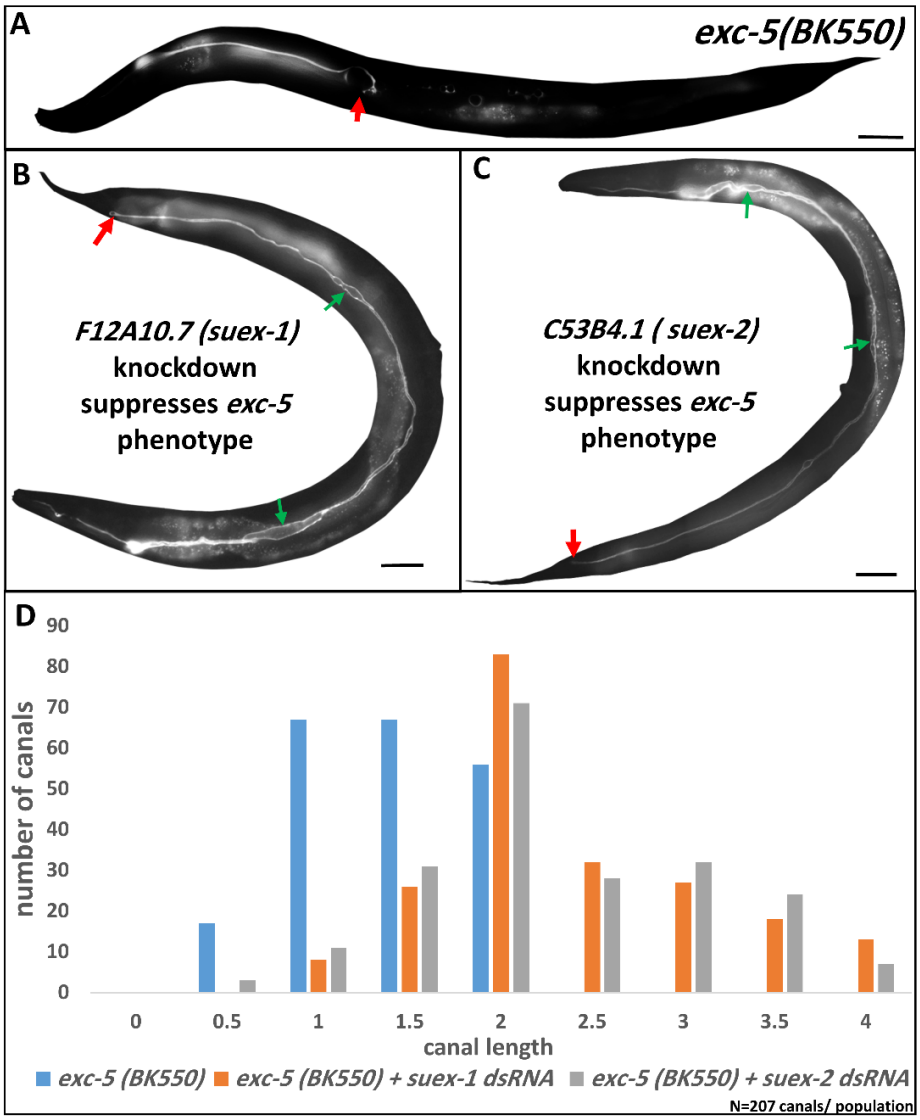


**Figure 7. Knockdown of two genes suppresses the Exc-5 phenotype.**

(A-C) GFP fluorescence of canals in null *exc-5*(*rh232*) mutant (BK545: *exc-5* sensitized via *rrf-3* mutation and containing a GFP canal marker) (A) and of animals showing strong suppression when knocked down for (B) F12A10.7 (*suex-1*), or (C) C53B4.1 (*suex-2*). Exc-5 phenotype typically includes very short normal diameter canals terminating in very large cysts {Shaye, 2015 #14}. Red arrows indicate termination of canals. Green arrows indicate areas of slight swelling of Suex canal lumen in both knockdowns. Bars, 50 µm. (D) Measurement of effect of *suex* suppression on canal length. Canals from mutant and mutant with *suex* knockdown were measured according to scale in Fig. 1A. Average canal length: *exc-5*(*rh232*): 1.4, *exc-5*(*rh232*); *suex-1*(*RNAi*): 2.3, *exc-5*(*rh232*);*suex-2*(*RNAi*): 2.3. N=207 for each genotype. The differences from wild type are highly significant: 3x2 Fisher Test (see Materials & Methods): $p=9.0\times10^{-17}$ for *suex-1*, $1.7\times10^{-13}$ for *suex-2*.

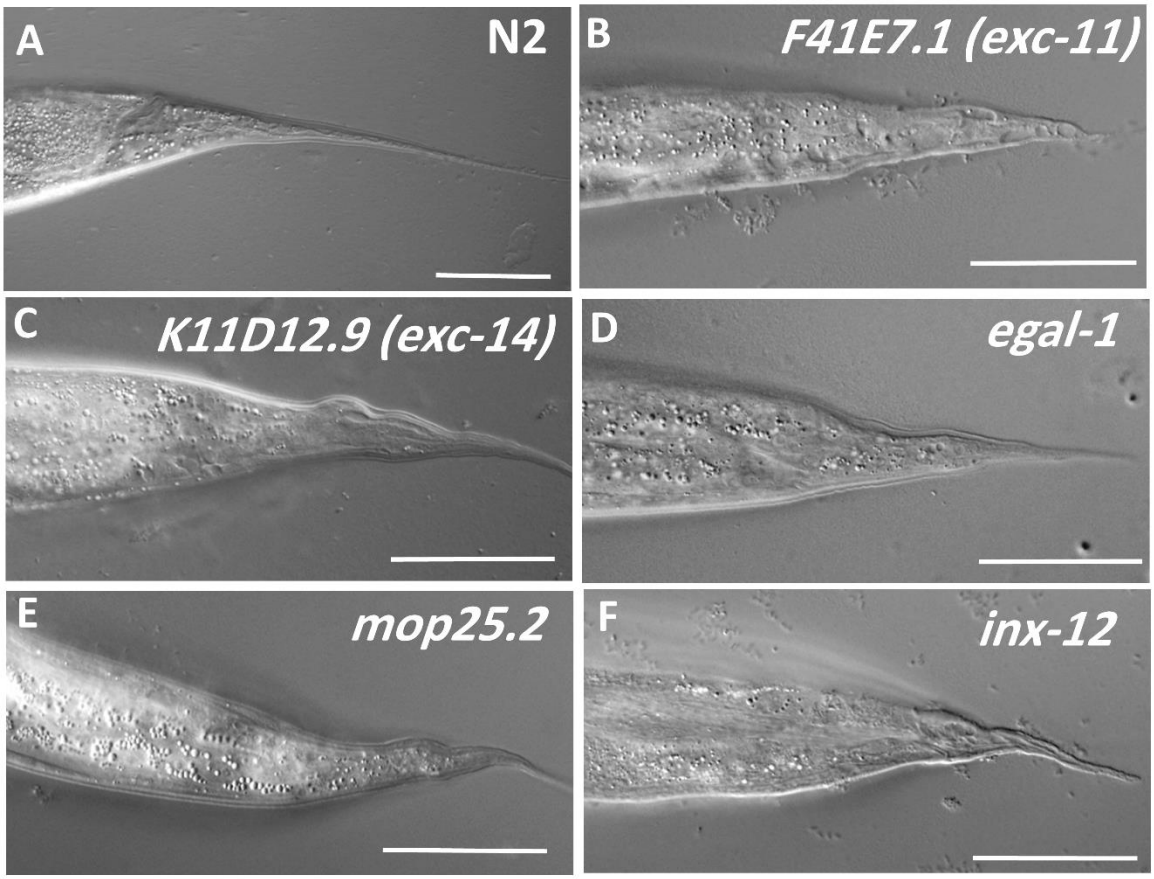


**Figure 8. Knockdown of some *exc* genes causes tailspike defect.**

DIC images of the narrow tail spike of adult hermaphrodite wild-type animal (A) and of adult mutants exhibiting RNAi knockdown for genes: (B) *F41E7.1* (*exc-11*); (d) *K11D12.9* (*exc-14*); (D) *egal-1*; (E) *mop-25.2*; (F) *inx-12*. Bars, 50µm.

### 3.4.5. Other Phenotypes

While the focus of this RNAi screen centered on excretory canal morphology, a few other phenotypes were noticed, including effects in some knockdown animals on fertility and effects on gonadal shape. In particular, the shape of the hermaphrodite tail spike is affected in many *exc* mutants and in multiple RNAi knockdowns in this screen (Fig. 8). The tail spike is formed from the interaction of hypodermal tissue hyp10 with a syncytium of two other hypodermal cells that later undergo cell death{Sulston, 1983 #50}. The tail spike cell expresses *exc-9* {Tong, 2008 #17}among other proteins. the screen tails. Strong defects in tail spike morphology were seen in animals with various genes knocked down (Fig. 9B-9F) with varied functions. In addition to the genes shown, tail spike defects were also seen in animals knocked down in homeobox protein CEH-6, VHA-5, sedoheptulose kinase EXC-10, aldo-keto reductase EXC-15, and innexin INX-13.

## 3.5. CONCLUSION

The RNAi screen was successful at identifying 26 genes that affect the formation of a normal lumen of the long excretory canals of *C. elegans*. These genes identified encode transcription factors, ion channels, innexins, and proteins involved vesicle trafficking; while these processes have been implicated previously in canal tubulogenesis, these proteins identify new actors that could provide insights into how these processes are integrated in single-cell tubulogenesis. Several other proteins have roles in sugar metabolism and redox, which are new processes to be involved in canal morphogenesis.

Finally, two genes were identified as suppressors of *exc-5* mutation. As the human

homologue FGD4 is involved in Schwann cell (which also forms single-cell tubules) morphology, determining the function of these suppressor proteins has the potential to increase understanding the maintenance of Schwann cell morphology during periods of rapid growth.

### 3.6. Supporting Data.

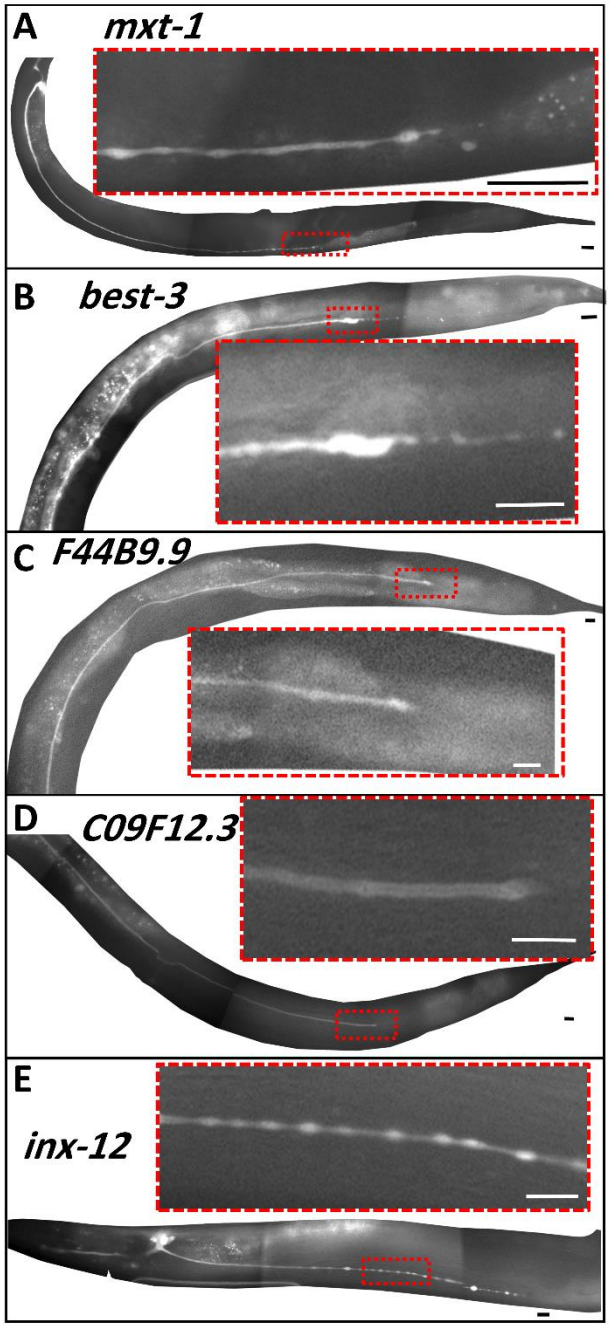


**Supplementary Figure 1.**

(A-E) GFP fluorescence images of short canals (A) *mxt-1*; (B) *best-3*; (C) *F44B9.9*; (D) *C09F12.3*; (E) *inx-12*. For each animal, the boxed area is enlarged on the right. In E' shows mild- cytoplasmic swellings in *inx-12* knockdown worm. Bar, 10µm.

**Table 3.2: A list of genes that are highly expressed in the canal along with the results for tested genes.**

| Gene Number | Gene | Clone ID | Gene ID | tested /not tested | result for tested |
|---|---|---|---|---|---|
| 1 | Y47H9C.2 | I-10A19 | *dhhc-2* | tested | Canal Phenotype |
| 2 | C07F11.2 | I-1E21 | | tested | No Canal Phenotype |
| 3 | Y8G1A.2 | I-1H11 | *inx-13* | tested | Canal Phenotype |
| 4 | ZK770.3 | I-1H15 | *inx-12* | tested | Canal Phenotype |
| 5 | F57C9.1 | I-2K08 | | tested | No Canal Phenotype |
| 6 | T23B3.2 | I-3C08 | | tested | No Canal Phenotype |
| 7 | H32K16.1 | I-4F01 | *slc-36.4* | tested | No Canal Phenotype |
| 8 | F36H2.1 | I-4H03 | *tat-5* | tested | No Canal Phenotype |
| 9 | F26E4.2 | I-4J18 | | tested | No Canal Phenotype |
| 10 | K02B12.1 | I-4M15 | *ceh-6* | tested | Canal Phenotype |
| 11 | C34B2.11 | I-5K08 | | tested | No Canal Phenotype |
| 12 | F36D1.7 | I-5L19 | | tested | No Canal Phenotype |
| 13 | Y18D10A.23 | I-6D07 | | tested | No Canal Phenotype |
| 14 | Y18D10A.8 | I-6D19 | *mxt-1* | tested | Canal Phenotype |
| 15 | R05D7.5 | I-6I03 | | tested | No Canal Phenotype |
| 16 | Y105E8A.22 | I-9C17 | *exc-4* | Not tested | Not Attempted |
| 17 | F36F2.7 | I-9M12 | | tested | No Canal Phenotype |
| 18 | C32D5.6 | II-10F06 | | tested | No Canal Phenotype |
| 18 | C32D5.6 | II-4N21 | | tested | No Canal Phenotype |
| 19 | K08A2.1 | II-10H01 | | tested | No Canal Phenotype |
| 20 | C30B5.6 | II-10M15 | | tested | No Canal Phenotype |
| 20 | C30B5.6 | II-4J13 | | No Bacterial Growth | Not Attempted |
| 21 | C01B12.3 | II-1A07 | *best-3* | tested | Canal Phenotype |
| 22 | C01B12.5 | II-1A09 | *best-4* | tested | Canal Phenotype |
| 22 | C01B12.5 | II-1A11 | *best-4* | tested | Canal Phenotype |
| 23 | F23F1.6 | II-1C05 | | tested | No Canal Phenotype |
| 24 | Y57G7A.1 | II-1F06 | | No Bacterial Growth | Not Attempted |
| 25 | K12H6.6 | II-2F22 | | No Bacterial Growth | Not Attempted |
| 26 | F12A10.7 | II-4O02 | *suex-1* | tested | Suppressor for *exc-5* |
| 27 | E04F6.4 | II-5B09 | | tested | No Canal Phenotype |
| 28 | E04F6.8 | II-5B17 | | tested | No Canal Phenotype |
| 29 | B0252.3 | II-5E06 | | tested | No Canal Phenotype |
| 30 | C06A8.8 | II-5H02 | | tested | No Canal Phenotype |
| 31 | T09A5.2 | II-5H18 | *klp-3* | tested | No Canal Phenotype |
| 31 | T09A5.2 | II-5H24 | *klp-3* | tested | No Canal Phenotype |
| 32 | D1022.3 | II-5J23 | | tested | No Canal Phenotype |
| 33 | T19D12.3 | II-5K01 | | tested | No Canal Phenotype |
| 34 | T19D12.7 | II-5K09 | *oig-8* | tested | No Canal Phenotype |

| Gene Number | Gene | Clone ID | Gene ID | tested /not tested | result for tested |
|---|---|---|---|---|---|
| 35 | T19D12.9 | II-5K13 | | tested | Canal Phenotype |
| 36 | T19D12.10 | II-5K15 | | tested | No Canal Phenotype |
| 37 | DH11.3 | II-5L24 | *pgp-11* | tested | No Canal Phenotype |
| 38 | T05C12.5 | II-6C11 | *mig-5* | tested | No Canal Phenotype |
| 38 | T05C12.5 | II-6C13 | *mig-5* | tested | No Canal Phenotype |
| 39 | F35C11.4 | II-6E19 | | tested | No Canal Phenotype |
| 40 | T26C5.1 | II-6J13 | *gst-13* | tested | No Canal Phenotype |
| 41 | Y53C12A.2 | II-6N18 | *glt-5* | tested | Canal Phenotype |
| 42 | Y53C12A.4 | II-6N22 | *mop-25.2* | tested | No Canal Phenotype |
| 43 | C05D12.1 | II-7D20 | | tested | No Canal Phenotype |
| 44 | W02B12.4 | II-7F20 | | tested | No Canal Phenotype |
| 45 | R03D7.6 | II-7H21 | *gst-5* | tested | No Canal Phenotype |
| 46 | F45E10.1 | II-7J23 | *unc-53* | No Bacterial Growth | Not Attempted |
| 47 | C14A4.11 | II-7M10 | *ccm-3* | tested | No Canal Phenotype |
| 48 | C14A4.12 | II-7M12 | | tested | No Canal Phenotype |
| 49 | F13D12.3 | II-7P22 | | tested | No Canal Phenotype |
| 50 | F13D12.8 | II-8A07 | | tested | No Canal Phenotype |
| 51 | Y38E10A.7 | II-8M20 | *lips-15* | No Bacterial Growth | Not Attempted |
| 52 | K02B7.3 | II-9C02 | | tested | No Canal Phenotype |
| 53 | Y53F4B.2 | II-9I08 | *elo-9* | No Bacterial Growth | Not Attempted |
| 54 | Y53F4B.31 | II-9O06 | *gst-28* | tested | Canal Phenotype |
| 55 | M01F1.5 | III-1F02 | *hmit-1.3* | tested | No Canal Phenotype |
| 56 | C46F11.2 | III-1H04 | *gsr-1* | tested | No Canal Phenotype |
| 57 | F58B6.2 | III-1K06 | *exc-6* | tested (Control) | Canal Phenotype |
| 58 | C44F1.3 | III-1L02 | *lec-4* | tested | No Canal Phenotype |
| 59 | C09F5.1 | III-1M19 | | tested | Canal Phenotype |
| 60 | H09G03.1 | III-1P09 | | tested | Canal Phenotype |
| 61 | B0285.6 | III-2M07 | | tested | No Canal Phenotype |
| 62 | R07E5.7 | III-2O13 | | tested | No Canal Phenotype |
| 63 | ZC155.1 | III-2P15 | *nex-1* | tested | No Canal Phenotype |
| 64 | ZK418.5 | III-3B10 | | tested | No Canal Phenotype |
| 65 | R13F6.3 | III-3H21 | *srv-1* | tested | No Canal Phenotype |
| 66 | C05D11.5 | III-3M02 | | tested | No Canal Phenotype |
| 67 | F11H8.4 | III-3P11 | *cyk-1* | tested | Canal Phenotype |
| 68 | F44B9.9 | III-4A16 | | tested | Canal Phenotype |
| 69 | K12H4.1 | III-4A18 | *pros-1* | tested | No Canal Phenotype |
| 70 | R13A5.1 | III-4A23 | *cup-5* | tested | No Canal Phenotype |
| 71 | R107.1 | III-4J02 | *nac-2* | tested | No Canal Phenotype |
| 72 | F09G8.9 | III-4K22 | *mps-4* | tested | No Canal Phenotype |
| 73 | F44B9.10 | III-4O23 | | tested | No Canal Phenotype |

| Gene Number | Gene | Clone ID | Gene ID | tested /not tested | result for tested |
|---|---|---|---|---|---|
| 74 | K11D9.3 | III-5D04 | | tested | No Canal Phenotype |
| 75 | K11H3.1 | III-5E02 | *gpdh-2* | tested | No Canal Phenotype |
| 76 | F55H2.1 | III-5E21 | *sod-4* | tested | No Canal Phenotype |
| 77 | T16H12.9 | III-5M20 | | tested | No Canal Phenotype |
| 78 | Y47D3A.15 | III-5P06 | *aakb-2* | tested | No Canal Phenotype |
| 79 | T05D4.3 | III-6B22 | | tested | Canal Phenotype |
| 80 | T25C8.1 | III-6D06 | | tested | Canal Phenotype |
| 80 | T25C8.1 | III-8C16 | | tested | lethal |
| 81 | Y41C4A.12 | III-6E21 | | tested | No Canal Phenotype |
| 82 | Y111B2A.8 | III-6I04 | *aakg-1* | tested | No Canal Phenotype |
| 82 | Y111B2A.8 | III-6I06 | *aakg-1* | tested | No Canal Phenotype |
| 82 | Y111B2A.8 | III-9A12 | *aakg-1* | tested | No Canal Phenotype |
| 83 | Y55B1BL.1 | III-7G08 | | No Bacterial Growth | Not Attempted |
| 84 | Y75B8A.26 | III-8A15 | *mrp-8* | tested | No Canal Phenotype |
| 85 | C05D10.4 | III-8E09 | | tested | No Canal Phenotype |
| 86 | ZK688.10 | III-8G12 | | tested | No Canal Phenotype |
| 87 | Y47D3B.11 | III-8H06 | *plr-1* | tested | No Canal Phenotype |
| 88 | T02C1.2 | III-8M08 | | tested | No Canal Phenotype |
| 89 | C35B1.5 | IV-10B15 | | tested | No Canal Phenotype |
| 90 | F20D12.5 | IV-10B16 | *exc-9* | tested | No Canal Phenotype |
| 91 | C50A2.3 | IV-1I18 | | tested | No Canal Phenotype |
| 92 | C09G12.8a | IV-1J04 | *ced-10* | tested | No Canal Phenotype |
| 93 | R05C11.3 | IV-1J15 | *mca-2* | No Bacterial Growth | Not Attempted |
| 94 | W03D2.5 | IV-2E05 | *wrt-5* | tested | No Canal Phenotype |
| 95 | C10G6.1 | IV-3A19 | *egal-1* | tested | Canal Phenotype |
| 96 | F55G1.15 | IV-3D10 | | tested | No Canal Phenotype |
| 97 | R05G6.6 | IV-3D22 | *glt-6* | tested | No Canal Phenotype |
| 98 | R13A1.2 | IV-3H09 | *kcc-1* | tested | No Canal Phenotype |
| 98 | R13A1.2 | IV-3H17 | *kcc-1* | tested | No Canal Phenotype |
| 98 | R13A1.2 | IV-3H19 | *kcc-1* | tested | No Canal Phenotype |
| 99 | D1046.4 | IV-4H01 | | tested | No Canal Phenotype |
| 100 | C53B4.1 | IV-4H05 | *suex-2* | tested | Suppressor for exc-5 |
| 101 | F42G8.11 | IV-4I15 | *sph-1* | tested | No Canal Phenotype |
| 102 | F56H11.2 | IV-4N20 | | tested | No Canal Phenotype |
| 103 | F35H10.4 | IV-4O13 | *vha-5* | tested | Canal Phenotype |
| 104 | C33D9.1 | IV-4O24 | *exc-5* | Not tested | Not Attempted |
| 105 | T05A1.5 | IV-4P10 | | tested | No Canal Phenotype |
| 105 | T05A1.5 | IV-4P12 | | tested | No Canal Phenotype |
| 105 | T05A1.5 | IV-4P16 | | tested | No Canal Phenotype |
| 106 | F27C8.1 | IV-4P18 | *aat-1* | tested | No Canal Phenotype |

| Gene Number | Gene | Clone ID | Gene ID | tested /not tested | result for tested |
|---|---|---|---|---|---|
| 107 | F27C8.2 | IV-4P20 | | tested | No Canal Phenotype |
| 108 | W09C2.3 | IV-5A07 | *mca-1* | tested | No Canal Phenotype |
| 109 | W01B6.3 | IV-5C04 | | tested | No Canal Phenotype |
| 110 | K08F4.4 | IV-5G22 | *glt-3* | tested | No Canal Phenotype |
| 111 | F32B6.9 | IV-5K21 | *best-13* | tested | No Canal Phenotype |
| 112 | F44D12.2 | IV-5O13 | | tested | No Canal Phenotype |
| 112 | F44D12.2 | IV-5O15 | | tested | No Canal Phenotype |
| 113 | C06G8.3 | IV-5P11 | | tested | No Canal Phenotype |
| 114 | F54D1.4 | IV-6C03 | *nhr-7* | tested | No Canal Phenotype |
| 115 | F54D1.5 | IV-6C05 | *gtl-2* | tested | No Canal Phenotype |
| 116 | H01G02.1 | IV-6C24 | | tested | No Canal Phenotype |
| 117 | K08E4.3 | IV-6M04 | | tested | No Canal Phenotype |
| 118 | ZK795.1 | IV-6N21 | | tested | No Canal Phenotype |
| 119 | C39E9.2 | IV-6P06 | *scl-5* | tested | No Canal Phenotype |
| 120 | C39E9.7 | IV-6P16 | | tested | No Canal Phenotype |
| 121 | B0564.3 | IV-7A11 | *best-1* | tested | No Canal Phenotype |
| 122 | Y37A1A.3 | IV-7I12 | | tested | No Canal Phenotype |
| 123 | Y45F10A.3 | IV-7M07 | *afmd-2* | No Bacterial Growth | Not Attempted |
| 124 | Y55F3BR.6 | IV-8N07 | | tested | No Canal Phenotype |
| 124 | Y55F3BR.6 | IV-8N05 | | No Bacterial Growth | Not Attempted |
| 125 | ZC168.1 | IV-9A13 | *ncx-3* | tested | No Canal Phenotype |
| 126 | H32C10.2 | IV-9D19 | *lin-33* | tested | No Canal Phenotype |
| 127 | Y37E11AR.5 | IV-9E06 | *ugt-45* | tested | No Canal Phenotype |
| 128 | C34D4.9 | IV-9F07 | *nas-8* | tested | No Canal Phenotype |
| 129 | Y51H4A.3 | IV-9L11 | *rho-1* | tested | Lethal |
| 130 | K08F4.12 | IV-9P14 | | tested | No Canal Phenotype |
| 131 | T06C12.10 | V-10D05 | *cgt-1* | tested | No Canal Phenotype |
| 132 | C55A1.6 | V-10E06 | | tested | No Canal Phenotype |
| 133 | F11A5.13 | V-10H10 | | tested | No Canal Phenotype |
| 134 | C18D4.4 | V-11B16 | | tested | No Canal Phenotype |
| 135 | Y59A8B.23 | V-11L08 | *gck-3* | tested | Canal Phenotype |
| 135 | Y59A8B.23 | V-11L10 | *gck-3* | tested | Canal Phenotype |
| 136 | Y43F8C.7 | V-12J11 | | tested | No Canal Phenotype |
| 137 | Y51A2D.5 | V-12K03 | *hmit-1.2* | tested | No Canal Phenotype |
| 138 | Y39B6A.27 | V-12K06 | | tested | No Canal Phenotype |
| 139 | Y39B6A.29 | V-12K08 | | tested | No Canal Phenotype |
| 140 | T13F3.5 | V-14C12 | *fbxa-2* | tested | No Canal Phenotype |
| 141 | Y43F8C.12 | V-14E13 | *mrp-7* | tested | No Canal Phenotype |
| 142 | K11D12.9 | V-14L15 | | tested | Canal Phenotype |
| 143 | T01G6.2 | V-14N17 | *nhr-131* | tested | No Canal Phenotype |

| Gene Number | Gene | Clone ID | Gene ID | tested /not tested | result for tested |
|---|---|---|---|---|---|
| 144 | B0222.3 | V-15G14 | *pitr-3* | tested | No Canal Phenotype |
| 145 | T28A11.11 | V-15P06 | *gst-23* | tested | No Canal Phenotype |
| 145 | T28A11.11 | V-2N04 | *gst-23* | tested | No Canal Phenotype |
| 146 | T22F3.6 | V-15P09 | *srh-212* | tested | No Canal Phenotype |
| 147 | C03G6.5 | V-16K12 | | tested | Canal Phenotype |
| 148 | F59D6.7 | V-2B12 | *chpf-2* | tested | No Canal Phenotype |
| 149 | K02G10.7 | V-2D20 | *aqp-8* | tested | No Canal Phenotype |
| 150 | T08H10.1 | V-3B06 | | tested | Canal Phenotype |
| 151 | R08F11.1 | V-3C24 | | tested | No Canal Phenotype |
| 152 | T24A6.20 | V-3M15 | | No Bacterial Growth | Not Attempted |
| 153 | T22F3.7 | V-3O19 | | tested | No Canal Phenotype |
| 154 | C24G6.2 | V-4C14 | | tested | No Canal Phenotype |
| 155 | C18C4.2 | V-4E06 | *cft-1* | tested | No Canal Phenotype |
| 156 | M03E7.2 | V-4G18 | | tested | No Canal Phenotype |
| 157 | T10H9.1 | V-4J08 | | tested | No Canal Phenotype |
| 158 | F44E7.6 | V-4M12 | *fbxa-183* | tested | Canal Phenotype |
| 158 | F44E7.6 | V-4M14 | *fbxa-183* | tested | Canal Phenotype |
| 159 | F44E7.8 | V-4M16 | *nhr-142* | tested | No Canal Phenotype |
| 160 | F19F10.3 | V-5B13 | | tested | No Canal Phenotype |
| 161 | T19F4.1 | V-5C05 | *frpr-18* | tested | No Canal Phenotype |
| 162 | C33G8.5 | V-5E15 | *srab-4* | tested | No Canal Phenotype |
| 163 | C03G6.17 | V-5G10 | | tested | No Canal Phenotype |
| 164 | T05B11.4 | V-5L01 | | tested | No Canal Phenotype |
| 165 | C08D8.2 | V-6A03 | *tmd-2* | tested | No Canal Phenotype |
| 166 | B0507.9 | V-6C02 | | tested | No Canal Phenotype |
| 167 | F40F9.2 | V-6D18 | *tag-120* | tested | No Canal Phenotype |
| 168 | C25E10.5 | V-6K06 | | tested | No Canal Phenotype |
| 169 | F57A8.7 | V-7A19 | | tested | No Canal Phenotype |
| 170 | F22E12.2 | V-7A20 | *chw-1* | tested | No Canal Phenotype |
| 171 | F58B4.1 | V-7B19 | *nas-31* | tested | No Canal Phenotype |
| 172 | Y32F6B.3 | V-7C06 | *crp-1* | tested | No Canal Phenotype |
| 173 | Y32F6B.3 | V-7C06 | *crp-1* | tested | No Canal Phenotype |
| 174 | F17C11.12 | V-7D03 | | tested | No Canal Phenotype |
| 175 | F32G8.3 | V-7E16 | | tested | No Canal Phenotype |
| 176 | C51E3.6 | V-7E23 | | tested | No Canal Phenotype |
| 177 | F53B7.7 | V-7F03 | | tested | No Canal Phenotype |
| 178 | R31.1 | V-8C09 | *sma-1* | Not tested | Not Attempted |
| 179 | F32H5.4 | V-8H02 | | tested | No Canal Phenotype |
| 180 | T07F10.1 | V-8H09 | | tested | No Canal Phenotype |
| 181 | C27A7.3 | V-8K19 | | tested | No Canal Phenotype |

| Gene Number | Gene | Clone ID | Gene ID | tested /not tested | result for tested |
|---|---|---|---|---|---|
| 182 | F53F4.1 | V-8P10 | | tested | No Canal Phenotype |
| 183 | F53F4.6 | V-8P20 | *rdy-2* | tested | No Canal Phenotype |
| 184 | F58G11.4 | V-9A23 | | tested | No Canal Phenotype |
| 185 | F47B8.8 | V-9M20 | | tested | No Canal Phenotype |
| 186 | M6.1 | X-1G15 | *ifc-2* | tested (Control) | Canal Phenotype |
| 187 | T19D7.7 | X-1I11 | | tested | No Canal Phenotype |
| 188 | ZK563.6 | X-2A10 | *acp-1* | tested | No Canal Phenotype |
| 189 | T06F4.2 | X-2D07 | *clh-4* | tested | No Canal Phenotype |
| 190 | K02G10.8 | X-2D22 | *dnj-14* | tested | No Canal Phenotype |
| 191 | F20B6.2 | X-2F09 | *vha-12* | No Bacterial Growth | Not Attempted |
| 192 | K05B2.3 | X-2J08 | *ifa-4* | Not tested | Not Attempted |
| 193 | H28G03.6 | X-3A07 | *mtm-5* | tested | No Canal Phenotype |
| 194 | C54D1.4 | X-3B14 | *alh-10* | tested | No Canal Phenotype |
| 194 | C54D1.4 | X-3B18 | *alh-10* | tested | No Canal Phenotype |
| 195 | F46H5.3 | X-3D18 | | tested | No Canal Phenotype |
| 196 | F35C8.6 | X-3E05 | *pfn-2* | tested | No Canal Phenotype |
| 197 | C45B2.8 | X-3E06 | | tested | No Canal Phenotype |
| 198 | T13C5.4 | X-3I10 | *ceh-54* | tested | No Canal Phenotype |
| 199 | C14F11.5 | X-3I24 | *hsp-43* | tested | No Canal Phenotype |
| 200 | W01C8.1 | X-3K11 | | tested | No Canal Phenotype |
| 201 | C01C10.3 | X-3L02 | *acl-12* | tested | No Canal Phenotype |
| 202 | F46C8.1 | X-3L24 | | tested | No Canal Phenotype |
| 203 | F46G11.2 | X-3M21 | | tested | No Canal Phenotype |
| 204 | F49E2.1 | X-4B24 | | tested | No Canal Phenotype |
| 205 | R09F10.4 | X-4C02 | *inx-5* | tested | No Canal Phenotype |
| 206 | F40B5.2 | X-4E04 | | tested | No Canal Phenotype |
| 207 | F16F9.1 | X-4G08 | | tested | No Canal Phenotype |
| 208 | F48C5.1 | X-5B17 | *igeg-2* | tested | No Canal Phenotype |
| 209 | T21B6.2 | X-5C22 | *pho-7* | tested | No Canal Phenotype |
| 210 | F41E7.1 | X-5E01 | | tested | Canal Phenotype |
| 211 | F41E7.2 | X-5E03 | | tested | No Canal Phenotype |
| 212 | F52D10.1 | X-5F03 | *abts-2* | tested | No Canal Phenotype |
| 213 | R07E3.7 | X-5G05 | | tested | No Canal Phenotype |
| 214 | R07A4.4 | X-5O13 | | tested | No Canal Phenotype |
| 214 | R07A4.4 | X-8L12 | | tested | No Canal Phenotype |
| 215 | ZK455.7 | X-8A21 | *pgp-3* | tested | No Canal Phenotype |
| 215 | ZK455.7 | X-5O16 | *pgp-3* | No Bacterial Growth | Not Attempted |
| 216 | F42E11.1 | X-5O20 | *pgp-4* | tested | No Canal Phenotype |
| 216 | F42E11.1 | X-8A22 | *pgp-4* | tested | No Canal Phenotype |
| 217 | F48F7.2 | X-6D17 | *syx-2* | tested | No Canal Phenotype |

| Gene Number | Gene | Clone ID | Gene ID | tested /not tested | result for tested |
|---|---|---|---|---|---|
| 217 | C09F12.3 | X-8B03 | | tested | No Canal Phenotype |
| 218 | C46E1.3 | X-8B08 | *exc-1* | tested (Control) | Canal Phenotype |
| 218 | F02C12.1 | X-6E02 | | tested | No Canal Phenotype |
| 219 | R01E6.3 | X-6I20 | *cah-4* | tested | No Canal Phenotype |
| 219 | Y34B4A.4 | X-8D15 | | tested | No Canal Phenotype |
| 220 | R03E1.1 | X-6J15 | *sym-4* | tested | No Canal Phenotype |
| 220 | C35C5.4 | X-8F03 | *mig-2* | tested | No Canal Phenotype |
| 221 | C37E2.5 | X-6L05 | *ceh-37* | tested | Canal Phenotype |
| 221 | R02E4.3 | X-8I06 | | tested | No Canal Phenotype |
| 222 | F09A5.2 | X-6M11 | | tested | No Canal Phenotype |
| 223 | F55F3.1 | X-6O16 | *aakb-1* | tested | No Canal Phenotype |
| 224 | T01C8.1 | X-7D05 | *aak-2* | tested | No Canal Phenotype |
| 225 | F39D8.4 | X-7I01 | *nas-13* | tested | No Canal Phenotype |
| 226 | K09A9.3 | X-7K19 | *ent-2* | tested | No Canal Phenotype |

# Chapter 4: Other projects and hindrances.

### 4.1 Detecting the subcellular location of *exc-1*:

#### 4.1.1 Rationale:

The cloning and characterization of *exc-1* gene was done by Dr. Kelly Grussendorf. She found that the *exc-1* gene encodes for an IRG-homologue protein, and via yeast 2-hybrid experiment she found that EXC-1 binds to EXC-9 directly. It was already established that the genes *exc-5, exc-1* and *exc-9* function in a common genetic pathway, in which *exc-9* is upstream of *exc-1*, and *exc-1* is upstream of *exc-5*. These genes work in the apical recycling-machinery, by transporting recycled material between the apical membrane and the recycling endosome. Dr. Grussendorf's work was published in *Genetics* volume 203, pp. 1789-1806, '16. My contribution in this work was to show that labeled EXC-1 is located throughout the cytoplasm of the canal, but is enriched at the apical membrane of the canal, where it is colocalized with the apical marker ERM-1. The subcellular localization helped in characterizing the function of EXC-1.

#### 4.1.2 Experimental plan:

The subcellular location of *exc-1* was identified through expressing plasmid pBK109, which contains *gfp*-tagged cDNA of *exc-1* expressed under the control of the *vha-1* promoter. This construct was expressed in a worm strain that harbored the *erm-1* gene tagged with *mCherry*, along with *rol-6*. ERM-1 served as an apical membrane for the canal. A confocal microscope was then used to detect the fluorescent signals. Finally, the results were quantified by use of ImageJ software to measure the intensity of each fluorophore signal along a path in a straight line perpendicular to the extension of the canal lumen.

### 4.1.3 Results and discussion:

EXC-1 was found throughout the canal cytoplasm, and the labeled protein overlapped with the apical marker ERM-1. These results are in agreement with EXC-1 functioning as a part of the transportation machinery at the apical membrane. In fact, a similar pattern of expression was shown for EXC-5, which further confirms a common function of these three EXC proteins in the canal.

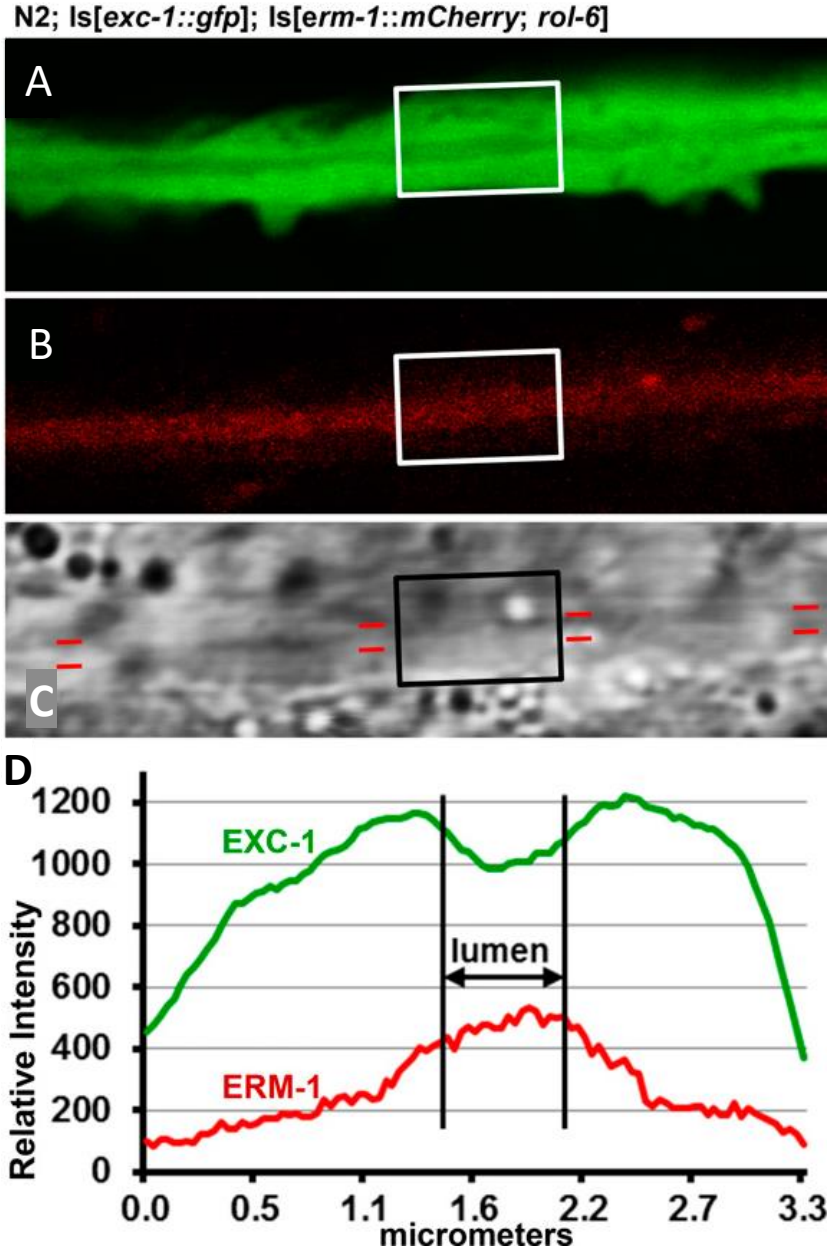


**Figure 4.1 Subcellular location of EXC-1 in the excretory canal.**

A confocal image of excretory canal expressing GFP tagged EXC-1 along with mCherry tagged ERM-1, as apical membrane marker.

A. GFP signal of EXC-1-tagged protein ($P_{vha\text{-}1}$*::exc-1::gfp*).
B. mCherry signal of ERM-1-tagged protein.
C. DIC image for the same section of the canal.
D. Plot measuring the intensity of each fluorophore signal. Adapted from [1].

### 4.2 Endosomal study in *exc-2* (*rh90*) mutants:

#### 4.2.1 Rationale:

The biological pathway of *exc-1*, *exc-5*, and *exc-9* was studied previously in our laboratory. In an epistasis study, *exc-9* was shown to work upstream of both *exc-1* and *exc-5* [36]. The same study suggested a possible role for *exc-2* in this pathway, as *exc-9* overexpression partially rescued *exc-2* mutants. This study was carried out at a time when *exc-2* was not cloned yet and its protein identity was unknown. As a result, such a role for *exc-2* in this pathway was not possible to confirm by injecting *exc-2* DNA into *exc-9* mutants. Since I faced a lot of complications during the process of cloning the *exc-2* gene, this piece of information attracted me to further investigate EXC-2's role in vesicle movement, while continuing attempts to clone the gene. I decided to study the endosomal compartments in *exc-2* mutants and investigate whether these endosomes show similar characteristics as seen in *exc-1* and *exc-5* mutants. In *exc-1* and in *exc-5* mutants, early endosomes show an enlargement in size as a presumed consequence of continued accumulation of recycled material into early endosomes. At the same time, these mutants show a reduction in recycling endosomes. I expected to find similar phenotypes in *exc-2* mutants if the protein functions in recycling machinery along with EXC-1 and EXC-5.

#### 4.2.2 Experimental plan:

Mutants of *exc-2*(*rh90*) were crossed to worms carrying mCherry-tagged endosomal markers. The *rab-5* and *eaa-1* genes were used as markers for early endosomes, and *rab-11* and *rme-1* as markers for recycling endosomes. Subsequently, the fluorescently-labelled vesicles (seen as small puncta) in the outcrossed strains were analyzed in terms of size and direction of

movement. Finally I performed Fluorescence Recovery After Photobleaching (FRAP) assays to examine the rapidity at which labelled vesicles moved within the canal cytoplasm. All of these studies were done via confocal microscopy. Puncta size and the FRAP-assay analysis were done using ImageJ software on samples taken from *exc-2* and from N2 worms as a control.

**4.2.3 Results:**

I found that *exc-2* mutants were unable to mimic the observations for both early and recycling endosomes as seen in *exc-1* and *exc-5* mutants. The sizes of early and recycling endosomes were normal and comparable with those in wild-type worms. Also, the puncta movements were comparable between *exc-2* mutants and wild-type animals. These puncta were active and moving in both directions, anteriorward and posteriorward. In fact, some puncta were seen changing directions (Figure 4.2).

For the FRAP assay, I bleached both cytosolic areas and individual puncta for both RAB-5-labelled early endosomes and for RAB-11 recycling endosomes in *exc-2* mutants and in wild-type backgrounds. Recovery of fluorescence of cytosolic molecules of labeled RAB-5 and RAB-11 are not affected by *exc-2* mutation. A difference was seen, however, with RAB-5 and RAB-11 bound to their target compartments. While puncta carrying marked RAB-5 recovered rapidly after bleaching in both wild-type and *exc-2* backgrounds (Figure 4.3). puncta of RAB-11 molecules exhibited a different behavior. In the wild-type background, bleached puncta recovered fluorescence fully within 180 seconds. When *exc-2* was mutated, however, recovery was essentially halted, with no significant increase in fluorescence visible after 280 seconds. This result suggests that EXC-2 function is required for turnover of RAB-11 on the recycling endosome (Figure 4.4).

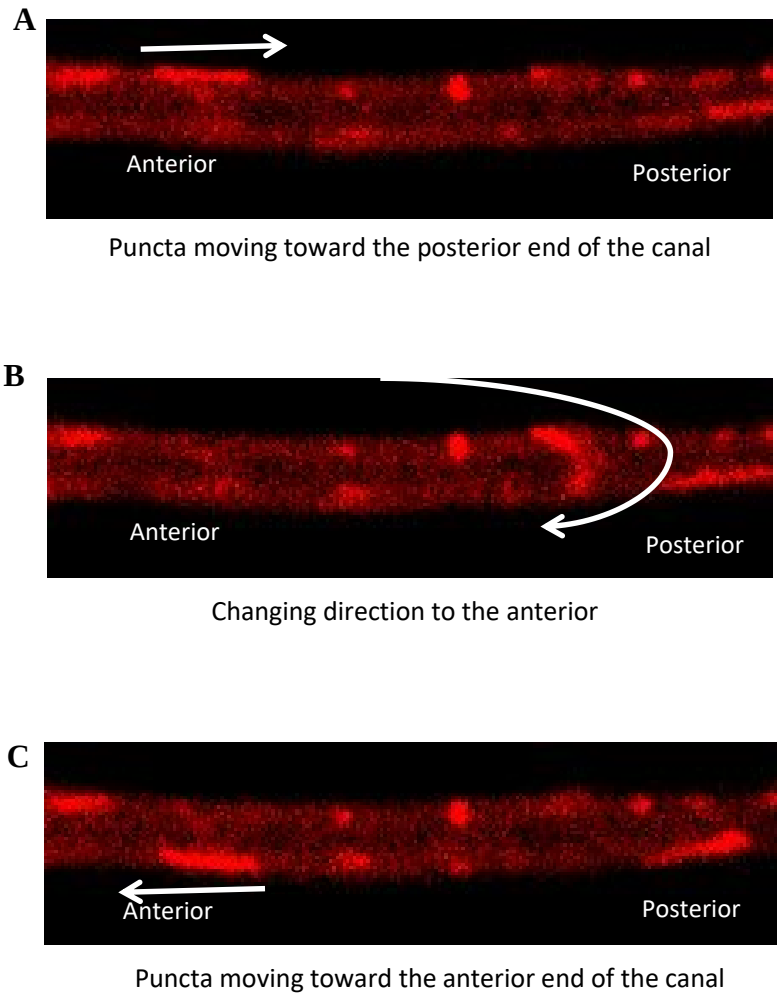


**Figure 4.2 Recycling endosome movement via RAB-11 labeling.**

Recycling endosome movement via RAB-11 labeling, in wild-type background. The traced punctum (recycling endosome) changes its direction of motion.

A. Punctum is moving from the anterior side of the canal toward the posterior end.
B. The punctum changes its direction and turns.
C. The punctum continues in the opposite direction toward the anterior end of the canal.

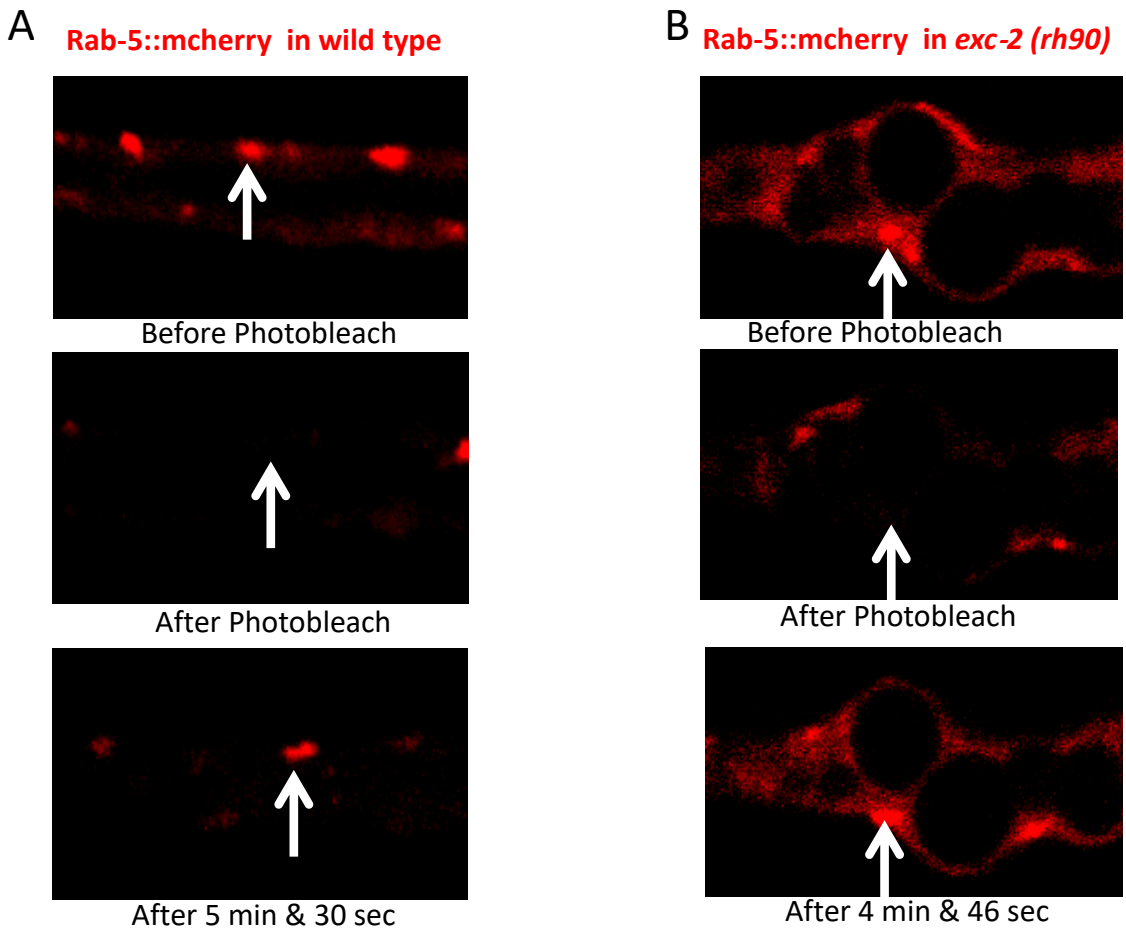


**Figure 4.3 FRAP assay of labeled RAB-5.**

RAB-5 (Early endosome) puncta reappear after photobleaching in wild-type & *exc-2* worms.

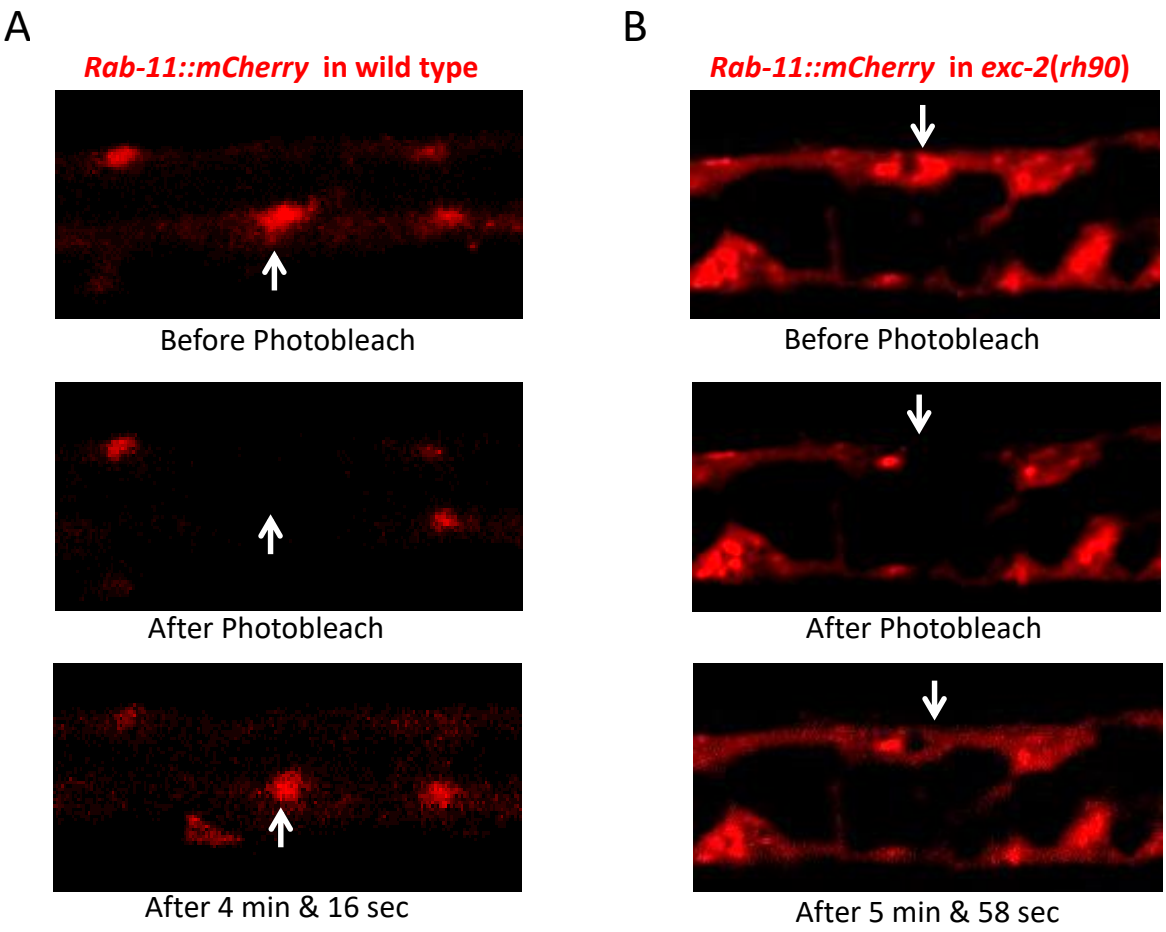


**Figure 4.4 FRAP assay of labeled RAB-11**

RAB-11 (Recycling endosome) puncta reappear after photobleaching in wild-type but NOT in *exc-2* worms.

### 4.3 *C. elegans* to study the virulence of *Enterococcus faecalis*:

#### 4.3.1 Rationales:

*Enterococcus faecalis* is a Gram-positive opportunistic and pathogenic bacterium. Due to its multi-drug resistance, it is considered one of the most problematic pathogens associated with hospital-acquired infections. Hospitalized patients with a compromised immune system, when treated with antibiotics, are susceptible to *E. faecalis* infections. The bacteria colonize the gut and subsequently propagate intensively in the colon [94].

Through conjugation, *E. faecalis* is able to exchange genetic material horizontally to acquire new virulence genes as well as drug resistance. The OligoPeptide Permease (Opp) is responsible for the import of peptide pheromones that initiate the conjugation step. The Opp complex is composed of five proteins (OppA, OppB, OppC, OppD, and OppF). The donor cell in the conjugation step acquires pheromone secreted from the recipient cell; acquiring this pheromone is vital to activate pheromone response in donor cells, and hence start the conjugation process [95-97].

The clinical isolate strain V583 is resistant to many antibiotics, including vancomycin, which often is considered as a last resort [98]. Despite its multidrug resistance, the strain V583 was shown to be sensitive to flora extracted from fecal samples [99]. It was shown by Dr. Hancock's laboratory, that this lethality is due to cross-talk between mobile elements in the shared environment, and that this cross-talk is induced by pheromones produced by fecal cultures [99].

Next, Dr. Hancock wanted to test whether the Opp complex, along with a novel second Opp complex (to be referred to here as Opp2, while the previous one is Opp1) contribute in

pheromone-mediated mating, and whether they play a role in bacterial biofilm development and virulence. One of the tests that evaluated the need for oligopeptide permease in terms of virulence was a worm-killing assay using *C. elegans*. Performing that assay was my contribution in this study.

The effect of *E. faecalis* on *C. elegans* has been described by many groups, and has been used as a model for infection by *E. faecalis* [100-102] Virulence factors often affect the ability of the bacteria to form a biofilm, and also contribute in its virulence in *C. elegans* [100, 102]. Even a small number of bacterial cells is enough to colonize and proliferate in the gut of *C. elegans*, and to kill the worm within five to ten days post-exposure [102]. I performed the worm-killing assay using strain V853 along with other mutant strains derived from V853 (V583Δ*opp1*, V583Δ*opp2*, and V583Δ*opp1*Δ*opp2*) in order to evaluate the effects of Opp1 and Opp2 on the virulence of *E. faecalis*. Strain Δ*pptAB* was utilized as a negative control for pheromone effects, since the Hancock lab has shown that this mutant strain fails to secrete the synthesized pheromone peptide outside of the bacterial cell. Furthermore, they showed that this strain forms an attenuated biofilm similar to that of a strain deleted for both *opp1* and *opp2*.

### 4.3.2 Experimental procedure:

BHI agar was used to culture different strains of *E. faecalis*: V583, V583 Δ*pptAB*, V583Δ*opp1*, V583Δ*opp2*, and V583Δ*opp1*Δ*opp2*. These bacteria were cultured at 37ºC for 24 hours until they formed bacterial lawns. Next, 10-15 worms at the L4-to-young adult stages were placed on the bacterial lawns, and their progeny's survival was evaluated every 24 hours for seven days. The results were recorded in a graph (GraphPad Prism, San Diego, CA), and statistically evaluated by use of the Mantle-Cox log-rank test.

### 4.3.3 Results and discussion:

As shown in Figure 4.3, the worms did not show a significant difference between response to the mutant V583Δ*opp2* and response to the wild-type, which suggests that the Opp2 complex exerts only a mild effect on bacterial virulence. In comparison to V583Δ*opp2,* the mutant V583Δ*opp1* exerted a significant difference than did the wild-type bacteria on nematode growth, which suggests that the Opp1 complex plays a more essential role for bacterial virulence (Figure 4.5 A).

On the other hand, the double mutant V583Δ*opp1*Δ*opp2* and the pheromone-transporter mutant V583 Δ*pptAB* showed similar attenuated killing in worms. In a different experiment, the Hancock laboratory showed that these mutants also showed a similar ineffectiveness in biofilm formation. These results indicate that both of the Opp protein complexes are needed for strong virulence of *E. faecalis,* as is the need for the peptide pheromone transporter PptAB (Figure 4.5 B).

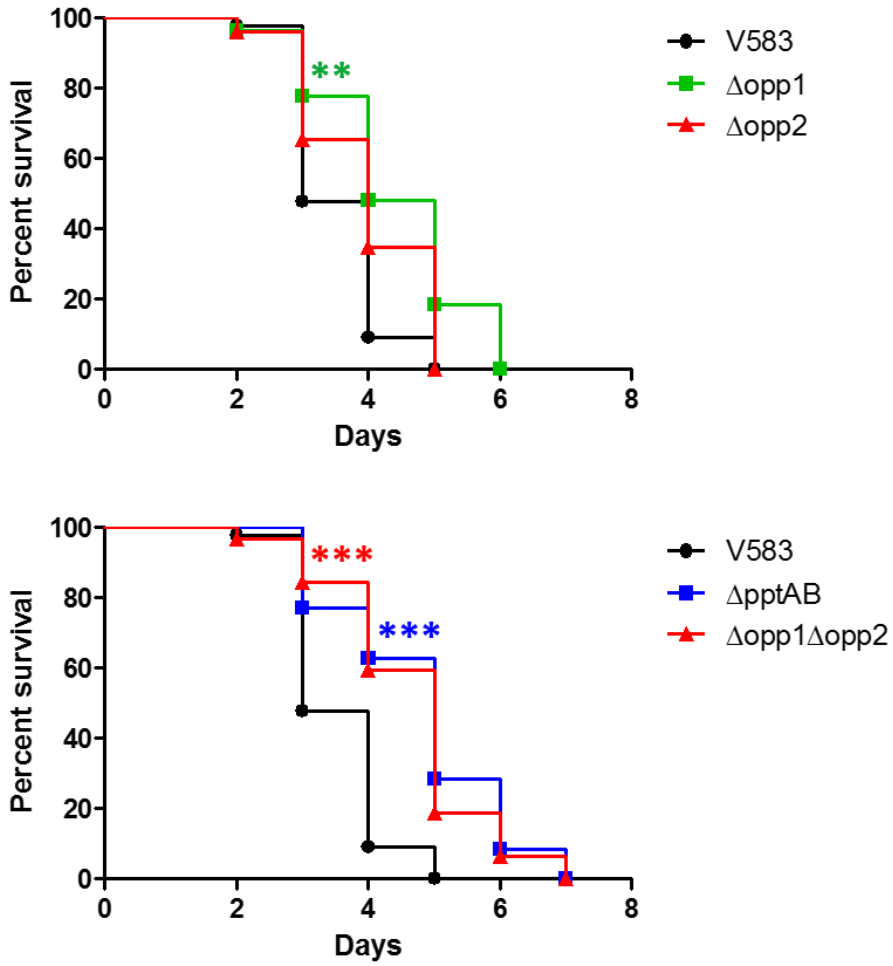


**Figure 4.5 The effect of the oligopeptide permease complexes 1 and 2 (Opp1 and Opp2) along with the pheromone-transporter on *E. faecalis* virulence via worm-killing assay.**

Effect on nematode longevity from growth on V583 (black), V583*Δopp1* (green), and V583*Δopp2*(red) bacteria.

Effect on nematode longevity from growth on V583 (black), V583*ΔpptAB* (blue), and V583*Δopp1Δopp2*(red).

### 4.4. Obstacles and hindrances:

#### 4.4.1 Cloning *exc-2*

Cloning and characterizing *exc-2* was my major project in the laboratory. Since the late nineties many previous lab members tried unsuccessfully to clone the gene and identify the DNA sequence of *exc-2*. The gene was previously-roughly mapped via three-point crosses towards the left side of chromosome X, between the genes *mec-2* and *dpy-8* [22]. This chromosomal region is about 450kb in length and contains a few more than 170 genes. Initially I injected 12 different fosmids covering most of this region. After injecting the 12 fosmids individually and in combinations of overlapping fosmids, I did not score any rescued worms, which indicates that either the fosmids do not cover that gene or the gene is not in the mapped region. To address the first possibility, a set of dsRNAs specific for the nine genes not included in fosmids in the region were injected into gonads of wild-type N2 worms, and the progeny were scored for a phenotype that mimics *exc-2*. None of these genes exhibited the Exc-2 phenotype in the canal (Figure 4.6).

Eventually, we decided to determine the site of the mutation in *exc-2*(*rh90*) through use of whole-genome sequencing. In order to confirm the locus of the gene, I outcrossed *exc-2* (*rh90*) animals to wild-type Hawaiian strain CB4856, picked cystic F2 worms from this cross, and subjected them to sequencing. The fact that all *exc-2* mutants are recessive guarantees that all the F2 worms picked were *exc-2* mutants as long as they were cystic. At the same time, the cross mixed the DNA sequences between two backgrounds (i.e. Single Nucleotide Polymorphisms (SNPs)) randomly among the F2 worms except for the area in proximity to the *exc-2* locus. Whole-genome sequencing of pooled F2 *exc-2* mutants shows the location of the *exc-2* gene as the locus where all of the SNPs correspond to those of the *exc-2* parent, derived

from the Bristol wild-type strain N2.

### 4.2.2 Whole-genome sequence reference error.

Comparison of sequences in the region predicted by whole-genome sequencing to have few Hawaiian SNPs showed that the *ifa-4* gene contained a frameshift mutation in comparison to the sequence of the wild-type N2 genome. The RNAi knockdown of the *ifa-4* gene showed a phenotype that mimics that of *exc-2*. Additionally, the knockout strain *ok1734* also showed a cystic canal similar to those found in *exc-2* mutants. The last step of confirming the link between the *ifa-4* and *exc-2* genes was to rescue *exc-2* mutants through microinjection of the cloned *ifa-4* gene. Surprisingly, the cDNA of *ifa-4* failed to rescue *exc-2* mutants, while it successfully rescued the *ifa-4* knockout mutant (*ok1734*). Furthermore, a complementation test showed that *exc-2*(*rh90*) and *ifa-4*(*ok1734*) were non-allelic, and instead that they were different genes! Furthermore, Sequencing *ifa-4* gene from wild-type worms also showed the same nucleotide insertion at the same position. It was a big surprise to find that the reference whole-genome sequence that was published by wormbase.org (WS220) had an erroneous one-nucleotide deletion that made our sequences appear to have a one-nucleotide insertion in comparison. This reference genome error was addressed in later versions in Wormbase. (Figure 4.8).

We had to start from the beginning, using three additional alleles of *exc-2*, all of which have different mutations in the same, correct gene, *ifc-2*, as described in Chapter 2. Nevertheless, this work provided the identity of a novel gene that contributes in canal maintenance that had not been previously reported, *ifa-4*. Interestingly, I found later on that both *ifa-4* and *exc-2*/*ifc-2* work together to provide the needed support to maintain the canal apical-membrane.

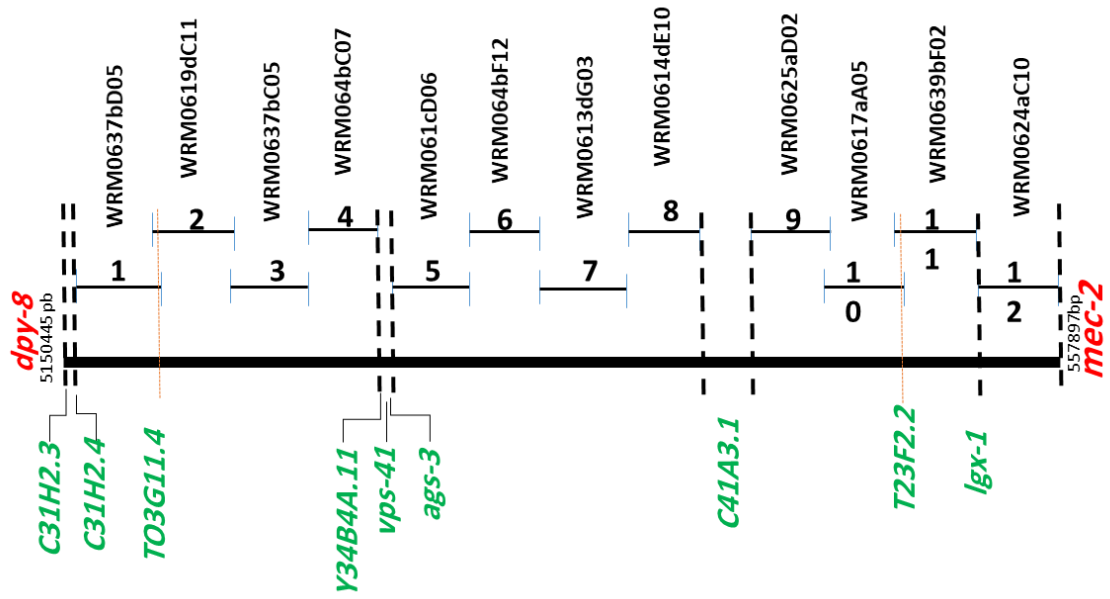


**Figure 4.6 Mapping of the *exc-2* gene via three-point crossing.**

To-scale scheme showing the region between *mec-2* and *dpy-8*. The region is mostly covered by DNA contained in twelve fosmids (1-12), while uncovered genes (in green) were knocked down through use of RNAi.

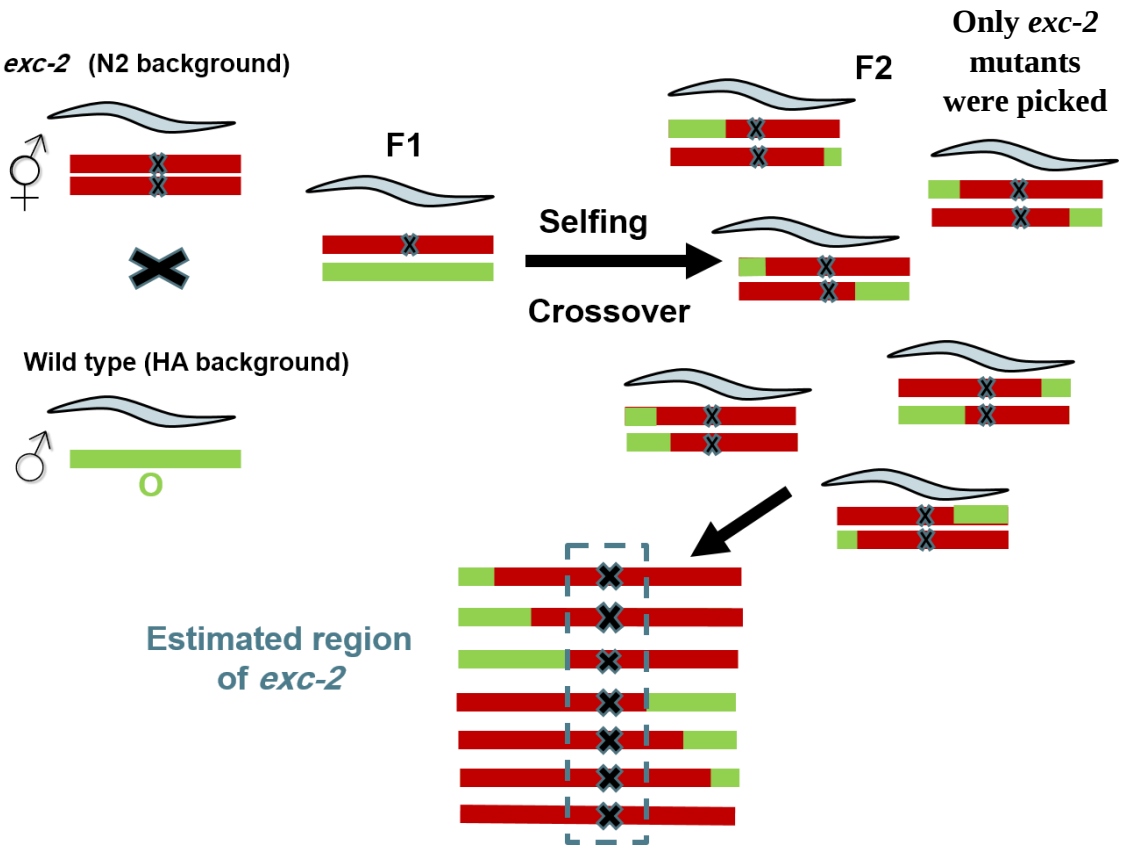


**Figure 4.7 Outcrossing *exc-2* mutants to Hawaiian wild-type.**

A schematic diagram showing the steps of outcrossing *exc-2* mutants to the Hawaiian wild-type strain. In order to narrow down the region of the *exc-2* gene, *exc-2* hermaphrodites were crossed to Hawaiian males. The F1 animals were all heterozygous and non-phenotypic for *exc-2* mutations. The F2 were picked only if cystic and hence *exc-2* mutant in both gene copies. Finally, genomes from 12 different F2 populations were subjected to whole-genome sequencing. Areas with all N2 SNPs indicate region of the *exc-2* gene.


**Figure 4.8 Genome reference of wild-type contained a nucleotide deletion in the gene *ifa-4*.**

Results of alignment of part of the *ifa-4* gene, showing DNA sequences in *exc-2*, *exc-1*, and *exc-3* strains along with the old (WS220) and current (WS246) whole-genome sequence of the N2 reference strain. All strains have the same nucleotide insertion in comparison to the obsolete genome reference (WS220). The later version genome reference (WS246) fixed the issue and shows the nucleotide at the position (X:4914716).

# Chapter 5: Conclusion.

I can divide my contribution into the field of tubulogenesis and tube maintenance into two main parts: cloning of *exc-2* and characterizing its function; and identifying novel genes that contribute in canal formation and/or maintenance. Some of these novel genes are of unknown function or phenotype in the worm, while others had not previously been reported to function in the excretory canal.

Since 1998, cloning of *exc-2* was undertaken in order to understand its function in the canal. The whole-genome sequencing enabled us to overcome difficulties in cloning this gene, most notably that expression of high concentrations of the gene also cause canal defects, as shown in Chapter 2. By sequencing multiple alleles, I increased the confidence of the results and identified the gene sequence. The identity of the gene as encoding for intermediate filament protein IFC-2 was not completely surprising, since many other cytoskeleton and cytoskeleton-related proteins contribute in canal maintenance. The surprise was in what was known about IFC-2 before it was identified as EXC-2.

The IFC-2 protein was previously reported to function in maintaining the tubular structure of the intestine, and had not been shown to express or function in the excretory canals. These observations contradicted what we learned about this protein, since all four alleles of *exc-2* exhibit canal cysts that can be visualized even through a dissecting microscope. At the same time, I never detected any phenotype in the intestine of these mutants, even under Nomarski microscopy at high magnification. By using robust experimental approaches, it was possible to resolve part of this contradiction. Using CRISPR/Cas9 *gfp*-knockin, I showed that *exc-2* is not expressed in the intestine, while it is expressed in other tissues including the excretory canal cell. The knock-in labels isoforms A, B, and C of the gene; it does not label isoform D which has a distinct promoter site within an intron of the other isoforms. Isoform D being responsible for the

intestinal phenotype is one possible explanation for the different observations. This hypothesis was further investigated, however, using dsRNAs that target isoform D, and the results showed that these dsRNA constructs did not induce phenotypes in the intestine. In addition, allele *rh105* harbors a deletion of an exon and splice site in Isoform D, and shows cysts in the excretory canal but no effects in the intestines.

I believe that the previous studies [71, 72] suggesting a function and expression of *exc-2* in the intestine are not accurate. Those studies relied on antibody staining to detect the location of EXC-2. Antibodies can be prone to cross-reactivity with other proteins and the intestine does have multiple intermediate filaments, such as IFB-1, which prevents cystic bulges in the intestinal lumen. In addition, it is easy to overlook staining of the narrow canals in fixed tissue, especially as the canals overlay the wide intestinal tube. In addition, more recent studies of tissue-specific expression [61] found that expression of *ifc-2* in the canal is 5-fold higher than baseline general expression, while *exc-2*/*ifa-4* is expressed below baseline levels in the intestine.

A working model of canal structure is proposed (Fig. 2.11) based on these studies and on what is known regarding intermediate filaments as structural proteins providing both support and elasticity. In this model, the formation of an intermediate-filament meshwork surrounding the apical membrane of the canal lumen gives the flexible support needed to the surface as the worm bends its body continuously during its movement. The rigid support needed for lumen extension and elongation is provided by actin filaments. The role of actin filaments may be more essential to canal formation than is the role of intermediate filaments; a mutation in the *erm-1* gene, needed for docking actin at the apical membrane, leads to almost unformed and very short canal lumens (Fig. 3.1).

There is still much to understand regarding EXC-2 and intermediate filaments in general, such as understanding the mechanism by which EXC-2 is located at and docked to the apical membrane of the canal. It would also be interesting to know if ERM-1 or its binding partners interact genetically or physically with EXC-2, since they are located at the same surface. Alternatively, since tagged EXC-2 and IFA-4 constructs have been constructed, it is now possible to perform a pull-down assay in order to identify binding partners of these proteins in the worm. The results may lead us to know the proteins that help in binding these intermediate filaments to the apical membrane, and greatly enhance our understanding of intermediate filaments in general.

In the second project to gain further insight toward tubulogenesis and tube maintenance, I performed a focused reverse genetic screen for genes highly expressed in the canal that affect the canal shape. The results led us to identify 29 genes that are needed for proper canal formation and/or maintenance. As described in chapter 3, these genes varied in phenotypes and phenotypic strength. Some of these genes affected the canal length, others affected the canal luminal diameter, and some affected both. The tested genes were also evaluated for a possible co-function with the other *exc* genes, by performing the screen in *exc-2*, *exc-3*, *exc-4*, *exc-5*, and *exc-7* backgrounds in addition to a wild-type background. The results identified two suppressor genes for *exc-5* mutants. EXC-5 is a guanine exchange factor and is homologous to human FGD proteins. As mutations in different human homologues of *exc-5* are the locus of Aarskog-Scott Syndrome and Charcot-Tooth-Marie Disease Type 4H, the identification of these suppressors may not only lead us to a better understanding to the biological function of the EXC-5/FGD proteins, but also advance our understanding of these human diseases.

# References

1. Grussendorf, K.A., et al., *Facilitation of Endosomal Recycling by an IRG Protein Homolog Maintains Apical Tubule Structure in Caenorhabditis elegans.* Genetics, 2016. **203**(4): p. 1789-806.
2. Baer, M.M., H. Chanut-Delalande, and M. Affolter, *Cellular and molecular mechanisms underlying the formation of biological tubes.* Curr Top Dev Biol, 2009. **89**: p. 137-62.
3. Fielenbach, N. and A. Antebi, *C. elegans dauer formation and the molecular basis of plasticity.* Genes Dev, 2008. **22**(16): p. 2149-65.
4. Sundaram, M.V. and M. Buechner, *The Caenorhabditis elegans Excretory System: A Model for Tubulogenesis, Cell Fate Specification, and Plasticity.* Genetics, 2016. **203**(1): p. 35-63.
5. Corsi, A.K., B. Wightman, and M. Chalfie, *A Transparent Window into Biology: A Primer on Caenorhabditis elegans.* Genetics, 2015. **200**(2): p. 387-407.
6. Martin-Belmonte, F. and K. Mostov, *Regulation of cell polarity during epithelial morphogenesis.* Curr Opin Cell Biol, 2008. **20**(2): p. 227-34.
7. Martin-Belmonte, F., et al., *PTEN-mediated apical segregation of phosphoinositides controls epithelial morphogenesis through Cdc42.* Cell, 2007. **128**(2): p. 383-97.
8. Gassama-Diagne, A., et al., *Phosphatidylinositol-3,4,5-trisphosphate regulates the formation of the basolateral plasma membrane in epithelial cells.* Nat Cell Biol, 2006. **8**(9): p. 963-70.
9. Bryant, D.M. and K.E. Mostov, *From cells to organs: building polarized tissue.* Nat Rev Mol Cell Biol, 2008. **9**(11): p. 887-901.

10. Meng, W. and M. Takeichi, *Adherens junction: molecular architecture and regulation.* Cold Spring Harb Perspect Biol, 2009. **1**(6): p. a002899.

11. Hartsock, A. and W.J. Nelson, *Adherens and tight junctions: structure, function and connections to the actin cytoskeleton.* Biochim Biophys Acta, 2008. **1778**(3): p. 660-9.

12. Lubarsky, B. and M.A. Krasnow, *Tube morphogenesis: making and shaping biological tubes.* Cell, 2003. **112**(1): p. 19-28.

13. Sundaram, M.V. and J.D. Cohen, *Time to make the doughnuts: Building and shaping seamless tubes.* Semin Cell Dev Biol, 2017. **67**: p. 123-131.

14. Wood, W.B., *1 Introduction to C. elegans Biology*. 1988. 1988.

15. Nelson, F.K. and D.L. Riddle, *Functional study of the Caenorhabditis elegans secretory-excretory system using laser microsurgery.* J Exp Zool, 1984. **231**(1): p. 45-56.

16. Brenner, S., *The genetics of Caenorhabditis elegans.* Genetics, 1974. **77**(1): p. 71-94.

17. Dickinson, D.J., et al., *Streamlined Genome Engineering with a Self-Excising Drug Selection Cassette.* Genetics, 2015. **200**(4): p. 1035-49.

18. Hammell, C.M. and G.J. Hannon, *Inducing RNAi in C. elegans by feeding with dsRNA-expressing E. coli.* Cold Spring Harb Protoc, 2012. **2012**(12).

19. Chalfie, M., et al., *Green fluorescent protein as a marker for gene expression.* Science, 1994. **263**(5148): p. 802-5.

20. Buechner, M., *Tubes and the single C. elegans excretory cell.* Trends Cell Biol, 2002. **12**(10): p. 479-84.

21. Berry, K.L., et al., *A C. elegans CLIC-like protein required for intracellular tube formation and maintenance.* Science, 2003. **302**(5653): p. 2134-7.

22. Buechner, M., et al., *Cystic Canal Mutants in Caenorhabditis elegans Are Defective in the Apical Membrane Domain of the Renal (Excretory) Cell.* Developmental Biology, 1999. **214**: p. 227–241.

23. Hedgecock, E.M., et al., *Genetics of cell and axon migrations in Caenorhabditis elegans.* Development, 1987. **100**(3): p. 365-82.

24. Kolotuev, I., et al., *A pathway for unicellular tube extension depending on the lymphatic vessel determinant Prox1 and on osmoregulation.* Nat Cell Biol, 2013. **15**(2): p. 157-68.

25. Khan, L.A., et al., *Intracellular lumen extension requires ERM-1-dependent apical membrane expansion and AQP-8-mediated flux.* Nat Cell Biol, 2013. **15**(2): p. 143-56.

26. Lee, S.K., et al., *Vacuolar (H+)-ATPases in Caenorhabditis elegans: what can we learn about giant H+ pumps from tiny worms?* Biochim Biophys Acta, 2010. **1797**(10): p. 1687-95.

27. Baranoski, J.F., et al., *Cerebral Cavernous Malformations: Review of the Genetic and Protein-Protein Interactions Resulting in Disease Pathogenesis.* Front Surg, 2016. **3**: p. 60.

28. Zhang, L. and R.E.t. Ward, *uninflatable encodes a novel ectodermal apical surface protein required for tracheal inflation in Drosophila.* Dev Biol, 2009. **336**(2): p. 201-12.

29. Ghabrial, A.S. and M.A. Krasnow, *Social interactions among epithelial cells during tracheal branching morphogenesis.* Nature, 2006. **441**(7094): p. 746-9.

30. Uv, A., R. Cantera, and C. Samakovlis, *Drosophila tracheal morphogenesis: intricate cellular solutions to basic plumbing problems.* Trends Cell Biol, 2003. **13**(6): p. 301-9.

31. Samakovlis, C., et al., *Development of the Drosophila tracheal system occurs by a series of morphologically distinct but genetically coupled branching events.* Development, 1996. **122**(5): p. 1395-407.

32. Lenard, A., et al., *Endothelial cell self-fusion during vascular pruning.* PLoS Biol, 2015. **13**(4): p. e1002126.

33. Lenard, A., et al., *In vivo analysis reveals a highly stereotypic morphogenetic pathway of vascular anastomosis.* Dev Cell, 2013. **25**(5): p. 492-506.

34. Herwig, L., et al., *Distinct cellular mechanisms of blood vessel fusion in the zebrafish embryo.* Curr Biol, 2011. **21**(22): p. 1942-8.

35. Mattingly, B.C. and M. Buechner, *The FGD homologue EXC-5 regulates apical trafficking in C. elegans tubules.* Dev Biol, 2011. **359**(1): p. 59-72.

36. Tong, X. and M. Buechner, *CRIP homologues maintain apical cytoskeleton to regulate tubule size in C. elegans.* Dev Biol, 2008. **317**(1): p. 225-33.

37. Fujita, M., et al., *The role of the ELAV homologue EXC-7 in the developmentof the Caenorhabditis elegans excretory canals.* Developmental Biology, 2003. **256**(2): p. 290-301.

38. Praitis, V., E. Ciccone, and J. Austin, *SMA-1 spectrin has essential roles in epithelial cell sheet morphogenesis in C. elegans.* Dev Biol, 2005. **283**(1): p. 157-70.

39. McKeown, C., V. Praitis, and J. Austin, *sma-1 encodes a betaH-spectrin homolog required for Caenorhabditis elegans morphogenesis.* Development, 1998. **125**(11): p. 2087-98.

40. Shaye, D.D. and I. Greenwald, *The disease-associated formin INF2/EXC-6 organizes lumen and cell outgrowth during tubulogenesis by regulating F-actin and microtubule cytoskeletons.* Dev Cell, 2015. **32**(6): p. 743-55.

41. Maruyama, R. and D.J. Andrew, *Drosophila as a model for epithelial tube formation.* Dev Dyn, 2012. **241**(1): p. 119-35.

42. Iruela-Arispe, M.L. and G.E. Davis, *Cellular and molecular mechanisms of vascular lumen formation.* Dev Cell, 2009. **16**(2): p. 222-31.

43. Sigurbjornsdottir, S., R. Mathew, and M. Leptin, *Molecular mechanisms of de novo lumen formation.* Nat Rev Mol Cell Biol, 2014. **15**(10): p. 665-76.

44. Nelson, F.K., P.S. Albert, and D.S. Riddle, *Fine structure of the Caenorhabditis elegans secretory-excretory system.* Journal of Ultrastructural Research, 1983. **82**: p. 156-171.

45. Hahn-Windgassen, A. and M.R. Van Gilst, *The Caenorhabditis elegans HNF4alpha Homolog, NHR-31, mediates excretory tube growth and function through coordinate regulation of the vacuolar ATPase.* PLoS Genet, 2009. **5**(7): p. e1000553.

46. Wang, X. and H.M. Chamberlin, *Multiple regulatory changes contribute to the evolution of the Caenorhabditis lin-48 ovo gene.* Genes Dev, 2002. **16**(18): p. 2345-9.

47. Pu, P., et al., *The Lipocalin LPR-1 Cooperates with LIN-3/EGF Signaling To Maintain Narrow Tube Integrity in Caenorhabditis elegans.* Genetics, 2017. **205**(3): p. 1247-1260.

48. Gill, H.K., et al., *Integrity of Narrow Epithelial Tubes in the C. elegans Excretory System Requires a Transient Luminal Matrix.* PLoS Genet, 2016. **12**(8): p. e1006205.

49. Mancuso, V.P., et al., *Extracellular leucine-rich repeat proteins are required to organize the apical extracellular matrix and maintain epithelial junction integrity in C. elegans.* Development, 2012. **139**(5): p. 979-90.

50. Jones, S.J. and D.L. Baillie, *Characterization of the let-653 gene in Caenorhabditis elegans.* Mol Gen Genet, 1995. **248**(6): p. 719-26.

51. Geisler, F., et al., *A novel function for the MAP kinase SMA-5 in intestinal tube stability.* Mol Biol Cell, 2016. **27**(24): p. 3855-3868.

52. Zhu, H., A.K. Sewell, and M. Han, *Intestinal apical polarity mediates regulation of TORC1 by glucosylceramide in C. elegans.* Genes Dev, 2015. **29**(12): p. 1218-23.

53. Carberry, K., et al., *The novel intestinal filament organizer IFO-1 contributes to epithelial integrity in concert with ERM-1 and DLG-1.* Development, 2012. **139**(10): p. 1851-62.

54. Zhang, H., et al., *Apicobasal domain identities of expanding tubular membranes depend on glycosphingolipid biosynthesis.* Nat Cell Biol, 2011. **13**(10): p. 1189-201.

55. Bossinger, O., et al., *The apical disposition of the Caenorhabditis elegans intestinal terminal web is maintained by LET-413.* Dev Biol, 2004. **268**(2): p. 448-56.

56. Lant, B., et al., *CCM-3/STRIPAK promotes seamless tube extension through endocytic recycling.* Nat Commun, 2015. **6**: p. 6449.

57. Armenti, S.T., E. Chan, and J. Nance, *Polarized exocyst-mediated vesicle fusion directs intracellular lumenogenesis within the C. elegans excretory cell.* Dev Biol, 2014. **394**(1): p. 110-21.

58. Gobel, V., et al., *Lumen morphogenesis in C. elegans requires the membrane-cytoskeleton linker erm-1.* Dev Cell, 2004. **6**(6): p. 865-73.

59. Karabinos, A., et al., *Essential roles for four cytoplasmic intermediate filament proteins in Caenorhabditis elegans development.* PNAS, 2001. **98**(14): p. 7863–7868.

60. Dodemont, H., et al., *Eight genes and alternative RNA processing pathways generate an unexpectedly large diversity of cytoplasmic intermediate filament proteins in the nematode Caenorhabditis elegans.* EMBO J, 1994. **13**(11): p. 2625-38.

61. Spencer, W.C., et al., *A spatial and temporal map of C. elegans gene expression.* Genome Res, 2011. **21**(2): p. 325-41.

62. Woo, W.M., et al., *Intermediate filaments are required for C. elegans epidermal elongation.* Dev Biol, 2004. **267**(1): p. 216-29.

63. Sulston, J.E. and J. Hodgkin, *Methods,* in *The Nematode Caenorhabditis elegans,* W.B. Wood, Editor. 1988, Cold Spring Harbor Press: Cold Spring Harbor, New York. p. 587-606.

64. Minevich, G., et al., *CloudMap: a cloud-based pipeline for analysis of mutant genome sequences.* Genetics, 2012. **192**(4): p. 1249-69.

65. Hodgkin, J. and T. Doniach, *Natural variation and copulatory plug formation in Caenorhabditis elegans.* Genetics, 1997. **146**(1): p. 149-64.

66. Wicks, S.R., et al., *Rapid gene mapping in Caenorhabditis elegans using a high density polymorphism map.* Nat Genet, 2001. **28**(2): p. 160-4.

67. Flibotte, S., et al., *Whole-genome profiling of mutagenesis in Caenorhabditis elegans.* Genetics, 2010. **185**(2): p. 431-41.

68. Buechner, M., et al., *Cystic Canal Mutants in Caenorhabditis elegans Are Defective in the Apical Membrane Domain of the Renal (Excretory) Cell.* Developmental Biology, 1999. **214**: p. 227-241.

69. Karabinos, A., J. Schunemann, and K. Weber, *Most genes encoding cytoplasmic intermediate filament (IF) proteins of the nematode Caenorhabditis elegans are required in late embryogenesis.* Eur J Cell Biol, 2004. **83**(9): p. 457-68.

70. Coch, R.A. and R.E. Leube, *Intermediate Filaments and Polarization in the Intestinal Epithelium.* Cells, 2016. **5**(3).

71. Husken, K., et al., *Maintenance of the intestinal tube in Caenorhabditis elegans: the role of the intermediate filament protein IFC-2.* Differentiation, 2008. **76**(8): p. 881-96.

72. Karabinos, A., et al., *<Expression profiles of the essential intermediate filament (IF) protein A2 and the IF protein C2 in the nematode Caenorhabditis elegans.pdf>*. Mechanisms of Development 2002. **117**: p. 311–314.

73. Karabinos, A., et al., *In vivo and in vitro evidence that the four essential intermediate filament (IF) proteins A1, A2, A3 and B1 of the nematode Caenorhabditis elegans form an obligate heteropolymeric IF system.* J Mol Biol, 2003. **333**(2): p. 307-19.

74. Zuela, N. and Y. Gruenbaum, *Intermediate Filaments in Caenorhabditis elegans.* Methods Enzymol, 2016. **568**: p. 661-79.

75. Jahnel, O., et al., *Mechanical Probing of the Intermediate Filament-Rich Caenorhabditis Elegans Intestine.* Methods Enzymol, 2016. **568**: p. 681-706.

76. Karabinos, A., J. Schunemann, and D.A. Parry, *Assembly studies of six intestinal intermediate filament (IF) proteins B2, C1, C2, D1, D2, and E1 in the nematode C. elegans.* Cytoskeleton (Hoboken), 2017. **74**(3): p. 107-113.

77. de Leeuw, R., Y. Gruenbaum, and O. Medalia, *Nuclear Lamins: Thin Filaments with Major Functions.* Trends Cell Biol, 2017.

78. Dechat, T., et al., *Nuclear lamins: major factors in the structural organization and function of the nucleus and chromatin.* Genes Dev, 2008. **22**(7): p. 832-53.

79. Fawcett, D.W., *On the occurrence of a fibrous lamina on the inner aspect of the nuclear envelope in certain cells of vertebrates.* Am J Anat, 1966. **119**(1): p. 129-45.

80. Webster, M., K.L. Witkin, and O. Cohen-Fix, *Sizing up the nucleus: nuclear shape, size and nuclear-envelope assembly.* J Cell Sci, 2009. **122**(Pt 10): p. 1477-86.

81. Grimm-Gunter, E.M., et al., *Plastin 1 binds to keratin and is required for terminal web assembly in the intestinal epithelium.* Mol Biol Cell, 2009. **20**(10): p. 2549-62.

82. Iwatsuki, H., C. Ogawa, and M. Suda, *Vimentin-positive cells in the villus epithelium of the rabbit small intestine.* Histochem Cell Biol, 2002. **117**(4): p. 363-70.

83. Forman-Rubinsky, R., J.D. Cohen, and M.V. Sundaram, *Lipocalins Are Required for Apical Extracellular Matrix Organization and Remodeling in Caenorhabditis elegans.* Genetics, 2017. **207**(2): p. 625-642.

84. McShea, M.A., et al., *Abelson interactor-1 (ABI-1) interacts with MRL adaptor protein MIG-10 and is required in guided cell migrations and process outgrowth in C. elegans.* Dev Biol, 2013. **373**(1): p. 1-13.

85. Fraser, A.G., et al., *Functional genomic analysis of C. elegans chromosome I by systematic RNA interference.* Nature, 2000. **408**(6810): p. 325-30.

86. Kim, E., et al., *Long-term imaging of Caenorhabditis elegans using nanoparticle-mediated immobilization.* PLoS One, 2013. **8**(1): p. e53419.

87. Kamath, R.S. and J. Ahringer, *Genome-wide RNAi screening in Caenorhabditis elegans.* Methods, 2003. **30**(4): p. 313-21.

88. Hedgecock, E.M., et al., *Axonal guidance mutants of Caenorhabditis elegans identified by filling sensory neurons with fluorescein dyes.* Dev Biol, 1985. **111**(1): p. 158-70.

89. Fujita, M., et al., *The role of the ELAV homologue EXC-7 in the development of the Caenorhabditis elegans excretory canals.* Dev Biol, 2003. **256**(2): p. 290-301.

90. Calixto, A., et al., *Enhanced neuronal RNAi in C. elegans using SID-1.* Nat Methods, 2010. **7**(7): p. 554-559.

91. Simmer, F., et al., *Loss of the putative RNA-directed RNA polymerase RRF-3 makes C. elegans hypersensitive to RNAi.* Curr Biol, 2002. **12**(15): p. 1317-9.

92. Armstrong, K.R. and H.M. Chamberlin, *Coordinate regulation of gene expression in the C. elegans excretory cell by the POU domain protein CEH-6.* Mol Genet Genomics, 2010. **283**(1): p. 73-87.

93. Burglin, T.R. and G. Ruvkun, *Regulation of ectodermal and excretory function by the C. elegans POU homeobox gene ceh-6.* Development, 2001. **128**(5): p. 779-90.

94. Gilmore, M.S., F. Lebreton, and W. van Schaik, *Genomic transition of enterococci from gut commensals to leading causes of multidrug-resistant hospital infection in the antibiotic era.* Curr Opin Microbiol, 2013. **16**(1): p. 10-6.

95. Tanimoto, K., F.Y. An, and D.B. Clewell, *Characterization of the traC determinant of the Enterococcus faecalis hemolysin-bacteriocin plasmid pAD1: binding of sex pheromone.* J Bacteriol, 1993. **175**(16): p. 5260-4.

96. Ruhfel, R.E., D.A. Manias, and G.M. Dunny, *Cloning and characterization of a region of the Enterococcus faecalis conjugative plasmid, pCF10, encoding a sex pheromone-binding function.* J Bacteriol, 1993. **175**(16): p. 5253-9.

97. Clewell, D.B., *Plasmids, drug resistance, and gene transfer in the genus Streptococcus.* Microbiol Rev, 1981. **45**(3): p. 409-36.

98. Sahm, D.F., et al., *In vitro susceptibility studies of vancomycin-resistant Enterococcus faecalis.* Antimicrob Agents Chemother, 1989. **33**(9): p. 1588-91.

99. Gilmore, M.S., et al., *Pheromone killing of multidrug-resistant Enterococcus faecalis V583 by native commensal strains.* Proc Natl Acad Sci U S A, 2015. **112**(23): p. 7273-8.

100. Bhatty, M., et al., *Enterococcus faecalis pCF10-encoded surface proteins PrgA, PrgB (aggregation substance) and PrgC contribute to plasmid transfer, biofilm formation and virulence.* Mol Microbiol, 2015. **95**(4): p. 660-77.

101. Maadani, A., et al., *Enterococcus faecalis mutations affecting virulence in the Caenorhabditis elegans model host.* Infect Immun, 2007. **75**(5): p. 2634-7.

102. Garsin, D.A., et al., *A simple model host for identifying Gram-positive virulence factors.* Proc Natl Acad Sci U S A, 2001. **98**(19): p. 10892-7.